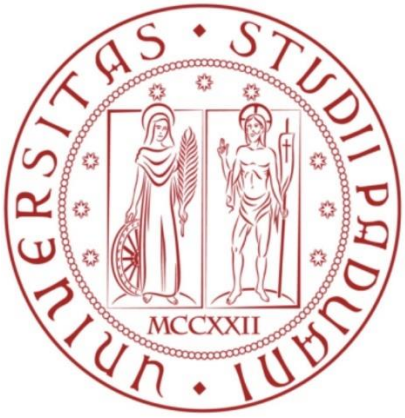

UNIVERSITÀ DEGLI STUDI DI PADOVA

SCHOOL OF SCIENCE

Department of Geoscience

MASTER THESIS IN GEOPHYSICS FOR NATURAL RISK AND RESOURCES

VALIDATING THE CANADIAN SEISMIC RISK MODEL

Supervisors: Prof. Lapo Boschi

Co-advisor: Dr. Tiegan Hobbs

Student: Somayeh Asadi Shekafti

Academic year

2022/2023

Abstract

Canada faces a scarcity of impactful earthquakes that can be used to validate seismic risk models, as the last significant damaging earthquakes occurred in the 1980s (Hobbs, Journeay, and Rotheram 2021). To overcome this limitation, this study aims to assess the reliability of the Canadian National Seismic Risk Model (CanadaSRM1) by analyzing the shaking intensities and physical impacts recorded from several recent events. These events include the 2010 Mw 5.5 Val-des-Bois and 2013 Mw 4.6 Ladysmith earthquakes in Eastern Canada, the 1985 M 6.9 Nahanni earthquake in Northern Canada, and the 2017 Mw 6.2 - 6.3 Mosquito Lake pair earthquakes in Western Canada. By evaluating the potential consequences of mentioned earthquakes in south-western Quebec, the Northwest Territories, and southern Yukon (near Whitehorse), the study aims to assess the potential impact on densely settled metropolitan areas across the country.

In order to support disaster risk reduction efforts and advance the objectives of the Sendai Framework for Disaster Risk Reduction, Natural Resources Canada (NRCan) partnered with Global Earthquake Model Foundation, Italy (GEM) to develop a public Canadian Seismic Risk Model (Hobbs et al. 2023). This collaborative effort involved creating a national exposure inventory, Canadian-specific fragility and vulnerability curves, and adjusting the Canadian Seismic Hazard Model, which is the basis for the seismic provisions in the National Building Code of Canada. The risk modeling process, using GEM's OpenQuake-Engine (OQ), utilizes deterministic and probabilistic calculations to assess seismic risk at the neighborhood level for all Dissemination Areas (DAUID) in Canada. By considering baseline and simulated retrofit conditions, the model provides risk metrics such as expected immediate physical impacts, including building damage, casualties, and direct economic losses. This approach of Seismic Risk Assessment (SRA) relies on previous earthquake knowledge to estimate the potential consequences of future earthquakes, enabling the evaluation of proposed mitigation and adaptation measures for disaster risk reduction.

This thesis presents a comprehensive analysis of the potential damage caused by benchmark scenario earthquakes, including shaking damage to buildings, financial losses, fatalities, and other impacts. The study utilizes the OQ Engine and the national exposure dataset, following the methodology of the CanadaSRM1.

The primary findings, such as damage distributions, loss exceedance curves, and annual average losses, offer an accessible and quantifiable foundation of evidence for decision-making at various levels - local, regional, and national. These results demonstrate a high degree of consistency with observed or predicted impacts, taking into account economic and population growth adjustments. Consequently, this confirms the reliability of the first generation Canadian Seismic Risk Model, aligning it with industry standards and enabling the reproduction of recent destructive earthquakes.

Given Canada's vast size, intricate seismic hazard model, and dispersed populations, this study holds unique significance. Nonetheless, the challenges faced, and solutions provided are likely to be valuable to other countries undertaking similar programs.

Acknowledgements

I extend my profound gratitude to Professor Lapo Boschi, the supervisor of this research endeavor, for his unwavering support and invaluable guidance throughout the entire duration of this project. Professor Boschi's expertise in the field of seismology has been indispensable, providing me with the necessary insights to comprehend and navigate the intricacies of this study. I am particularly thankful for his time, unwavering patience, and constant encouragement, all of which played a pivotal role in the triumphant culmination of this thesis.

Additionally, I wish to convey my sincere thanks to my co-advisor, Dr. Tiegan Hobbs from the University of British Columbia, for her countless support and invaluable guidance throughout this project. Dr. Hobbs's profound knowledge and experience in seismic risk assessment have significantly contributed to my understanding and adept navigation of the complexities inherent in this study. I am especially appreciative of her generous allocation of time, patience, and encouragement, which have been instrumental in the successful completion of this thesis. Without her expertise and unwavering support, my research journey would not have been possible, even amidst her demanding schedules. Her patience and dedication as a mentor have left an indelible mark on my academic pursuits.

I would also like to express my deep appreciation to the program coordinator of the master's program, Professor Giorgio Cassiani, whose adept structuring of the program laid a solid foundation and provided the necessary tools for this research. The entire Geoscience department deserves my thanks for their unwavering support and guidance. I extend my gratitude to all my knowledgeable professors, whose classes significantly contributed to my learning, realization of my aspirations, and paved the way for both my future academic journey and job opportunities.

Finally, I want to express heartfelt gratitude to my siblings, Dr. Fatemeh, Eng. Mohammadreza, Dr. Samira, for their unwavering support and encouragement throughout my academic journey. I am also grateful to my loving family and friends for their invaluable support and encouragement during this engagement. Their belief in me and unwavering support have been pivotal in my ability to conduct and successfully complete this research.

Dedication

This dissertation is affectionately dedicated to my soul and heart

My Mother and Father

Pure spirits who have bestowed profound meaning upon my life

To my beloved homeland, wounded yet resilient, with a rich cultural heritage

IRAN

"In the garden of the mind, sow the seeds of wisdom,

Water them with curiosity, watch the blooms of knowledge blossom.

Rumi tends this garden, where the soul finds its light,

In the dance of understanding, darkness takes its flight."

(Jalāl al-Dīn Muḥammad Rūmī)

13th-century Persian poet

Table of Contents

List of Tables

List of Figures

List of Acronyms

SRA	Seismic Risk Assessment
DSHA	Deterministic Seismic Hazard Assessment
PSHA	Probabilistic Seismic Hazard Assessment
SDC	Scenario Damage Calculator
SRC	Scenario Risk Calculator
CanadaSHM6	6th Generation Seismic Hazard Model of Canada
CanadaSRM1	Canadian National Seismic Risk Model
OQ Engine	OpenQuake-Engine Software
GEM	Global Earthquake Model Foundation, Italy
HAZUS	The United States Federal Emergency Management Agency's methodology for estimating potential losses from disasters
FEMA	Federal Emergency Management Agency
Mw	Moment Magnitude
PGA	Peak Ground Acceleration
PGV	Peak Ground Velocity
SA	Spectral Acceleration
GMM	Ground Motion Model
GMPE	Ground Motion Prediction Equation
GMF	Ground motion field
MMI	Modified Mercalli Intensity
DAUID	Dissemination Areas Unique Identifier
DA	Census Dissemination Area
CAD	Canadian Dollars
GIS	Geographic Information System
GSC	Geological Survey of Canada
USGS	United States Geological Survey
NRCan	Natural Resources Canada
CDD	Canadian Disaster Database (Public Safety Canada 2022)
EM-DAT	Center for Research on Epidemiology of Disasters 2022
CatIQ	Catastrophe Loss Database 2023

Chapter 1 : Introduction

"It was at nighttime that the land shook… a big wave smashed into the beach…the Pachena Bay people were lost…"
Pacheenaht Elder, Vancouver Island
(Arima, 1991)

1.1. Introduction

Canada, a seismically active country, faces the potential for future earthquakes that could result in significant damage and loss. Understanding and mitigating the consequences of such disasters is crucial, especially considering the interdependencies among critical infrastructure networks that provide essential services to the population.

The Canadian Seismic Risk Model, developed by Natural Resources Canada (NRCan) in collaboration with the Global Earthquake Model Foundation, Italy (GEM), supports disaster risk reduction efforts at various levels of government and across industries (Tiegan Hobbs et al. 2023) (Hobbs et al. 2022). The model, known as CanadaSRM1 (the first generation of Canadian National Seismic Risk Model), includes both a probabilistic assessment of expected damages and losses at different time intervals, and a catalog of deterministic scenarios that assess damage, financial losses, human impacts, and other associated consequences. This model aligns with Canada's adoption of the Sendai Framework for Disaster Risk Reduction (Sendai Framework for Disaster Risk Reduction 2015 - 2030, n.d.). The model integrates a new physical exposure model covering the entire country (Journeay et al. 2022), earthquake building performance functions adapted for Canada based on HAZUS (The United States Federal Emergency Management Agency's methodology for estimating potential losses from disasters, stands for Hazard US) (Tiegan E Hobbs et al. 2023), and the 6th Generation National Seismic Hazard Model (CanadaSHM6) (Kolaj, Halchuk, and Adams 2023), which forms the foundation for the seismic provisions of the National Building Code of Canada.

Utilizing OpenQuake-Engine Software (OQ Engine) (Pagani et al. 2014) provided by GEM the risk modeling process involves deterministic and probabilistic calculations under both baseline and simulated retrofit conditions (Hobbs et al. 2023). The model generates outputs for all settled regions in Canada, providing information at the neighborhood or smaller scales. However, before the model can be utilized, it needs to undergo validation. The validation process ideally involves using data from previous earthquakes and the cumulative losses over relevant time periods.

1.2. Seismic risk assessment background

Seismic Risk Assessment (SRA) involves evaluating the potential negative impacts that individuals and society may face as a consequence of future earthquakes ("The Basics of Seismic Risk Analysis" 1989). This assessment consists of three main components: seismic hazard, vulnerability of structures in the area, and an inventory of the buildings and inhabitants, which is known as exposure model. To estimate the level of ground shaking at a particular location, seismic hazard assessment methodologies are used. Factors such as earthquake source characteristics (magnitude and fault type), wave travel path effects, and local site conditions influence the ground shaking. Local site conditions encompass aspects like soil amplification. The goal is to estimate the damage of potential earthquakes in order to reduce the impact of seismic events (Thibert 2008).

To perform seismic risk assessment, regional building data needs to be collected and stored in a building inventory. This data can include information like the building's name, address, occupancy, as well as structural details such as height, age, materials, and lateral force resisting system. Rather than analyzing each building individually, buildings in the Canadian database are grouped based on similar structural characteristics. This allows for earthquake risk assessment to be conducted more efficiently, as safety measures and policies can be applied to entire groups of buildings that share these common features, rather than addressing each building individually. This classification system assists in understanding and managing seismic risks across a wide range of structures by sorting buildings into categories. Damage estimation relies on ground motion-damage relationships developed for these building prototypes, which determine the anticipated amount of structural and non-structural damage caused by a given level of earthquake intensity (Hazus-MH 2003).

Losses are estimated based on the outcome of the damage assessment. Monetary losses are calculated considering both structural and non-structural damage, as well as the replacement value of the building (Hobbs et al. 2023). The replacement value depends on the use of the facility, with non-structural components and contents often comprising the largest portion, thereby impacting the economic losses resulting from earthquake damage. The number of casualties is determined by considering the structural damage and the number of occupants present in the building during the earthquake, and the relationship between shaking and fatalities (Hobbs et al. 2023).

1.3. Research motivation

Large earthquakes are less common in stable continental regions, but they can still pose a significant threat to both people and infrastructure. The devastating New Madrid earthquake sequence with magnitudes above 7.0 on the winter of 1811–1812 serves as evidence of this (Hough 2009). Canada, similar to numerous other regions, faces the risk of significant earthquakes that can lead to extensive destruction and the loss of human lives (Hobbs, Journeay, and Rotheram 2021). Even in Canada, there have been damaging and deadly earthquakes in the past, such as the Moment Magnitude (Mw) 7 earthquake in Charlevoix, in 1663 and the Mw 7.2 earthquake off of Grand Banks, Newfoundland, in 1929, which resulted in a tsunami and the loss of 27 lives (M. Lamontagne et al. 2008).

According to Canada's national hazard map, most Canadians live in areas prone to earthquakes, particularly in urban regions where more than 75% of the population resides (Adams et al. 2002). This means that the highest risk of earthquakes in Canada is concentrated in these urbanized areas. Therefore, the occurrence of a major earthquake near densely populated areas could have disastrous social and economic consequences. Past earthquakes have emphasized the significance of safeguarding buildings, prioritizing the safety of residents, and taking proactive steps to mitigate the impact of earthquakes (Fereidoni 2014). Therefore, it is crucial to evaluate the seismic risk model of Canada accurately and reliably in order to implement effective measures to mitigate impact.

1.4. Aims and objectives

The objective of this study is to conduct a benchmark assessment of the CanadaSRM1 model by comparing observations from recent earthquakes in Eastern, Northern, and Western Canada with the estimated impacts of these events determined using the CanSRM1 model. The aim is to evaluate the model's reliability in predicting the effect of future events, with the goal of providing valuable information for decision makers in Canada to justify plans and take appropriate actions to mitigate seismic risk in the country.

To achieve this, the research proposes a computational method to assess the risks associated with different seismic scenarios in three regions of Canada: east, north, and west. OQ engine, an open-source software, is utilized to combine seismic hazard data in the form of shakemaps, exposure models, and building vulnerability information to validate the initial version of Canada's national seismic risk model. The method involves selecting earthquake scenarios based on magnitude and location distributions for each area, sampling damage states for each event using ground-motion shaking intensity data from the United States Geological Survey (USGS) shakemaps and comparing the computed results with actual data.

While this research contributes to the understanding and evaluation of Canada's initial seismic risk model by quantifying the likelihood of various levels of loss, it's important to note that the study does not cover the effects of earthquakes on infrastructure and secondary losses like induced landslides. Nonetheless, the estimation of uncertainty in the data will help assess its quality and determine its appropriate use in decision-making processes. To achieve this goal, the following steps will be taken:

1. Development of a dataset of recent earthquakes that occurred in the study areas:
   - Due to a shortage of relevant catastrophic disaster events in Canada, we will focus on recent earthquakes that are not featured in major databases but still caused modest damage in western, northern, and eastern Canada.
   - Calculation of the expected physical impacts and cumulative losses from previous earthquakes will be done, using USGS shakemaps and the OQ Engine. This approach mostly aligns with the methodology of the CanadaSRM1 model.

2. Adjustment of the outputs for economic and population growth from the model's generation year, 2016, to the year of the events' occurrence.

3. Collecting reports of the impacts of these events using information acquired from Disaster databases, Catastrophe Loss Database (CatIQ), and Geological Survey of Canada (GSC).

4. Analysis and comparison of the adjusted outcomes of recent earthquakes (CanadaSRM1) with the determined threshold.

5. Validating of the CanadaSRM1 model.

1.5. Limitation and scope

Assessing seismic risk is challenging due to the interactions between risk drivers. Seismic hazard is inherently uncertain because it relies on previous knowledge that may be limited or poorly understood (Dowrick 2003). The evaluation of both structural and non-structural damage involved following assumptions:

1. This approach is not capable of determining the specific damage to individual components or systems, such as mechanical, electrical, and plumbing systems of the non-structural components of a building.
2. The approach used in this study is focused on evaluating regions rather than individual buildings, so detailed structural analyses were not conducted. Instead, buildings were categorized into prototypes. However, it's important to note that this simplification introduces uncertainties in the estimation of damages. For site specific impacts it is important to conduct site specific analyses. Additionally, estimating earthquake casualties involves various uncertainties, relying on factors such as assessing structural damage, understanding the relationship between damage and casualties (casualty rate), and determining the number of individuals present in the affected buildings during the event.
3. The study focused solely on evaluating the damage caused by the shaking of buildings during an earthquake. Other associated risks like landslides, liquefaction, fires triggered by earthquakes, and flooding were not considered in this research.
4. The mentioned monetary losses do not take into account the additional losses incurred through business interruption. Calculating these indirect losses is not solely based on the physical damage suffered by a building, but also involves assessing the duration of downtime which is determined by the time required for repairing the damage. Due to the complexity involved and the constraints of time and resources, the monetary losses were only calculated for the direct damages.

1.6. Thesis outline

This thesis covers several topics, presented in the following order of discussion: After the first introductory chapter, chapter 2 provides an overview of general risk assessment methods and a discussion of techniques used for national-scale seismic risk analyses. It explains various tools and software used in this field, comparing their effectiveness. Finally, the main methods that are currently used in risk assessment are critically discussed. Chapter 3 presents a comprehensive overview of the three study areas. This includes a detailed description of the geological formation, tectonic situation, seismicity, and seismic history of each area.

Chapter 4 delves into the research methodology for assessing the CanadaSRM1, covering aspects such as workflow, input parameters, data processing, and theoretical concepts like seismic risk analysis. Additionally, it establishes the theoretical framework and methodological design for SRA, discussing key requirements and presenting a roadmap for the SRA methodology. Chapter 5 presents research findings and estimated outcomes from seismic damage and risk assessments conducted on five earthquakes in various regions of Canada. Utilizing the OQ Engine and the CanadaSRM1 framework, the study employed calculators to simulate damage states and loss ratios

for buildings and assets in the exposure model. The mean damage distribution and aggregated statistics for the entire portfolio were calculated, including fatalities and mean financial losses.

Chapter 6 provides a comprehensive analysis of SRA in the western, eastern, and northern regions of Canada. It explores the implications of probability of exceedance across different damage states, assessing variations among provinces exposed to earthquakes. The chapter also delves into the economic losses and fatalities resulting from studied earthquakes, while examining the relationship between probability of exceedance and loss ratio. Furthermore, this chapter is dedicated to the comparison and evaluation of a proposed system, addressing testing and results in relation to research objectives.

In the concluding chapter of the thesis, final conclusions are drawn from the research, accompanied by an acknowledgment of limitations associated with the methods and software used. This section not only offers valuable recommendations for potential future research but also tailors them to the specific scope of the study, as detailed in Chapter 7.

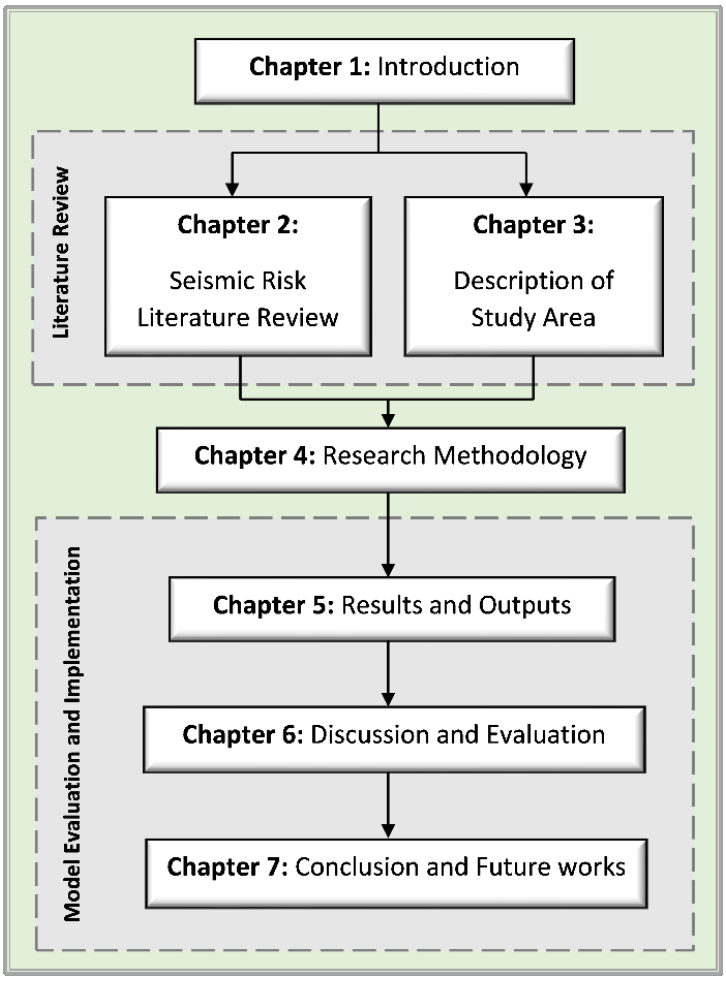

Figure 1.1. Outlines the structural layout of the thesis, offering a visual overview of how key chapters or sections are interconnected. This figure serves as a guide for readers to understand the logical flow and organization of this document.

Chapter 2 : Literature Review

2.1. Introduction

In recent years, research in various fields, spanning from seismology to social sciences, has greatly enhanced our comprehension of global disasters. This chapter offers a concise overview of seismic risk methodologies, elucidating key terms in seismic risk. Additionally, it delves into the evolution of notable SRA software programs, ultimately spotlighting the ones selected and employed in this thesis.

2.2. Seismic risk methods

Strong earthquakes have severe consequences, such as economic impacts, building damage, casualties, and harm to essential facilities, lifelines, transport networks, cultural heritage, and the environment ("Global Assessment Report on Disaster Risk Reduction 2015" n.d.). To address these risks, an SRA process is conducted, aiming to measure the potential negative impacts and their likelihood. This assessment informs emergency managers and decision-makers, enabling them to take appropriate actions (Newman et al. 2017). Accurate estimation of seismic risk requires detailed information about ground shaking intensity, exposed buildings and infrastructure, and their vulnerabilities. Risk assessment results may quantify some combination of physical damage, economic and social losses, and their probabilities.

Seismic losses have been increasing significantly in terms of both magnitude and frequency, resulting in severe impacts on societies and economies. This rise is primarily due to the rapid growth of population and infrastructure in earthquake-prone areas worldwide. To effectively respond to and recover from these events, it is crucial to have a better understanding and accurate estimation of seismic risks. As a result, research communities have been focusing on developing software tools for modeling and analyzing seismic risk.(Hosseinpour et al. 2021)

In recent years, significant efforts have been made to develop software for estimating seismic losses. Various tools, such as HAZUS (Hazus-MH 2003), Haz-Taiwan, SELENA (S. Molina, Lang, and Lindholm 2010), HazCan , InaSAFE (Pranantyo and Fadmastuti 2014), CAPRA (Bernal and Cardona 2018), DBELA, OQ Engine (Pagani et al. 2023), and ER2 web application (Abo El Ezz et al. 2019), have been created for seismic loss estimation. Some countries have their customized versions, while global projects like the GEM are working on tools with worldwide capabilities (Silva et al. 2014a).

This section provides a critical review of existing methods and software used for seismic risk analysis. It discusses the essential steps of hazard assessment, exposure modeling, and vulnerability assessment, with a particular emphasis on evaluating different approaches to vulnerability evaluation. The strengths and limitations of various software programs are highlighted, and a comparative analysis of major seismic risk software is presented.

2.3. Overview of earthquake loss assessment

Four main factors contribute to the calculation of seismic loss:

- ***Exposure:*** It refers to the level of human activity in areas prone to seismic hazards, determined by the presence of buildings, infrastructure, and inhabitants in those locations (De Bono and Mora 2014b).

- ***Vulnerability:*** This factor assesses the susceptibility of infrastructure to damage from shaking (Tyagunov et al. 2004).
- ***Hazard:*** It represents the likelihood of specific intensity ground motions occurring at a particular location over a given period of time, which can be determined through various methods such as scenario modeling which is Deterministic Seismic Hazard Assessment (DSHA) and Probabilistic Seismic Hazard Assessment (PSHA) (J. J. Bommer 2002).
- ***Damage loss conversion:*** This factor quantifies the damage in terms of repair and restoration costs or social impact, including injuries, homelessness, and fatalities (Daniell 2011).

Due to the diverse approaches used to determine these components, there is a wide range of earthquake loss estimation methods available (Daniell 2011). The suitability of a particular method may vary depending on the region, considering the reduction of uncertainties related to data collection, scientific assumptions, and regional factors like source, path, and site characteristics. An earthquake loss estimation can be performed either proactively (pre-earthquake scenario modeling) or reactively (post-earthquake fixed scenario modeling) (Daniell 2011).

2.4. Loss assessment software

There are different types of software packages for seismic analysis. These packages can be proprietary, open access, or open-source, and they are usually designed for specific regions with their unique geological and construction characteristics. Table 2.1 provides a summary of the SRA software. OQ Engine is being considered for this current study, and the rationale behind this choice will be discussed in the following.

2.4.1. ER2-Earthquake

ER2-Earthquake, developed by NRCan, is a user-friendly web-based software for assessing seismic risk (Abo El Ezz, Nollet, and Nastev 2014). It's unique in its usability for both experts and non-experts, offering assessment using scenario earthquakes or probabilistic scenarios over various return periods. Built with Java and Python, it efficiently computes results, using an innovative non-iterative algorithm to determine structural response (Porter 2009). By employing HAZUS fragility functions, it calculates probabilities of building damage states linked to spectral displacement (Nollet et al. 2018). These probabilities are linked to the intensity measures of the input spectrum.

What sets ER2 apart is its database storage of multiple scenario results, reducing the need for time-consuming iterations, and it provides quick, reliable outcomes akin to HAZUS but with the added benefits of short runtime and minimal user input (Abo El Ezz et al. 2019). This accessibility makes ER2 highly valuable for planning and operational drills, particularly in regions with low to moderate seismic activity.

2.4.2. HAZUS

The U.S. Federal Emergency Management Agency (FEMA) created the HAZUS software in the 1990s to assess the effects of earthquakes and other hazards on buildings, infrastructure, casualties, shelter needs, and economic losses (Kircher, Whitman, and Holmes 2006). The

software uses C++ and Visual Basic algorithms, Microsoft SQL for the database, and ArcGIS for visualization. It is developed by private companies as closed-source software with comprehensive guidelines and parameters for damage assessment ("Hazus User & Technical Manuals | FEMA.Gov" n.d.).

Table 2.1. Seismic risk assessment software packages (Silva et al. 2014a) (Jena et al. 2020) (Hosseinpour et al. 2022).

Software	ER2	HAZUS (HazCan)	HAZUS-MH	Ergo (MAEviz)	CAPRA	EQRM	SELENA	OQ
Lunched by	Canada (Quebec City)	Canada	U.S.	U.S.	Central America (Nicaragua)	Australia	Norway	Italy
Developed by	NRCan, CSSP	NRCan	FEMA (NHRAP)	Uni. Illinois	World Bank (GFDRR)	Geoscience Australia	NORSAR	GEM (Stakeholder worldwide)
Programming Language	Java and Python	VB6, C++	VB6, C++	Java	Visual Basic, NET	Python, MATLAB	MATLAB, C++	Python (Web-based)
Open source	No	No	No	Yes	Yes	Yes	Yes	Yes
Graphic user interface	Yes	Yes	Yes	Yes	Yes	No	Yes	No
Input data	seismic hazard data, structural information on buildings, infrastructure, and population data	Buildings, infrastructure and demographic data	Buildings, critical facilities, transportation and demographic data	building data, infrastructure details, human behavior models, and environmental factors	Population, building inventory data, PGA, and infrastructure	Active fault Types, Event scenario, Attenuation, Threshold Distance, Amplification, Building classification	Building Demographical data and seismic data, different soil class	Population, global land cover, building data, global GDP data
Methodology	assess structural vulnerabilities and risks related to earthquakes, focuses on building characteristic, soil types	incorporate Canadian seismic hazard models and regional geological data, Building vulnerability assessment map, Estimation of damage and Casualty, Estimate loss	Prepare shakemap, Building vulnerability assessment map, Estimation of damage and Casualty, Estimate loss	building performance evaluation, evacuation modeling, infrastructure analysis, and environmental considerations	Seismic hazard Evaluation, Identifying inventory, Application of Vulnerability functions, Estimation of losses	Generation of Synthetic earthquake catalog, Preparation of attenuation relation, Account of Interaction between geology and seismic waves, preparing probability of every earthquake and hazard, using buildings and population risk analysis can be done	Prepare seismic risk map, produce building vulnerability map, Estimate damage and casualty	Seismic risk evaluation, Use of analytical and empirical methods for vulnerability analysis, Socioeconomic impact and losses estimation
Output	detailed structural assessments, including building-specific damage predictions and risk analyses	loss estimates, considering economic, social, and infrastructure damage	Loss estimates for utilities and lifelines, Estimation of vulnerability and casualties, Estimation of economic and social loss	building performance analysis, evacuation strategies, infrastructure resilience, and environmental impact assessment	Physical and economic losses approximated per property, Probable % of loss, annually expected economic losses	Probability estimation, Level of damage estimation, financial loss, Computation of risk	Physical damage estimation, Estimation of total economic loss, Damage, and casualty	Loss of life and Property, Damage Estimation, Social and Economic changes due to disruption

HAZUS v.4.2, released in May 2019, offers high-resolution shake-maps and an updated fire following earthquake module. It provides pre-packaged input data and links to additional

information sources. The software incorporates 15 categories of building types, differentiated by structural features and materials, multiplied by building height and design level to generate 128 building types. HAZUS also considers seven major occupancy categories, which impact building performance and resulting social and economic losses. Ongoing efforts aim to modernize HAZUS and eliminate the need for commercial software (Otto 2010).

The HAZUS methodology has been adapted in various locations worldwide to assess losses in other areas. Examples include Turkey (J. Bommer et al. 2002), Norway (SELENA) (Sergio Molina and Lindholm 2005), Taiwan (using a modified version called Haz-Taiwan) (Yeh, Loh, and Tsai 2006), Canada (HazCan) (Nastev 2014), Risk-UE (Mouroux and Le Brun 2006), EQRM (D. Robinson, Fulford, and Dhu 2005), ER2-Earthquake (Abo El Ezz et al. 2019), and Ergo (formerly known as MAEviz). HAZUS employs a user-friendly GUI for data input and presents output in a GIS-based platform. It can estimate losses for different infrastructures like lifelines, essential facilities, and transportation systems. Additionally, it considers damage from post-earthquake fires and indirect economic losses. However, HAZUS has some limitations, including the requirement of an ArcGIS license and difficulties in software installation. It's worth noting that while HAZUS can be used for locations outside the U.S., the reliability of loss estimation results may be compromised due to varying seismic and structural conditions (Daniell 2011).

2.4.3. ERGO (MAEviz, mHARP, Hazturk)

Ergo, previously known as MAEviz and mHARP, is a loss estimation software developed by the Mid-America Earthquake Centre and the National Centre for Supercomputing Applications at the University of Illinois (Makhoul and Argyroudis 2018) (“Ergo – Multi-Hazard Assessment, Response, and Planning” n.d.). It is designed for SRA in the central U.S. states. Ergo is an open-source software written in Java programming language and has a user-friendly graphical user interface. It includes a built-in Geographic Information System (GIS) for representing input and output data without requiring any commercial package.

The software is built on the open-source Eclipse Rich Client Platform. It supports various plug-ins and allows users to incorporate their own hazard data (Elnashai et al. 2008). The software considers hazards like liquefaction and ground shaking. It provides default earthquake scenarios and probabilistic hazard maps in its catalogue, but users can also upload their own hazard data within the GUI. It follows a consequence-based risk management approach to assess and mitigate potential losses from disasters (Elnashai et al. 2008). Ergo has been integrated into various platforms, including HAZTurk (Turkey's seismic risk assessment platform) (Karaman, Şahin, and Elnashai 2008), EQvis (European platform) (Schäfer and Wenzel 2013), and the SYNER-G project, which incorporates a large fragility function manager system (Pitilakis, Crowley, and Kaynia 2014).

2.4.4. CAPRA-Earthquake

CAPRA is an open-source risk assessment platform supported by the World Bank (“CAPRA-GIS | CAPRA | Probabilistic Risk Assessment Platform” n.d.). It was released in 2008 and offers various modules for evaluating risks related to natural hazards, with a focus on earthquakes. The main module, CAPRA-GIS, calculates losses caused by different hazards once the necessary input

files are imported. CAPRA-GIS relies on a hazard model generated by the CRISIS 2015 module, which incorporates stochastic scenarios and spatial distribution of intensity (Bernal and Cardona 2018). CAPRA also includes modules for analyzing strong motion signals, soil response, and conducting PSHAs.

To assess damage, CAPRA utilizes vulnerability functions specific to each building type. These functions are developed using the ERN-Vulnerabilidad module, which allows for the creation of custom functions and considers uncertainty by adjusting the variance (Aguilar Meléndez et al. 2017). The outputs provided by CAPRA include loss exceedance curves, probable maximum loss, and average annual loss for individual buildings or a set of buildings.

In addition to the existing modules, a new module called CAPRA-EQ is currently being developed to enhance seismic hazard modeling for risk analysis, reduction, and management. CAPRA serves as a user-friendly platform with a graphical interface programmed in Visual Basic language, making it accessible and easy to understand ("CAPRA-GIS | CAPRA | Probabilistic Risk Assessment Platform" n.d.).

2.4.5. EQRM

The EQRM (Earthquake Risk Model) is an open-source software developed by Geo-Science Australia specifically for assessing seismic risks and damage in Australian (D. J. Robinson, Dhu, and Row 2007). It was created using Python and MATLAB and lacks a graphical user interface or integration with GIS (D. Robinson, Fulford, and Dhu 2005).

The software applies the HAZUS methodology for damage assessment but with some variations. It considers a wider range of periods in the response spectrum and soil amplification compared to HAZUS. Instead of incorporating variability in damage thresholds, capacity curves, and ground shaking, EQRM focuses only on the variability of damage states in its fragility curves. The software utilizes uniform hazard spectra and the Modified Mercalli Intensity (MMI) scale. It performs probabilistic seismic hazard and risk analysis using an event-based approach, calculating ground shaking parameters and losses for each event and aggregating the results for probabilistic risk estimates (Dhu et al. 2008). EQRM provides various outputs such as seismic hazard maps, hazard exceedance curves, uniform hazard spectra, risk exceedance curves, and aggregated/disaggregated annualized losses ("Daniell J, Simpson A, Murnane R, Tijssen A, Nunez A, Deparday V, Gunasekera R, Baca A, Ishizawa O, Schäfer A. Review of Open Source and Open Access Software Packages Available to Quantify Risk from Natural Hazards. Washington, DC: World Bank and Global Facility for Disaster Reduction and Recovery. 2014." n.d.).

2.4.6. InaSAFE

InaSAFE is a free and open-source software developed collaboratively by the Indonesia National Disaster Agency, the Australian Government, and international organizations ("Inasafe.Org | 521: Web Server Is Down" n.d.). It functions as a plugin for QGIS, a GIS platform, and aims to aid disaster managers in understanding the potential impacts of specific disasters (Pranantyo and Fadmastuti 2014). InaSAFE, as same as HAZUS, includes tools to calculate shelter needs based on estimated displaced populations and utilizes MMI as a hazard measure. It calculates

economic losses considering building values and areas, and estimates fatalities using a model developed by Institute Teknologi Bandung (Vecere, Monteiro, and Ammann 2016). However, the ITB model tends to over-predict fatality rates at high MMI levels, and its associated uncertainty has not been addressed (Jaiswal, Wald, and Hearne 2010).

Object-oriented framework for infrastructure modelling and simulation (OOFIMS) OOFIMS Seismic Loss Estimation software, developed as part of the SYNER-G project, evaluates the seismic vulnerability of urban areas, including buildings, transportation systems, and lifelines (Pitilakis, Crowley, and Kaynia 2014). It is an open-source software written in MATLAB and can now handle multiple hazards such as floods and volcanic events (Hosseinpour et al. 2021). The latest version, OOFIMS V.4.4, released in 2018, includes the Boore and Atkinson Ground Motion Prediction Equation (GMPE) and HAZUS fragility models for water supply systems (Boore and Atkinson 2008). OOFIMS can analyze the vulnerability of interconnected infrastructure systems and building portfolios, including natural gas transition infrastructure, water supply systems, electrical power networks, and transportation systems (Franchin and Cavalieri 2013). It has been successfully applied to transportation and electric networks and gas distribution systems in Italy (Esposito et al. 2015).

2.4.7. SELENA

SELENA (Seismic Loss Estimation for Normal Earthquake Scenarios) is a software developed by the International Centre for Geohazards in collaboration with NORSAR and the University of Alicante. It uses a logic tree approach to assess uncertainties in seismic risk estimation (S. Molina 0). SELENA 6.5, the latest version coded in MATLAB, allows users to input data in a specific format to calculate shake maps, damage probabilities, economic losses, and casualty estimates. Unlike other tools, SELENA is independent of a GIS and can be integrated with any GIS system for result visualization (Sergio Molina et al. 2017). It incorporates various ground-motion parameter calculation methods and offers multiple vulnerability methodologies for computing building damage ("ATC-40 Seismic Evaluation and Retrofit of Concrete Buildings | PDF | Economic Sectors | Solid Mechanics" n.d.). This method differs from other methods by using a logic tree approach which allows for incorporating uncertainties related to different input parameters, offering final results along with corresponding confidence levels (S. Molina, Lang, and Lindholm 2010). Additionally, SELENA accounts for topographic effects in hilly regions through user-selectable amplification procedures based on different approaches (Sergio Molina et al. 2017).

2.4.8. OpenQuake Engine

The OQ Engine is software developed by GEM that allows for the assessment of seismic hazard and risk at various scales. It is coded in Python and the current version is v3.16.3, which is open source. The OQ Engine utilizes the Natural Hazard's Risk Markup Language, an XML-based language developed alongside the GEM project, to read input parameters and conduct loss analyses (Global Earthquake Maps | Global Earthquake Model Foundation | Italy n.d.). OQ is a transparent software that can be used with GEM or other user-created models to perform scenario-based or probabilistic hazard and risk analyses and generate hazard and loss outputs. It can also model spatial correlation of ground motion residuals and vulnerability uncertainty.

The OQ Engine includes various calculation algorithms such as the Scenario Risk Calculator (SRC), Scenario Damage Calculator (SDC), classic PSHA-based risk, probabilistic event-based risk, and retrofitting benefit-cost ratio (Silva et al. 2014b). The Probabilistic Event Based calculator is a particularly innovative module that utilizes the Monte Carlo method to generate a stochastic event set representing potential seismicity. GMFs are calculated for each event in the set. The event based PSHA calculator uses this set of GMFs to compute hazard curves for each site, representing the potential shaking scenarios over a given time period. However, this procedure can be computationally intensive and may not be suitable for large study areas (Pagani et al., n.d.).

The GEM project also developed a framework for evaluating and selecting existing fragility curves for new studies (Rossetto et al. 2014). This framework helps users assess the quality and relevance of fragility curves and improve the selection process, which can often be subjective. It requires a deep understanding of structural dynamic response and the evaluated fragility curves. The inventory of assets at risk, including structural and non-structural parameters, vulnerability curves, and content parameters, was then considered. The final step involved computing the negative impacts. The exposure dataset could also be prepared independently in a spreadsheet format and imported.

Figure 2.1 illustrates how QGIS, an open-source GIS platform, is utilized to assess the impact of an earthquake scenario. The process begins with users inputting necessary data using the Input Preparation toolkit. They then select the type of calculation they wish to conduct, be it event-based or seismic risk and hazard assessment scenarios. Each calculation stage yields diverse outputs, such as average asset loss, GMFs, and comprehensive calculation reports. The final phase involves visualizing these results through the QGIS software for a comprehensive understanding of the scenario's effects.

This section presents a review of various seismic loss estimation software options and concludes that OQ Engine is the preferred choice. OQ Engine distinguishes itself through its implementation of a user-friendly graphical interface, utilization of open-source codes, ability to incorporate probabilistic seismic shake maps from the USGS, and provision of visual representations of input and output parameters (Crowley and Bommer 2006). Furthermore, it offers free web-based access and incorporates a logic tree to account for uncertainties in modeling. OQ Engine enables users to input their own data and customize the analysis according to their needs. In comparison to alternative software, OQ Engine provides comprehensive user and technical manuals and is particularly accessible for users with moderate knowledge. Additionally, it appropriately considers uncertainties in seismic hazard assessment. Considering the limitations of other software options and the challenges related to data acquisition, seismic vulnerability assessment, and probabilistic risk assessment, OQ Engine emerges as a reliable and user-friendly tool for conducting seismic loss assessments in this thesis.

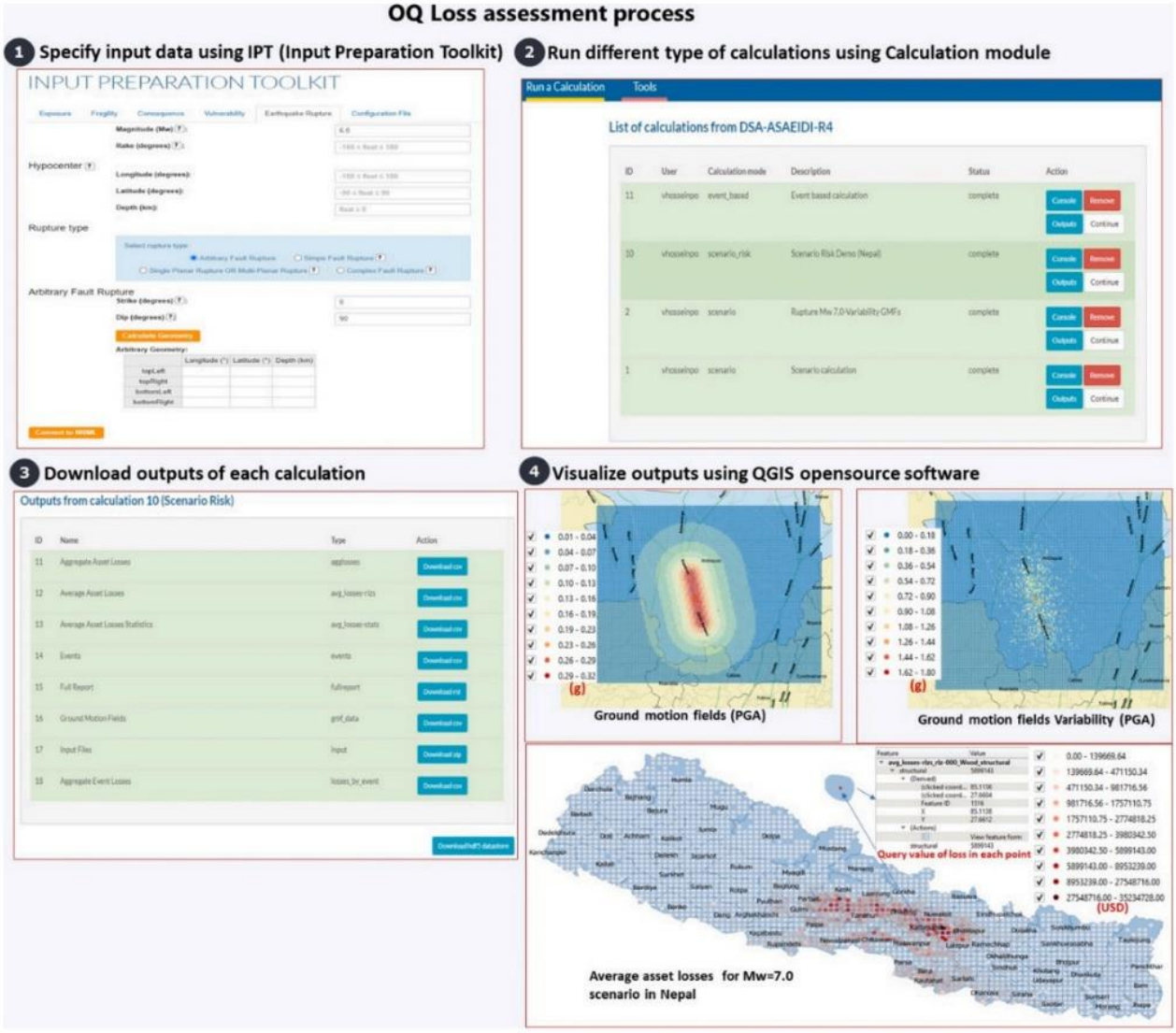

Figure 2.1. OQ Engine loss estimation process and visualization of loss results. In this specific example, Mw 7.0 earthquake scenario was simulated with a uniform shear wave velocity of 760 m/s across the study area to account for local site amplification. The figures provided show screen captures of input tables and the visualization of results (reprinted from Bhattacharya, Basu, and Ma 2001).

2.5. Selection rationale for OpenQuake Engine

The OQ Engine, employed in this research, presents distinct advantages in SRA when compared to other SRA software, such as ER2, HAZUS (HazCan), HAZUS-MH, Ergo (MAEviz), CAPRA, EQRM, and SELENA. Here is a detailed analysis of the key points of comparison:

ER2 boasts advanced seismic hazard analysis capabilities, including integration with GIS for enhanced visualization. However, its drawback lies in limited flexibility for customization, and it may not garner the same level of community support as open-source alternatives (Abo El Ezz et al. 2019). HAZUS (HazCan) and HAZUS-MH are extensively used in the U.S. and Canada for earthquake risk assessment. While they encompass various building types and occupancy classes

and seamlessly integrate with GIS, their primary design for the U.S. may limit their applicability in other regions (Daniell 2011). Moreover, these non-open-source tools may lack flexibility for customization, disregarding certain local building characteristics. Ergo (MAEviz) features a user-friendly interface and integration with other risk assessment tools. Nevertheless, it may lack some advanced features found in competing tools and offers limited flexibility for customization (Elnashai et al. 2008).

CAPRA stands out with comprehensive risk assessment capabilities and the ability to conduct PSHAs. However, it may demand significant computational resources and possesses a steep learning curve for users unfamiliar with PSHAs (Bernal and Cardona 2018). EQRM, being open-source and customizable, is suitable for SRA in various regions. Yet, it requires substantial knowledge of seismic hazard modeling and has limitations in certain risk assessment components (D. Robinson, Fulford, and Dhu 2005). SELENA, developed for SRA in Europe, seamlessly integrates with GIS. However, its applicability outside of Europe may be limited, and it has a smaller user community compared to more widely used tools (Sergio Molina et al. 2017).

In the context of validating the first seismic risk model for Canada in this thesis, the OQ Engine emerges as a robust candidate. Its open-source nature facilitates adaptation to regional requirements, and the incorporation of state-of-the-art seismic hazard models provides a strong foundation for risk assessments (Pagani et al. 2023). Despite the learning curve associated with its use, the flexibility and comprehensive capabilities of the OQ Engine make it a favorable choice for SRA in the Canadian context.

Chapter 3 : Study Area

3.1. Introduction

The purpose of the chapter is two-fold: first, to describe the geological setting, seismicity of Canada including the tectonic mechanism and active faults, and recognize the earthquake zones of western, eastern, and northern Canada; and second, to summarize the effects of Canada's noteworthy scenario and recent earthquakes, used as the case studies in this thesis, reminding readers that destructive earthquakes have happened in the past and will occur again in the future.

3.2. Geological setting of Canada

Canada is a country with diverse and complex geological settings due to its vast size and varied landscapes (Figure 3.1). The geological history of Canada spans billions of years and includes a wide range of geological features, including mountains, plains, plateaus, and the world's longest coastline.

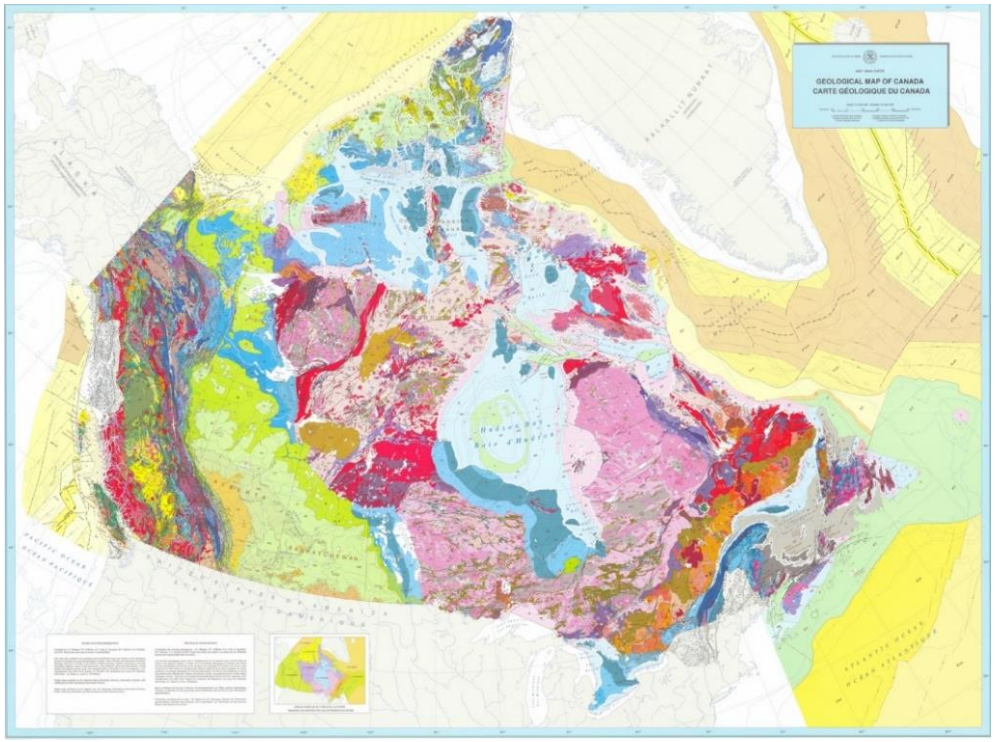

Figure 3.1. Geological map of Canada. Source: National Resources Canada (1996).

The prairies in Alberta and Saskatchewan have flat landscapes due to the presence of sedimentary rocks deposited by an ancient sea (C. E. Ventura and Schuster 1994). British Columbia and the Yukon Territory are mountainous regions with volcanoes formed by tectonic plate collisions (J F Cassidy, Rogers, and Halchuk 2010). In the Rocky Mountains, the geological record shows three distinct sequences from the Cretaceous period. These sequences indicate the movement of underwater deposits, transitioning from marine shale to deltaic sandstones and conglomerates. They're important sources of coal, oil, and gas (Stott 1984).

The Canadian Shield in the Northwest Territories, Nunavut, Manitoba, Ontario, and Quebec is known for its lakes and rocky landscapes and contains some of the oldest rocks on Earth, forming the core of the continent (Langford 2018). The Appalachian Mountains in southern Quebec were

once as high as the Rockies but have eroded over time (Brooks and Perret 2023). Along the East coast, Newfoundland showcases rocks with ancient multicellular fossils, and the continental shelf in the Atlantic Ocean is covered by thick sediment layers.

3.3. Seismicity of Canada

The GSC, an agency under NRCan, is responsible for studying and documenting earthquakes in the country. Presently, seismologists detect over 4000 earthquakes annually in Canada, but only around 100 of them are noticeable to humans (Ludwin et al. 2007). The majority of these earthquakes are relatively small, with a magnitude below 3, and go unnoticed (Fereidoni 2014). However, Canada has also witnessed numerous significant earthquakes, some occurring in remote regions while others have struck populated areas, resulting in destruction, injuries, and even rare fatalities. These substantial earthquakes generally register a magnitude of 6 or higher (Fereidoni 2014).

The distribution of earthquakes can largely be explained by the tectonic setting. Most earthquakes occur along the active plate boundaries off the west coast. However, significant seismic activity is also observed in the Cordillera region, particularly in the Yukon and Northwest Territories, along the Arctic margin, in the Ottawa and St. Lawrence river valleys, in the northern Appalachians, and along the eastern offshore margin (J. F. Cassidy et al. 2010).The least number of earthquakes occur in the stable craton, including the plains of Saskatchewan and Manitoba. Figure 3.2 shows a map of earthquakes in or near Canada for a period of almost four centuries from 1627 to 2022 and had a magnitude of 3 or higher.

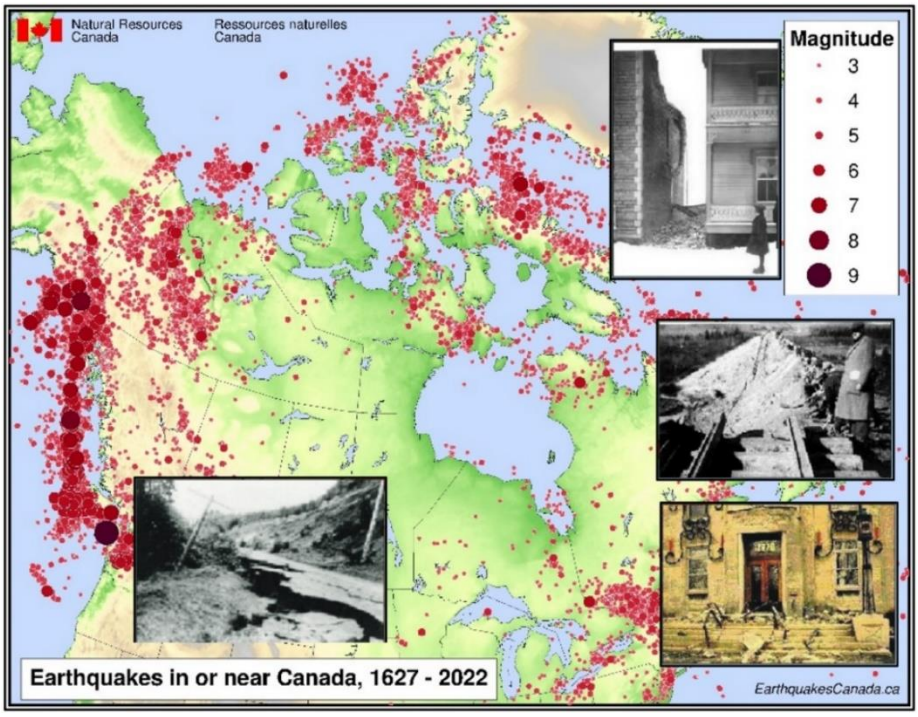

Figure 3.2. Seismic Activity in Canada Over Time. This map illustrates the historical earthquakes that have occurred in or near Canada between 1627 and 2022, with the size of the red circles indicating the magnitude (Source: GSC). It's evident that smaller earthquakes are more frequent compared to stronger ones (N. R. C. Government of Canada n.d.).

Globally, approximately one-third of the world's population is exposed to earthquakes (Pesaresi et al. 2016). In Canada, a similar proportion of people are at risk of experiencing ground shaking that could lead to structural damage, especially in high hazard areas like British Columbia (BC) and Quebec, where the risk is closer to one in two residents (Hobbs et al., 2023). While many Canadians have not witnessed destructive earthquakes, historical events confirm their occurrence (J F Cassidy, Rogers, and Halchuk 2010), and as our population grows and development expands into high-risk zones, this becomes increasingly concerning (Hobbs et al., 2021).

The seismic hazard map in Figure 3.3 shows where the likelihood of experiencing strong ground shaking, measured as Peak Ground Acceleration (PGA), with a 10% chance of happening in 50 years is highest. Average annual loss is the yearly average of expected damages due to earthquake ground shaking for residential, commercial, and industrial buildings, including both structural and non-structural components and contents. The average annual loss ratio for a country or subdivision is the average annual loss divided by the total value of assets that could be replaced in that area.

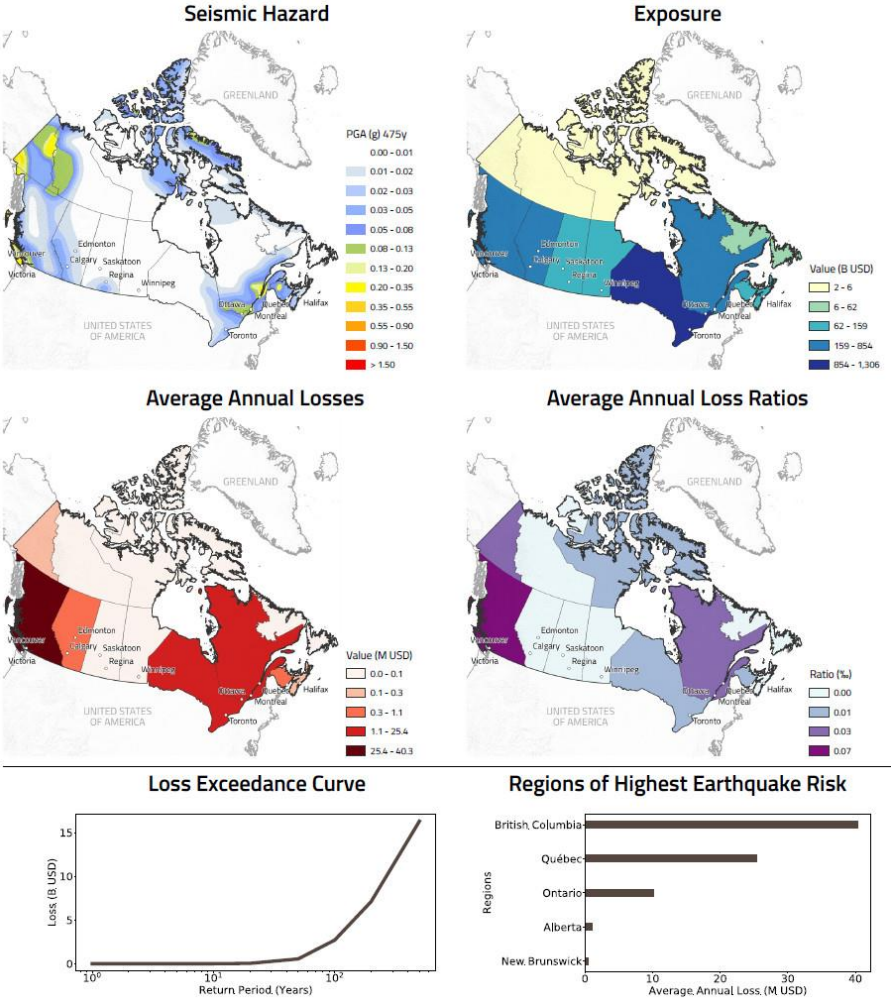

Figure 3.3. Seismic hazard map, national exposure model, average annual economic losses and loss ratio of Canada (Nations n.d.). These maps, found in country profiles, are based on the 2018.1 version of the Global Seismic Hazard Map from GEM (Silva et al. 2020).

The 200-year return period loss represents the average expected loss due to earthquake ground shaking for buildings (structural and non-structural) and contents, but it's something that is anticipated to occur or be exceeded roughly once every 200 years. This country profile relies on the most reliable and publicly accessible data and models. The seismic hazard, exposure, and vulnerability models used were either supplied by national institutions or developed through regional programs and collaborations (Hobbs et al. 2023).

3.4. Earthquake zones in Canada

In essence, earthquake zones are areas where earthquakes frequently occur due to a common underlying cause. These areas are known as seismic zones and are crucial for assessing earthquake risks (Heidebrecht 1995).

3.4.1. Earthquake zones in western Canada

The largest and most frequent earthquakes happen along the west coast, primarily associated with plate motions and active faults (Bostwick 1984). Seismologists from the GSC monitor and locate over 1000 earthquakes annually in western Canada, with the Pacific Coast being the most susceptible region (Bent et al. 2018). In the past 70 years, more than 100 earthquakes with a magnitude of 5 or higher have occurred offshore west of Vancouver Island (Lochead, Gillespie, and Hand 2012). These earthquakes could have caused significant damage if they had been closer to land (Fowler et al., 1990).

The Queen Charlotte Fault, where the Pacific and North American plates separate, experienced Canada's largest recorded earthquake in 1949 (Lay et al. 2013). The Cascadia Subduction Zone, off the west coast from Vancouver Island to northern California, generates various types of earthquakes due to the Juan de Fuca plate subducting beneath North America. The Juan de Fuca and North America plates are currently locked together, causing strain and leading to both small and potentially destructive earthquakes, which are known as "megathrust", occur approximately every 300-800 years along this coast (Walker et al. 2021).

Other earthquake-prone regions in Western Canada include the St. Elias Region and the Southwestern Yukon, where significant seismic activity has been observed (Bruhn et al. 2012), and the Northern Cordillera, which experienced its largest recorded earthquake with Mw 6.9 in 1985 (John F. Cassidy, Rogers, and Ristau 2005). The Southern Cordillera, located south of the 60th parallel, has decreased seismic activity, with the most powerful earthquake occurring in 1918 (Gutenberg 2013). Finally, the Interior Platform, below 60 N latitude, focuses on southern Saskatchewan, where seismic activity is concentrated, and notable earthquakes, including those related to potash mining, have been documented (Bakun, Stickney, and Rogers 2011).

3.4.2. Earthquake zones in eastern Canada

Eastern Canada, situated on the stable North American Plate, generally experiences fewer earthquakes than the western region. Despite its stability, significant and potentially destructive earthquakes have occurred and are anticipated in the future. On average, about 450 earthquakes transpire annually in eastern Canada, with four exceeding Mw 4, thirty surpassing Mw 3, and approximately twenty-five being perceptible (Sadegh 2012).

Unlike areas near plate boundaries where seismic activity is directly linked to plate interactions, eastern Canada, situated in the stable interior of the North American Plate (refer to Figure 3.1), sees seismic activity influenced by regional stress patterns. Clusters of earthquake activity have been identified, occurring at depths ranging from the surface to 30 km (Asgharzadeh Sadegh 2012). Several specific earthquake zones exist in eastern Canada. Northern Ontario experiences minimal seismic activity, with only one or two earthquakes of Mw 2.5 or higher recorded between 1970 and 1999 (Agrawal 2018). The Southern Great Lakes region encounters relatively few and mild earthquakes, with only three moderate-sized earthquakes (Mw 5) in the past 250 years (Dineva, Eaton, and Mereu 2004). The Charlevoix-Kamouraska Seismic Zone near Quebec City is highly active, considered the highest earthquake risk area in eastern Canada. Earthquakes happen there approximately every day and a half due to geological faults in the Canadian Shield (Brooks and Perret 2023).

The Lower St. Lawrence Seismic Zone, along the St. Lawrence River east of Quebec City, is active but hasn't experienced major earthquakes like the Charlevoix Seismic Zone. It sees around 60 smaller earthquakes annually within a defined area (Maurice Lamontagne et al. 2004). The Northern Appalachians Seismic Zone, spanning from New Brunswick to Boston, experienced notable earthquakes in 1982 in central New Brunswick (Wetmiller et al. 1984). The Laurentian Slope Seismic Zone, off the southeastern coast of Canada, including the Grand Banks of Newfoundland, saw a powerful earthquake in 1929 with Mw 7.2, causing a destructive tsunami (Hasegawa 1991).

The Western Quebec Seismic Zone covers a large area, including Montreal, Ottawa, and Eastern Ontario (Hunter et al. 2010). It consistently experiences earthquakes, including historical events like the 1732 Montreal earthquake (Mw 5.8) and the 1935 Temiscaming earthquake (Mw 6.2). Recent earthquakes in this zone include a 1990 Mw 5 quake near Mont-Laurier (Lamontagne 2002).

3.4.3. Earthquake zones in northern Canada

In Northern Canada, earthquake risk is generally low in the central region, but moderate seismic activity is estimated in the Arctic areas (Milne and Davenport 1969). A 2021 study in northwestern Canada by Estève et al. used local earthquakes to examine the Earth's crust and upper mantle, creating a 3D model of seismic velocity (Estève et al. 2021). The study noted changes in the shape of the northwestern North American craton edge, suggesting subduction of a segment of the Pacific plate beneath the Wrangell volcanic field in southeastern Alaska. These findings have significant implications for understanding the tectonic evolution of the northern Canadian region (Estève et al. 2021).

3.5. Analysis of recent earthquakes as case studies

This thesis examines a total of five previous earthquakes to determine whether their observed impacts match those anticipated by CanSRM1: two in eastern Canada, two in western Canada, and one in northern Canada. The geographical location of these earthquakes is provided in Figure 3.4.

Table 3.1 presents a compilation of noteworthy earthquakes that have occurred in Western, Northern, and Eastern Canada, which have been selected as the focus of study for this thesis.

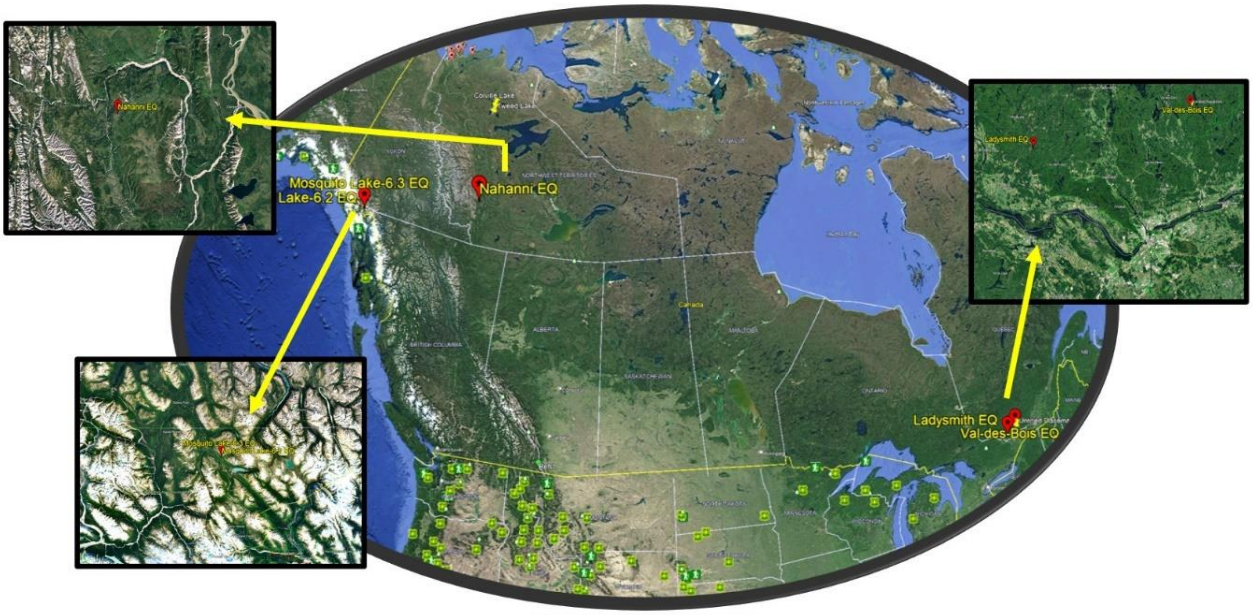

Figure 3.4. Location of the selected sites where the interested earthquakes occurred. This figure highlights 2 earthquakes in eastern Canada, namely Val-des-Bois and Ladysmith, as well as 2 earthquakes in western Canada known as the Mosquito Lake pair earthquakes, and 1 earthquake in northern Canada, referred to as Nahanni. Background images sourced from Landsat 8 and Google Earth.

Table 3.1. Overview of past earthquakes employed as research locations in this thesis, (Feng et al. 2019, 201), (He et al. 2018), (Bent et al. 2015), (Mitchell, Tinawi, and Law 1990), (Perret et al. 2017).

Year	Lat (°N)	Long (°W)	Mw	Depth (km)	Location	Region	MMI	Comment
2017	59.87	136.66	6.2	5.1	West Canada	Mosquito Lake, Alaska (near Whitehorse) Northwest British Columbia; 109 km SE of Haines Jct.	VI	Widely felt in B.C., localized damage, no landslide, no tsunami, no deaths
2017	59.87	136.66	6.3	2.5	West Canada	Mosquito Lake, Alaska (near Whitehorse) Northwest British Columbia; 109 km SE of Haines Jct.	V	Widely felt in north-western B.C., localized damage, associated landslide, no tsunami, no deaths
2013	45.74	76.34	4.6	13.5	East Canada	Ladysmith, Southwest Quebec	VII	Widely felt, most damaging quake in western Canada, no landslide, no tsunami, no deaths
2010	45.88	75.48	5.0	22.1	East Canada	Val-des-Bois, Southwest Quebec	VIII	Widely felt, minor damage, associated landslide, no tsunami, no deaths
1985	62.21	124.22	6.9	5	North Canada	North Nahanni River, Northwest Territories.	IX	Widely felt, minor damage, associated landslide, no tsunami, no deaths

3.5.1. Earthquakes in the west

In May 2017, a pair of earthquakes with Mw 6.2 and 6.3, referred to as EQ 1 and EQ 2, occurred in the southern Yukon Territory and Alaska, near the U.S.-Canada border, near the junction of the

eastern Denali fault and Duke River fault. EQ 1 was a reverse fault event and EQ 2 was a strike-slip event (He et al. 2018). Figure 3.5 illustrates the tectonic environment and seismic events in Southeastern Alaska.

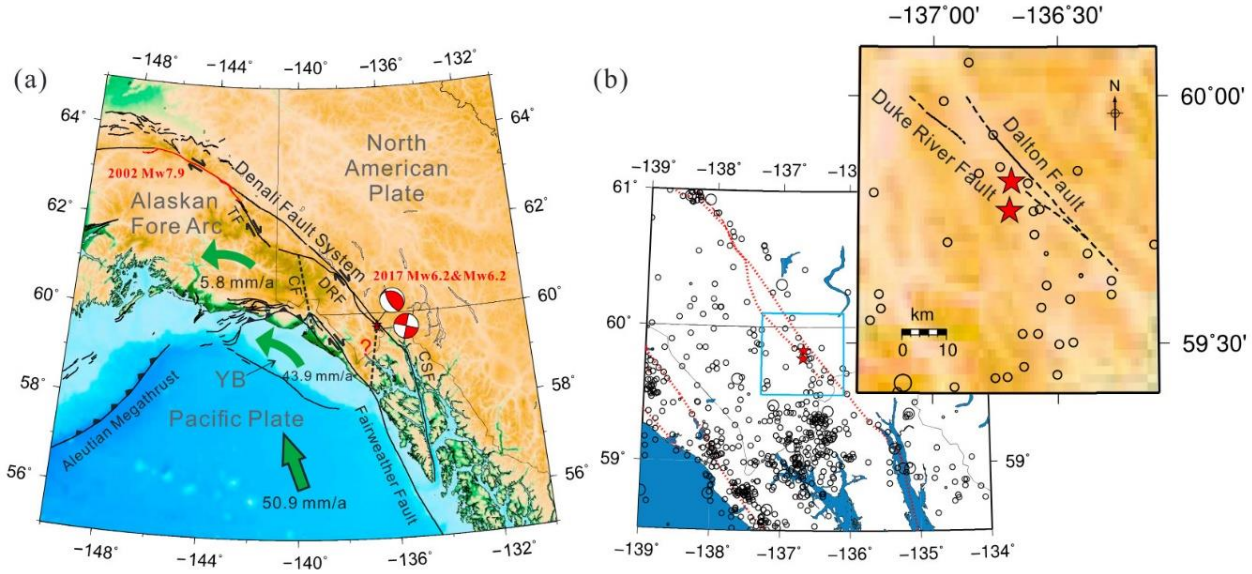

Figure 3.5. Overview of Southeastern Alaska's Tectonic Setting and Seismic Activity. a) Representation of the 2017 MW6.2 and MW6.3 earthquake doublet using beach balls, with red lines indicating surface rupture from the 2002 Denali earthquake. Arrows indicate tectonic motion relative to the North American Plate, based on studies by DeMets & Dixon (1999), Leonard et al. (2007, 2008). b) Historical seismic activity (M5+ since 1900 and M2.5+ since 1973) sourced from USGS-PDE and ISC-GEM catalogs, along with major Quaternary faults. Solid, dashed, and dotted lines represent well-constrained, approximate, and inferred faults. Red stars denote the British Columbia earthquake doublet. The inset in the top right corner offers a closer view of the region outlined in the blue box (Doser and Rodriguez 2011).

3.5.1.1. 2017: Mw 6.2 - 47 km NW of Mosquito Lake, Alaska, pair earthquakes: Western Canada

On May 1, 2017, at 12:31:55 (UTC), there was an earthquake designated as EQ 1. It occurred at around [59.821° N, 136.711° W] coordinates and had a Mw of 6.2. The earthquake's hypocenter was located approximately 5.1 kilometers below the Earth's surface (U. S. Geological Survey 2017). There have been no reports of landslides or tsunamis associated with this earthquake. Because of the sparse population in the affected areas, there were no reported casualties or significant economic losses, with only isolated damages observed in the surrounding areas of the earthquakes (Feng et al. 2019). The earthquake had an estimated intensity of VI and was strongly felt in several areas, including Whitehorse, Haines Junction, Atlin, Teslin, Carmacks, and Watson Lake (He et al. 2018). Additionally, there were avalanches triggered near Mount Logan, and there was also another earthquake, with Mw 6.3, following the initial earthquake.

3.5.1.2. 2017: M 6.3 - 48 km NW of Mosquito Lake, Alaska, pair earthquakes: Western Canada

Two hours later, the second earthquake (EQ 2) occurred at 14:18:15 (UTC), 1.3 km northeast of the location of EQ 1 with a Mw of 6.3 (He et al. 2018). The earthquake's hypocenter was located approximately 2.5 kilometers below the Earth's surface. Some avalanches and landslides were observed during a field survey conducted two months later by the Yukon Geological Survey (U. S. Geological Survey 2017).

These 2017 earthquakes were notable as the largest seismic events in the northern Canadian Arctic region in recent years. They occurred in a tectonically complex area between the Duke River and Eastern Denali faults, driven by the collision of the North American and Pacific plates (He et al. 2018). This collision has caused significant crustal deformation and seismic activity in the region. The Denali fault, a major strike-slip fault, is active in this region and has experienced substantial displacement over millions of years (Feng et al. 2019, 201).

3.5.2. Earthquakes in the east

3.5.2.1. 2010: Mw 5.0 Val-des-Bois earthquake: Eastern Canada (SW Quebec)

On June 23, 2010, a significant earthquake with Mw 5.0 struck Val-des-Bois, Quebec at 13:41:41 (EDT). This earthquake was located about 60 kilometers north of Ottawa, at a depth of 22 kilometers (Perret et al. 2017). It had a northwest-striking thrust motion and was notable for its widespread effects, spanning approximately 3 million square kilometers. This impact extended beyond its epicenter, affecting regions in Quebec, Ontario, and several U.S. states, from Maine to Illinois and Kentucky (Ma and Motazedian 2012). What made this earthquake particularly significant was that it resulted in the strongest shaking ever recorded in Canada's capital city, Ottawa, and it generated an unprecedented response on the “Did You Feel It?” online platform, with over 57,000 reports from individuals who experienced the tremors (Marano, Wald, and Allen 2010).

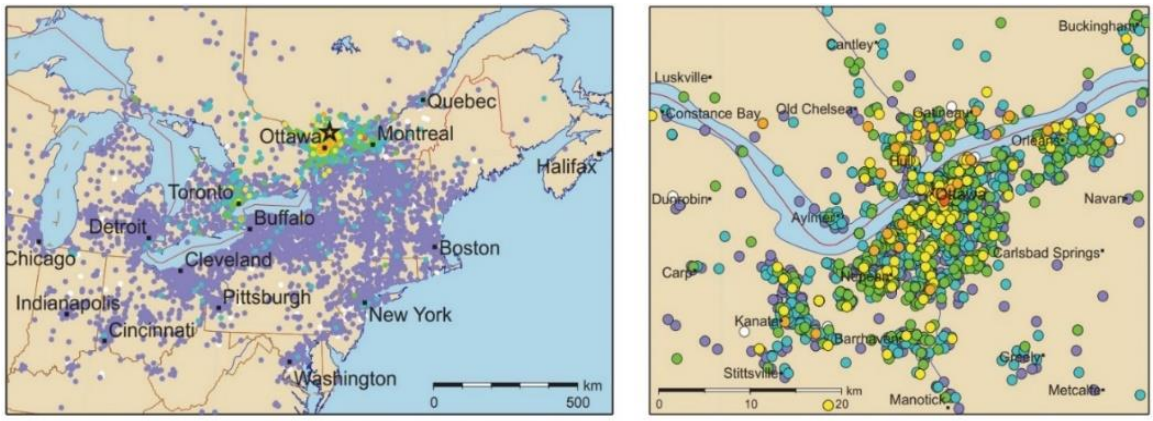

INTENSITY	I	II - III	IV	V	VI	VII	VIII	IX	X+
SHAKING	Not felt	Weak	Light	Moderate	Strong	Very Strong	Severe	Violent	Extreme
DAMAGE	none	none	none	Very light	Light	Moderate	Moderate/Heavy	Heavy	Very Heavy

Figure 3.6. Intensity map of the 2010 M 5.0 Val-des-Bois Earthquake based on the number of reports received by the GSC and U.S. Geological Survey via their 'Did You Feel It?' online forms in response to the Val-des-Bois mainshock (reprinted from Marano, Wald, and Allen 2010).

In terms of seismic significance, the Val-des-Bois earthquake marked a major event in southeastern Canada and the northeastern United States since the 2002 earthquake in Au Sable Forks, New York, which also had Mw 5.0. The Val-des-Bois earthquake was measured at intensity level VIII on the MMI scale (CBC News, June 23, 2010). It caused minor damage to structures within the epicenter area, including a damaged church steeple and cracked masonry (Marano, Wald, and Allen 2010). Damage was also recorded in Ottawa, where buildings such as City Hall

suffered broken windows, and numerous structures, including the Parliament buildings, had to be evacuated. Additionally, there was some damage to roads and bridges in the epicenter area, primarily attributed to embankment failures (Perret et al. 2017).

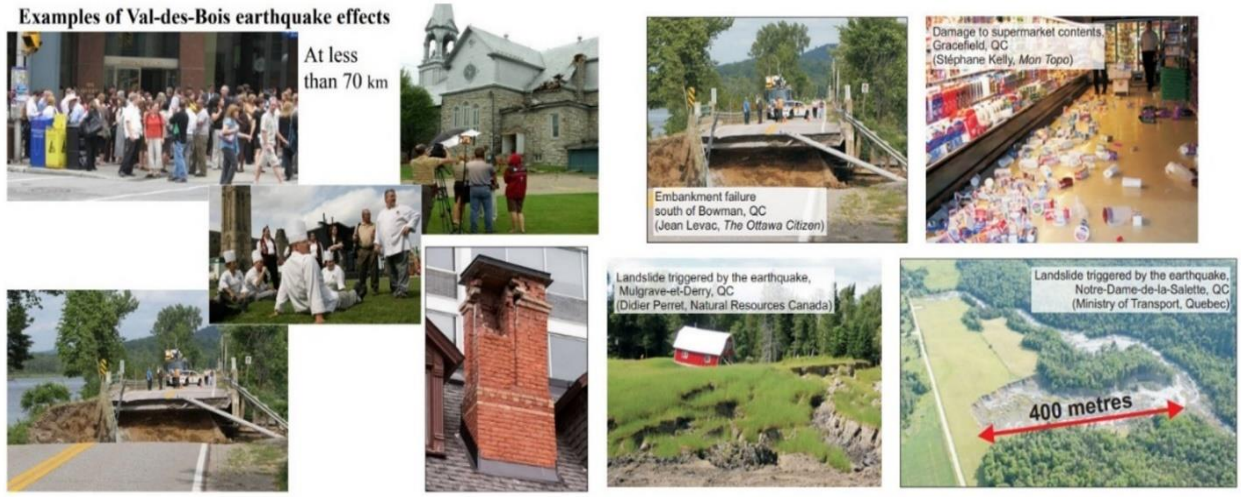

Figure 3.7. Visualizing the Impact of the 2010 M 5.0 Val-des-Bois Earthquake on buildings and infrastructures (News · 2011), (N. R. C. Government of Canada n.d.).

From a scientific perspective, the Val-des-Bois earthquake provided an extensive dataset for analysis. It involved 120 instrumental recording stations within a 1,000-kilometer radius of the epicenter, including nine stations with detailed three-component records at distances less than 100 kilometers (Perret et al. 2017), which is illustrated in Figure 3.8. These contours are created using MMI values derived from the recorded Peak Ground Velocity (PGV) data.

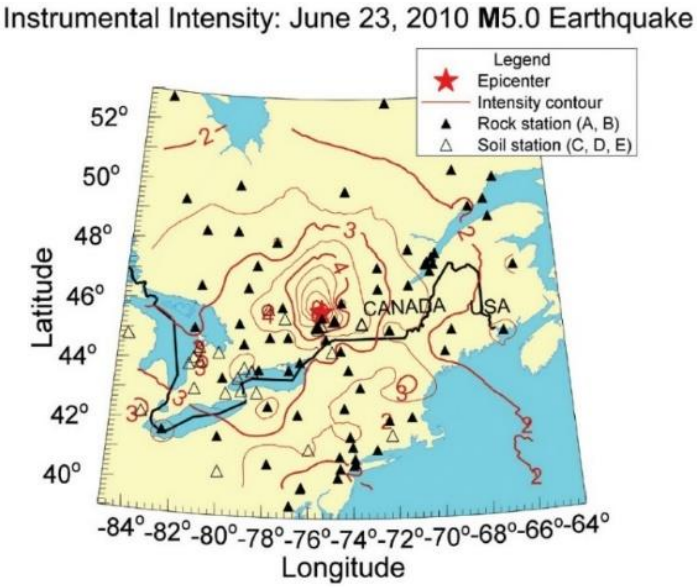

Figure 3.8. Visualizing Ground Motion: Mapping the Impact of the 2010 M 5.0 Val-des-Bois Earthquake. Station locations are marked with symbols, while contour lines represent MMI values derived from recorded PGV data, following the methodology of Atkinson and Kaka (2007) (Earthquake Engineering Research Institute n.d.).

3.5.2.2. 2013: Mw 4.6 Ladysmith earthquake: Eastern Canada (SW Quebec)

On May 17, 2013, at 09:43 Eastern Daylight Time (13:43 Coordinated Universal Time), there was a moderate earthquake with Mw 4.6 in Shawville, southwestern Quebec, near Ladysmith (Esmaeilzadeh and Motazedian, n.d.). This earthquake was felt across a wide area, from Montreal to Toronto, and even as far as New York and Vermont. While it didn't cause significant damage, some buildings developed cracks, and there were minor rockfalls (Bent et al. 2015). After the main earthquake, there were several aftershocks, with the largest one having Mw 3.6 occurring about 10 minutes later. This aftershock sequence was unusual because there were many relatively large aftershocks (Ma and Audet 2014). A total of 46 aftershocks were recorded up until March 2014.

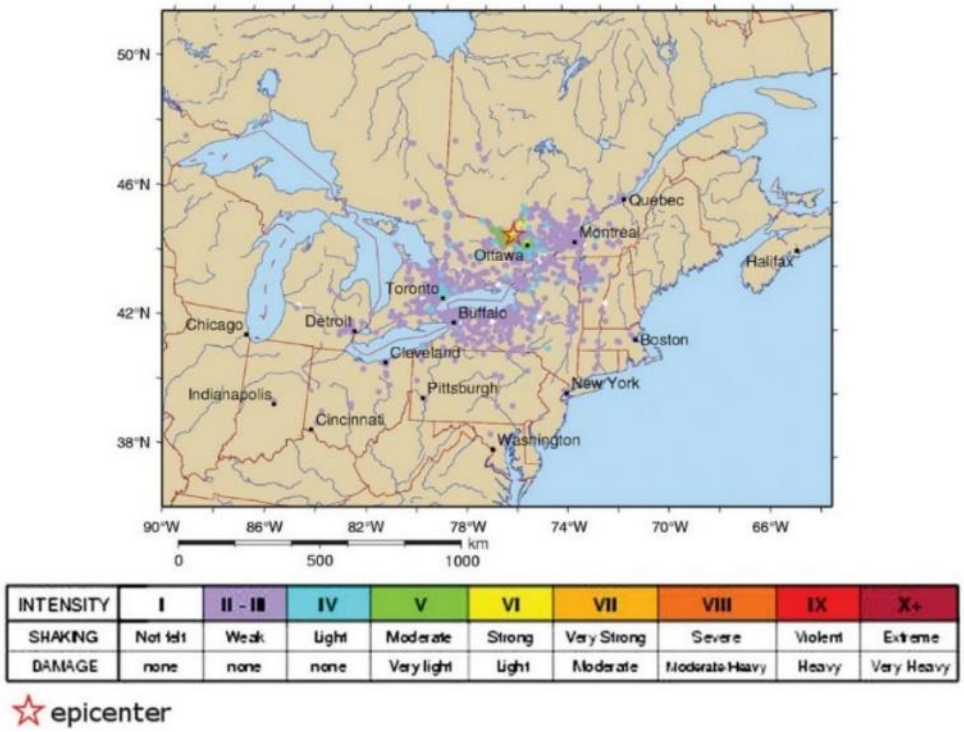

Figure 3.9. Intensity map of Ladysmith earthquake based on the number of reports received by the GSC and U.S. Geological Survey via their 'Did You Feel It?' online forms in response to the Ladysmith mainshock. A total of 4,273 reports were submitted (J F Cassidy, Rogers, and Halchuk 2010).

The earthquake took place in the western Quebec seismic zone, an area known for moderate earthquake activity. The Canadian National Seismograph Network (CNSN) and U.S. Transportable Array (USTA) stations recorded the event extensively, allowing for detailed analysis. The earthquake resulted from thrust faulting on a northwest-striking plane and had a depth estimated to be between 12 and 15 kilometers (Bent et al. 2015).

The strong-motion data from this event contributed to a study on soil amplification and basin effects. The earthquake was felt over a vast distance, with more than 4300 people filling out a "Did You Feel It?" survey online, providing valuable information on its effects (Bent et al. 2015). Visits to Ladysmith and nearby areas showed minor damage, mostly limited to the epicentral region. While the earthquake's correlation with known faults in the region is challenging to establish, some

local-scale features in the epicentral area trend similarly to the nodal planes of the earthquake's focal mechanism.

3.5.3. Earthquakes in the north

3.5.3.1. 1985: M 6.9 Nahanni earthquake: Northern Canada (Northwest Territories)

Between 1985 and 1988, a series of earthquakes occurred in the northern Canadian Cordillera, in the Mackenzie Mountain range, with the main event being the M 6.9 Nahanni earthquake on December 23, 1985, followed by another M 6 event in 1988 (Mitchell, Tinawi, and Law 1990). These earthquakes were felt up to a distance of 1500 km, but since no community was closer than 100 km to the epicenters, no major structural damage was reported (J. F. Cassidy et al. 2010). However, there were noticeable effects such as ground rolling, vehicle bouncing, and tree and power line movements in the area. The Mackenzie River also experienced slumping of its banks, and homes had furniture displacement and other disturbances (M. Lamontagne, Halchuk, and Adams, n.d.).

The December 23 earthquake triggered a large rock avalanche, resulting in a significant landslide (Choy and Boatwright 1988). Aftershocks reveal that the earthquake sequence involved thrusting along a shallow fault that was 50 km long and 15 km wide, dipping towards the west (Wetmiller et al. 1988). This quake was the strongest of a series of earthquakes that took place in the region in the last months of 1985.

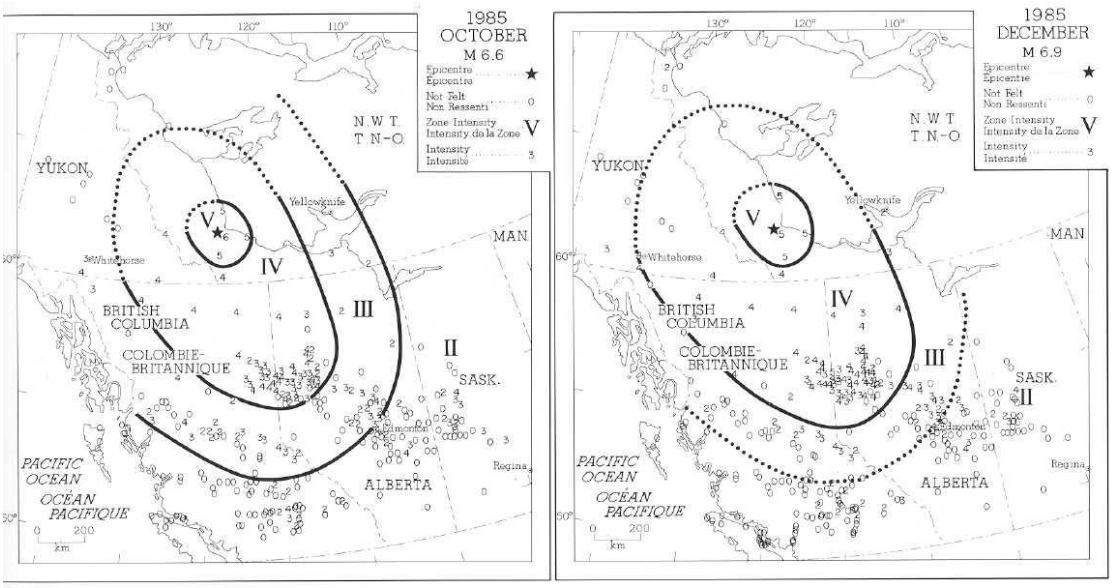

Figure 3.10. Modified Mercalli Intensity Scale Map Showing Impact Zones of Two Major Earthquakes, Graded by MMI Scale from Minor Tremors (I) to Total Devastation (XII) (J F Cassidy, Rogers, and Halchuk 2010).

The earthquake had an estimated intensity of IX and was felt in areas including the western Northwest Territories, southeastern Yukon, northern Alberta, and British Columbia. It resulted in significant landslides, rockfalls, and a major rock avalanche at the epicenter, with around 5 to 7 million cubic meters of rocks tumbling 1.6 kilometers from the top to the bottom of the slope. Numerous aftershocks were documented in the months that followed by (Horner, Lamontagne, and Wet-miller 1987).

Chapter 4 : Methodology and Theory

4.1. Introduction

The chapter focuses on the research methodology and procedures employed to achieve the objectives outlined in the first chapter. The methodology begins by outlining the workflow used to assess the CanadaSRM1. It then introduces the input parameters used in this dissertation, followed by an explanation of the various data processing procedures. Meanwhile, it offers a comprehensive overview of the theoretical concepts employed in seismic risk analysis, which includes seismic risk assessment, ground motion intensity, exposure model and building inventory collection, vulnerability and fragility functions, uncertainties, and a brief description of the OQ Engine, the software utilized in this thesis.

4.2. Methodology of seismic damage and risk assessment for model validation

In Canada, there is a lack of useful events for validating seismic risk models, as the last significantly damaging earthquakes occurred in the 1980s (Hyndman and Rogers 2010). Therefore, this study focuses on the benchmarking of CanadaSRM1, using shaking intensities and physical impacts recorded from a few recent earthquakes in various regions of Canada (west, east, and north) that are not featured in prominent databases and resulted in minor damage. These include the Mosquito Lake earthquakes in 2017 out west Canada in the northwestern corner of British Columbia, the Val-des-Bois earthquake in 2010 and the Ladysmith earthquake in 2013 out east Canada in the southern margin of Quebec, as well as the Nahanni earthquake in 1985 out north Canada in the south of Northwest Territories.

For recent events, acquired shaking data, including shakemaps, exposure models, and vulnerability-fragility models, is employed. The shaking data is then input into the CanadaSRM1 model to calculate expected building damage and financial losses. These outcomes are compared with the observed impacts from the five recent events. All monetary values are in Canadian Dollars (CAD), unless stated otherwise. Notably, it doesn't include any secondary hazards due to computational challenges or data limitations in Canada. The methodology of validation CanadaSRM1 is visually represented in Figure 4.1, illustrating each step of the process. Furthermore, the step-by-step description of this figure is provided in detail in the subsequent sections of this thesis.

4.2.1. Step 1: Data collection

Risk assessment requires three input layers: the seismic hazard model, exposure model, and vulnerability or fragility functions. USGS shakemaps are used as the Ground Motion Field (GMF) (Silva and Horspool 2019) (Hazus-MH 2003) for damage and loss calculations in this thesis. A national exposure model (Journeay et al. 2022) is used, and adjusted fragility and vulnerability curves are derived from the CanadaSRM1 curves, focusing on functions dependent on a Spectral Acceleration (SA) of 0.6 seconds (Hobbs et al. 2022). As a result, the initial step involves the preparation of these input layers, as elaborated in detail on in Section 4.4.

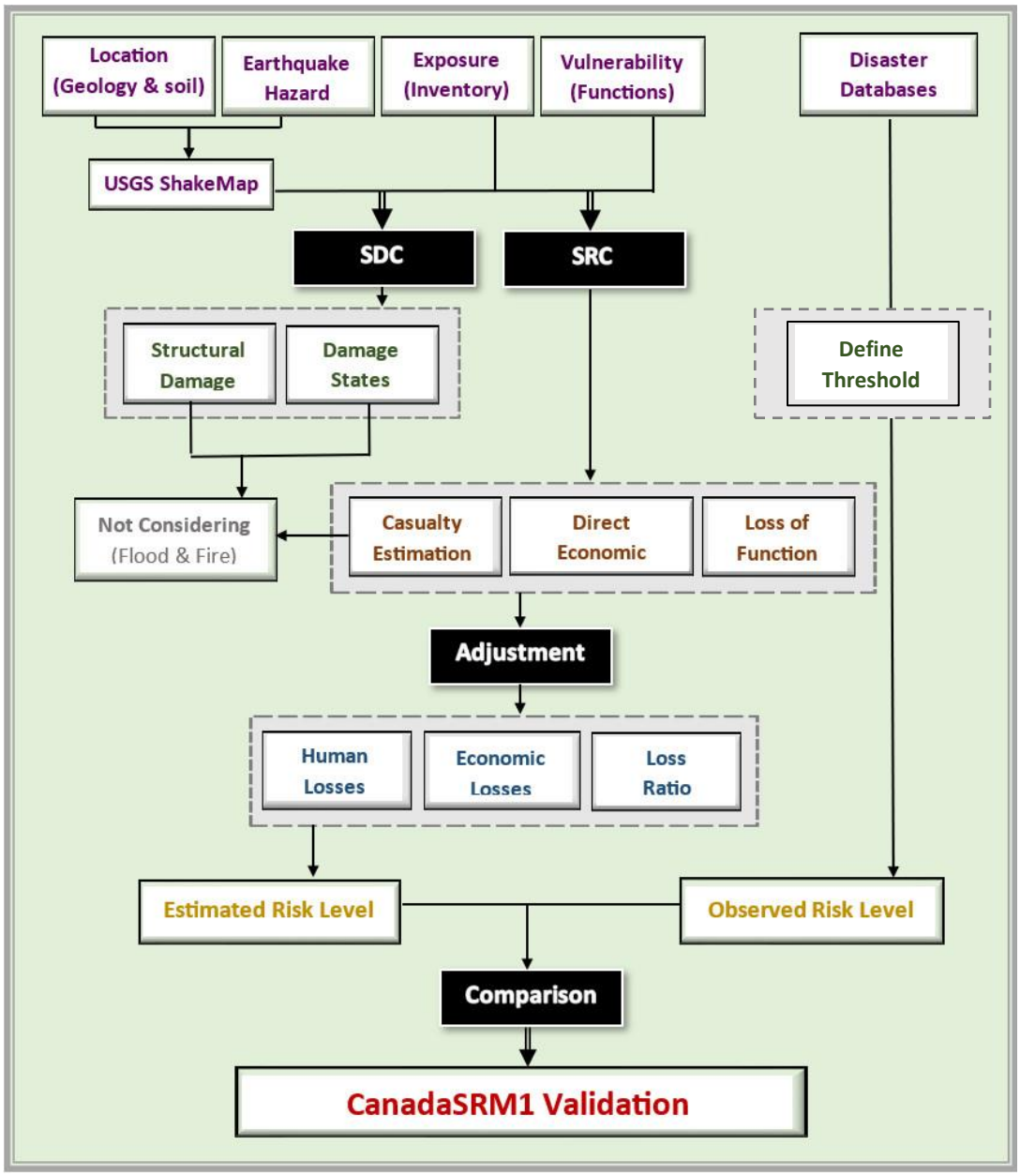

Figure 4.1. Methodology outline for validating the seismic risk model (CanadaSRM1). The diagram outlines key steps, including data collection, model development, and validation techniques. SDC and SRC refers to OQ calculators, which stands for Scenario Damage Calculator and Scenario Risk Calculator, respectively.

4.2.2. Step 2: Structural damage assessment

In this step, after the preparation of three input layers, SDC is conducted for each of the five earthquakes. The total damage resulting from these events, encompassing all stages of damage (no-damage, slight, moderate, extensive, and complete damage), are determined from the SDC.

4.2.3. Step 3: Loss estimation

Subsequently, the process is repeated for scenario risk assessment (SRC), and losses incurred by structural and non-structural elements, contents, and occupants are computed through the utilization of SRC in OQ Engine.

4.2.4. Step 4: Result correlation and adjustment

The financial losses and fatalities calculated in step 4 are based on data from 2016 (Journeay et al. 2022). Consequently, to establish a dependable basis for comparing the estimated outcomes with actual observed data for the respective earthquake years, the results derived from SRC must be modified to align with the year of each earthquake's occurrence. This adjustment involves accounting for the inflation rate from the year of each earthquake's occurrence to 2016 and incorporating the population growth rate to adjust the fatalities.

4.2.5. Step 5: Comparison and model verification

The CanadaSRM1 model is validated in the final step by comparing the actual losses from five earthquakes to the estimated retrospective losses for these events, using the CanadaSRM1 model. The observed or actual impacts of these events were determined by referring to reported and documented information from disaster databases such as EM-DAT, CDD, and CatIQ, as detailed in Chapter 6. It should be noted that the calculations of losses were restricted to the Canadian side of the border, in line with the primary focus of this work on the Canadian risk model.

4.3. Seismic risk assessment

Risk refers to the potential damages and anticipated losses expected from a specific hazard in a specific area within a certain time frame (Coordinator 1980). When it comes to seismic risk, it pertains to the probability of damage or losses resulting from potential future earthquakes. It can be represented by the spatial and temporal combination of three factors: hazard, vulnerability, and exposure. Seismic hazard quantifies the likelihood of earthquakes or ground motions occurring at specific location (Hosseinpour et al. 2022) and is obtained through DSHA/ PSHA.

Fragility/vulnerability curves are used to describe the seismic vulnerability of structures, indicating the probability of various damage/risk levels based on the seismic intensity (Karaca and Luco 2008) (Porter 2015). Exposure pertains to man-made environment and all assets subjected to seismic risk in a particular region (Journeay et al. 2022), and in the case of buildings, it requires a building inventory with information on the number of buildings, residents, and their distribution across different vulnerability classes (Sabetta et al. 2023).

$$\boldsymbol{Risk} = \boldsymbol{hazard} * \boldsymbol{vulnerability} * \boldsymbol{exposure} \qquad (4\text{-}1)$$

4.4. Input data sets

The subsequent sections outline the fundamental elements needed to calculate risk, encompassing exposure models, fragility models, and vulnerability models.

4.4.1. Seismic hazard model

Seismic hazard, which is typically quantified as the anticipated intensity of ground shaking over a defined timeframe, is indicative of the threat posed by earthquakes in a particular region.

4.4.1.1. Probabilistic seismic hazard assessment (PSHA)

The PSHA estimates ground motions with a specific probability of exceedance for the intermediate term, considering all potential seismic sources. The Probability of Exceedance (PE) quantifies the likelihood of surpassing a specific loss value in the future (Wyss and Toya 2000). PSHA assumes earthquakes follow a Poisson distribution in time and space (Baker 2008). A logic tree weighs different models, producing hazard curves, uniform hazard spectra, and hazard maps. OQ Engine offers two calculators: the Classical PSHA for seismic design codes and the Event-based PSHA for risk assessment, both generating valuable outputs for understanding and mitigating seismic risks (Pagani et al. 2023).

4.4.1.2. Deterministic seismic hazard assessment (DSHA)

The effects of a single earthquake scenario are analyzed by DSHA, characterizing each event by magnitude, hypocenter, fault information, and rupture type. Unlike PSHA, DSHA uses a single value per parameter and employs a ground shaking intensity model based on macroseismic intensity and strong motion records (Pagani et al. 2023). This scenario-based approach results in a GMF that assigns a ground motion measure to each location.

DSHA calculates ground motions using attenuation equations, considering earthquake wave propagation and local site conditions. Both DSHA and PSHA methods contribute to seismic hazard assessments, offering complementary insights (TOOLKiT 2015). The OQ Engine 's scenario calculator generates a stochastically based GMF for a single seismic event, incorporating seismic source characteristics, rupture-produced GMF, and site effects (refer to Figure 4.2). This GMF informs the intensity of shaking in the study area (Bay et al. 2005).

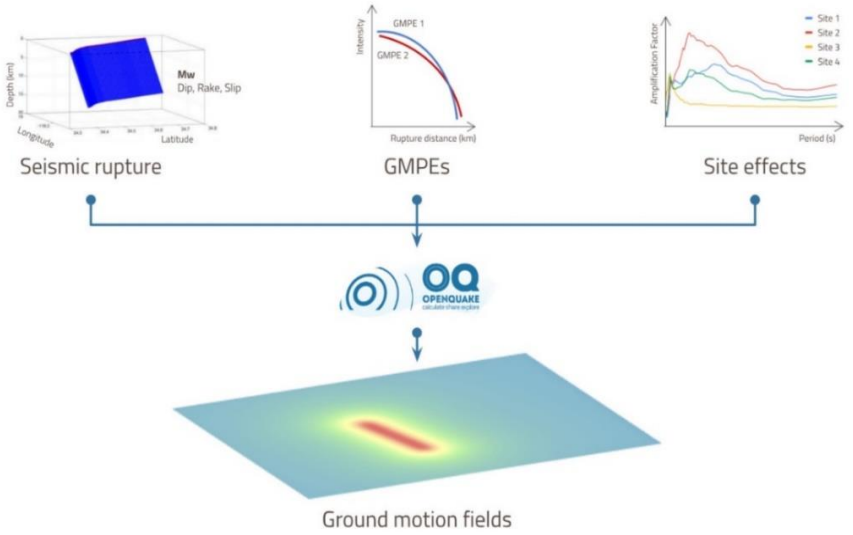

Figure 4.2. OQ Engine scenario hazard calculator, showcasing its functionality with three key inputs—seismic rupture, GMPEs, and site effect curves. The resulting output is a comprehensive seismic hazard model presented in the form of GMFs (Global Earthquake Maps | Global Earthquake Model Foundation | Italy n.d.).

4.4.1.3. Seismic source characteristics

Seismic hazard assessment evaluates the likelihood of potentially destructive events occurring over time, specifically earthquakes. When dealing with earthquakes, this process includes estimating how often various magnitudes of earthquakes might occur from active faults in the area of concern and assessing the level of ground shaking they could produce. To describe the seismic source, the initial step involves identifying the type, geometry, and location of seismic faults, along with the factors associated with their potential rupture (Hobbs et al. 2023).

Fractures or breaks in the Earth's crust, known as faults, result from compressional or tensional forces, causing movement between rocks on opposite sides. These fractures vary in size and displacement, ranging from centimeters to hundreds of kilometers (McGuire 2004). Faults create planes of discontinuity, allowing independent movement of adjacent blocks. Earthquakes, occurring along faults, stem from seismic activity. During seismic events, only a portion of the fault breaks, termed a rupture, representing the movement within the Earth's crust. Seismic hazard modeling often simplifies ruptures as flat features in earthquake analysis (Pagani et al. 2014).

4.4.1.4. Ground motion parameters and intensity metrics

The spatial distribution of ground shaking generated by a rupture event, known as the GMF, is characterized by intensity levels at places of interest relative to the distance from the epicenter. The modeling of GMFs, calculated using GMPEs, is employed to estimate the anticipated ground shaking resulting from earthquakes. These estimates are based on the characteristics of the rupture and the distances to sites within the study area (Hobbs et al. 2022).

- **Intensity metrics**

Ground motion parameters, such as PGA and PGV, must be transformed into an earthquake intensity scale for damage assessments. PGA suits shorter buildings, correlating well with their design, while PGV is relevant for taller structures, posing a challenge in linking velocity to force for design purposes (Trifunac and Brady 1975). SA, used in seismic analysis, models the impact on buildings during an earthquake. Despite its potential, the relationship between SA and design force is more intricate than that of PGA due to the influence of vibration period (Atik et al. 2010).

While PGA, PGV, and SA provide approximations for building demand/design, their accuracy is complicated by the diverse vibration modes of buildings (Bay et al. 2005). Some research suggests that nonlinear response weakly depends on earthquake magnitude and distance, favoring SA as a potentially more reliable index for demand/design.

Intensity, denoting the effects of an earthquake on structures, differs from magnitude scales. Unlike Richter Magnitude and Moment Magnitude, which measure energy release, intensity offers a qualitative assessment of damage (Wald et al. 1999). Shaking intensity can be portrayed using metrics like PGA or SA or non-mathematical scales like MMI, as outlined in Table 4.1.

Table 4.1. Ground motion parameters (intensity measure types) used to quantify shaking hazard.

Acronym	Intensity measure type	Units	Description
MMI	Modified Mercalli Intensity	Roman numeral	A discrete scale that indicated the severity of earthquake effects
PGA	Peak Ground Acceleration	$[m/s^2]$, $[\%g]$	The highest acceleration experienced on the ground
PGV	Peak Ground Velocity	$[m/s]$, $[cm/s]$	The highest velocity experienced on the ground
SA (T)	Spectral Acceleration	$[m/s^2]$, $[\%g]$	The acceleration experienced by a structure with natural vibrational period T
…	…	…	…

Researchers commonly employ MMI scale for assessing damage in terms of intensity (Langhammer et al. 2006), as indicated by equations (4-2) and (4-3).

$$\boldsymbol{II = 3.66(PGA) - 1.66} \quad \textit{(4-2)}$$

$$\boldsymbol{II = 3.47(PGV) - 2.35} \quad \textit{(4-3)}$$

where, II denotes Instrumental Intensity, PGA is measured in cm/s^2, and PGV is measured in m/s.

For intensities lower than VII, it is recommended to use a relationship based on acceleration, while for intensities greater than VII, a relationship based on velocity should be used. The provided equations and Table 4.2 allow for quick conversion from PGA or PGV to the Instrumental Intensity scale. While intensity to peak ground motion relationships have been developed for various regions, there are no specific ones available for whole Canada. Therefore, relationships based on strong motion data from other regions, such as those proposed by Neumann in 1945 (Neumann 1954), Trifunac and Brady in 1975 (Trifunac and Brady 1975), McCormack and Rad in 1997 (McCormack and Rad 1997), and Wald in 1999 (Wald et al. 1999) using equations (4-2) and (4-3), are currently being used by the USGS to rapidly generate earthquake intensity maps ("SHAKEMAP") for earthquakes worldwide.

Table 4.2. Instrumental intensity scale based on MMI scale, PGA, or PGV (Wald et al. 1999).

PERCEIVED SHAKING	Not felt	Weak	Light	Moderate	Strong	Very strong	Severe	Violent	Extreme
POTENTIAL DAMAGE	none	none	none	Very light	Light	Moderate	Moderate/Heavy	Heavy	Very Heavy
PEAK ACC.(%g)	*<.17*	*.17-1.4*	*1.4-3.9*	*3.9-9.2*	*9.2-18*	18-34	34-65	65-124	>124
PEAK VEL.(cm/s)	<0.1	0.1-1.1	1.1-3.4	3.4-8.1	8.1-16	*16-31*	*31-60*	*60-116*	*>116*
INSTRUMENTAL INTENSITY	I	II-III	IV	V	VI	VII	VIII	IX	X+

In simple terms, a Ground Motion Model (GMM) is a mathematical equation utilized to estimate the average ground motion intensity during an earthquake. This equation incorporates various parameters:

$$Y = C_1 + C_2 m + C_m m^{c4} + C_5 ln\, r + f(F) + f(HW) + f(S) \quad (4\text{-}4)$$

where Y represents the expected ground motion intensity (measured as PGA, SA), m is the earthquake's magnitude, r is the distance from earthquake's source to the site, F relates to the type of fault mechanism, HW considers the site's location in relation to the fault plane, and S accounts for the local site conditions, which help estimate how ground shaking will vary across the site during an earthquake.

In a more concise way, the ground motion intensities must be calculated as:

$$L(Y) = f(Rup, Mag, Dis) + variability \quad (4\text{-}5)$$

where $L(Y)$ is the intensity, Rup, Mag, Dis stand for rupture, magnitude, and distance, respectively.

4.4.1.5. USGS Shakemap

The input hazard model in this thesis is constituted by the utilization of shakemaps. The USGS shakemap system, initially developed in response to the 1994 Northridge earthquake and subsequently adopted globally, is a robust tool for swiftly assessing earthquake-induced shaking (Bay et al. 2005). It addresses the distribution of shaking intensity instead of only considering the earthquake magnitude and location, by leveraging seismic recording stations, community reports, and GMMs. This comprehensive approach, which incorporates data grids, fault geometry adjustments, variability reduction, and site effect considerations (Wald et al. 1999), estimates shaking in areas lacking sensors and provides detailed maps for various shaking measures such as peak ground velocity, PGA and multiple periods of SA. For locations close to seismic monitoring stations, the system heavily relies on the actual ground motion recorded by these stations. For areas further away from these stations, it uses a prediction equation to estimate ground motion. The generated ground motion maps are compatible with the OQ Engine (Pagani et al. 2023). shakemaps used in this thesis are depicted in Figure 4.3 - Figure 4.5.

Additional information about the selected shakemaps, such as their USGS ID, the type of GMPEs employed, magnitude, maximum intensity, PGA/PGV, and SA, can be found in Table 4.3.

4.4.2. Exposure model

Exposure refers to the human-made environment that faces the risk of seismic activity. This refers to the potential losses that assets could face due to earthquake shaking, encompasses economic and social elements, such as residential buildings, schools, and their occupants, as well as the services they provide, which can all suffer damage or disruption during a seismic event (J. J. Bommer, Crowley, and Pinho 2015). Additionally, valuable cultural and heritage assets like religious temples and historical monuments can also be considered as exposed elements (Hobbs et al. 2022). To model exposure accurately, it's essential to identify and characterize all the elements involved in a risk assessment.

Val-des-Bois-2010 **Ladysmith-2013**

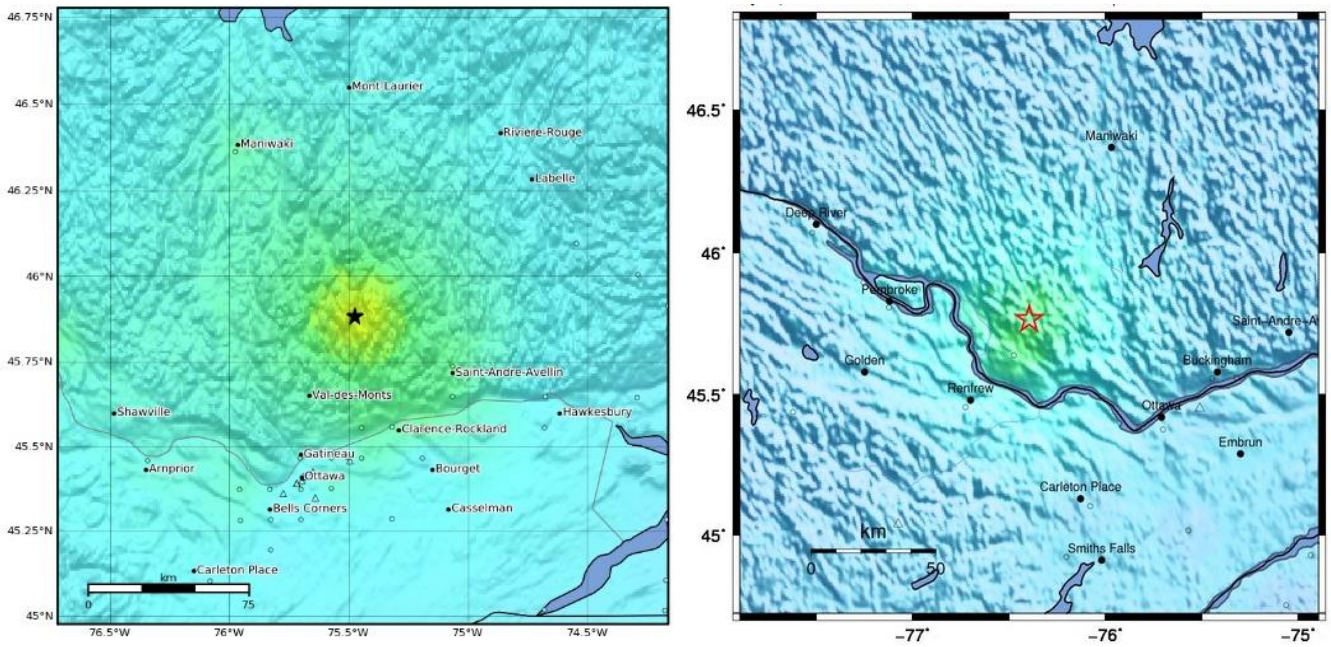

Figure 4.3. The shakemaps of the eastern earthquakes examined as case studies in this thesis (USGS Website n.d.).

6.2 Mosquito Lake-2017 **6.3 Mosquito Lake-2017**

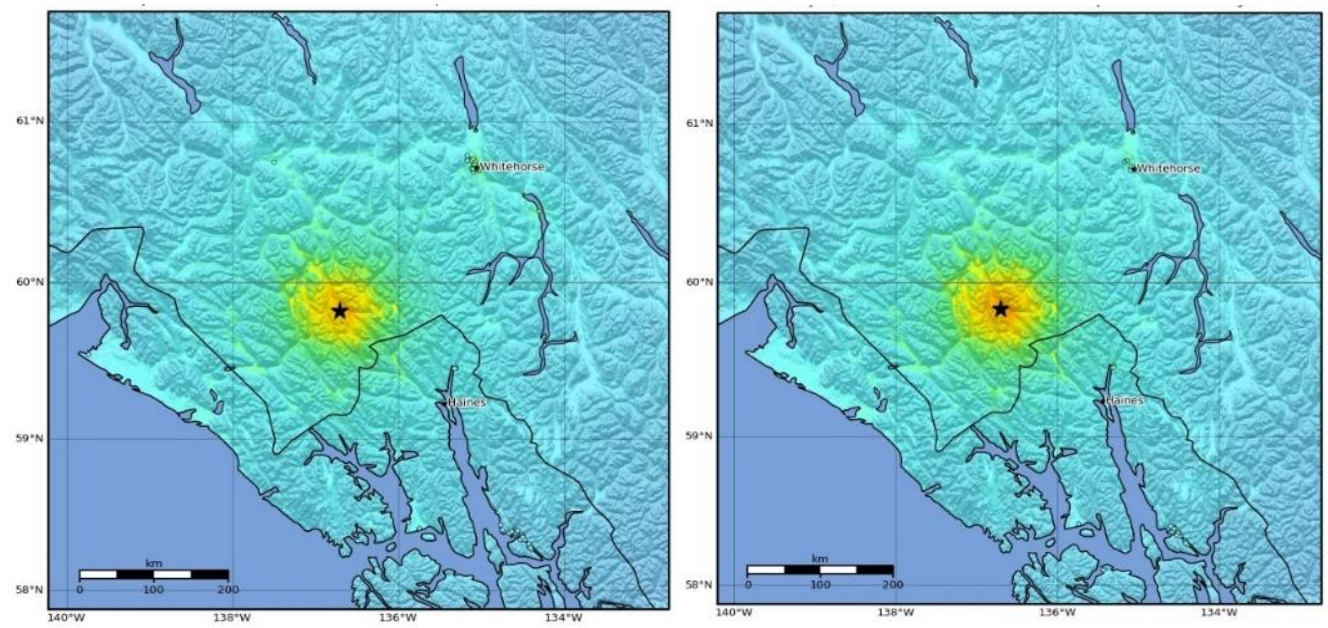

Figure 4.4. The shakemaps of the western earthquakes examined as case studies in this thesis (USGS Website n.d.).

Nahanni-1985

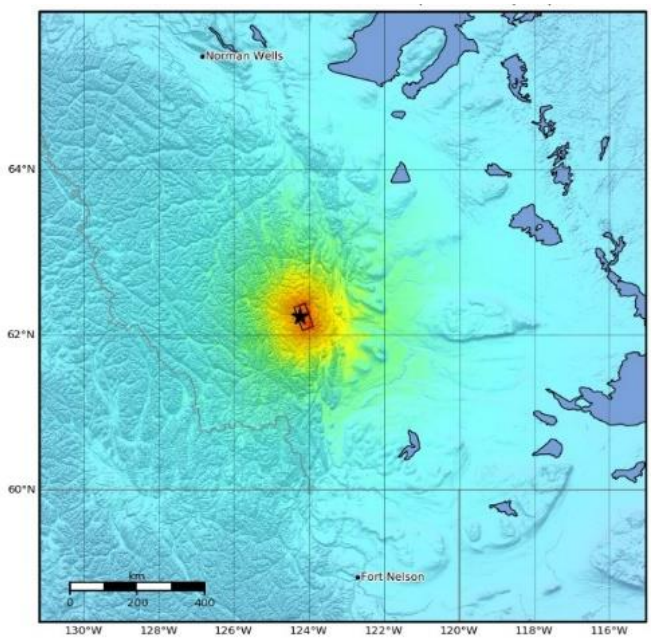

Figure 4.5. The shakemap of the northern earthquake examined as case studies in this thesis (USGS Website n.d.).

Table 4.3. GMPE and USGS ID of each shakemap used in this study (USGS Website n.d.).

Earthquake	USGS ID	GMPE	Mw	MMI	PGA (g)	PGV (cms)	SA(0.3s) (g)	SA(1.0s) (g)	SA(3.0s) (g)
Val-des-Bois	ld2010062300	Gmpe-ld2010062300-custom	5.0	5.856	0.129	2.138	0.244	0.087	0.013
Ladysmith	ld60040526	AB06-ENA-BC	4.6	4.96	8.7	3.06	8.79	1.02	0.05
Mosquito Lake	us10008mel	Gmpe-us10008mel-custom	6.2	7.577	0.384	3.628	0.799	0.425	0.101
Mosquito Lake	us10008mgu	Gmpe-us10008mgu-custom	6.3	8.036	0.465	3.938	1.055	0.57	0.146
Nahanni	usp0002p9m	Gmpe-usp0002p9m-custom	6.6	8.706	0.948	4.487	1.793	0.961	0.234

This involves using descriptive attributes that cover aspects like usage, content, economic and human value, physical characteristics, and connectivity of what is exposed to the seismic hazard (Pagani et al. 2023). In essence, exposure pertains to the constructed environment, its contents, and its occupants that are susceptible to seismic hazards. Certain attributes are necessary for conducting damage and loss assessments. The development of an exposure model can be adapted to different scales, depending on the scope of the risk assessment. In all cases, it requires the identification, manipulation, and management of geographic, demographic, and socio-economic data to accurately assess what's at risk.

Regardless of the model's scale, OQ Engine enables users to perform risk analysis using exposure models, provided they meet the minimum attribute requirements (Pagani et al. 2014). Furthermore, apart from the number of elements within the exposure model, modelers can also consider replacement costs by distinguishing the value of various components. For instance, these components may include structural elements, non-structural elements, contents, and losses due to business interruptions. Occupancy levels, such as day, night, and transit occupants, can also be factored in (TOOLKiT 2015). This allows for the analysis of insured portfolios with defined limits and deductibles, and even the incorporation of personalized information through labels. For instance, it's possible to differentiate between elements in the same construction category based on the socioeconomic status of the house or its built area.

Key factors to consider in exposure modeling include:

- Limits and deductibles
- Average area per building class
- Tages (custom user information)
- Number of assets
- Occupants (day/night/transit)
- Economic value (replacement cost) for various components: structural, non-structural, contents, and business interruption.

In the study by Journeay et al. (2022), they provide a comprehensive overview of their exposure model, its development process, and important findings regarding the current state of Canada's building inventory. This exposure model, which is used in this thesis, focuses on creating a detailed representation of various aspects related to buildings and their seismic risk within Canada.

This model encompasses a national inventory of buildings, their occupants, and the replacement value of these buildings, all analyzed on the scale of a Dissemination Area Unique Identifier (DAUID). These DAUIDs serve as the smallest census units (polygons) used for calculating seismic risk in CanadaSRM1 and define areas of building development across Canada (Hobbs et al. 2022). In urban regions, DAUIDs typically cover less than a square kilometer. In rural areas, DAUIDs can be extensive and non-contiguous, approximating the locations of building clusters.

Within this model, a representative building inventory consists of points situated at the centroids of DAUIDs. Each point represents a group of buildings with similar occupancy, construction type, and seismic design levels, referred to as 'building archetypes.' The inventory also summarizes the number of occupants in these buildings at different times of the day and the replacement value of the buildings and their contents. The classification of building occupancy and construction type is based on standard HAZUS classifications, with adaptations to account for Canadian building conditions (FEMA, 2021). Seismic design levels are determined based on building code requirements at the time of construction, assuming that all buildings met these standards during their construction, as well as geographic location relative to seismic hazard. The composition of buildings with various occupancies is derived from national census data and georeferenced business listings (Journeay et al. 2022).

The distinct building archetypes within each DAUID are determined using mapping schemes that relate land use characteristics to the mix of specific building occupancies and construction

types typical for a given location and time period (Journeay et al. 2022). The model estimates the number of occupants in buildings during daytime, nighttime, and transit hours. Occupants in residential buildings are estimated based on housing statistics and nighttime occupancy proportions (Statistics Canada, 2016). Non-residential building occupants are estimated based on the average number of people per 1,000 square feet and the total finished building area (Hamburger et. al., 2012).

Table 4.4. Sample exposure model used for Ontario damage and risk assessment.

	A	B	C	D	E	F	G	H	I	J	K	L	M	N	O	P	Q	R	S	T	U	V	W	X	Y	Z	AA	AB	AC	AD	AE	AF	AG	AH	AI	AJ
1	id	lon	lat	taxonomy	number	structural	nonstruct	contents	retrofittin	day	night	transit	LandUse	GenOcc	OccType	OccClass	GenType	BldgType	BldEpoch	SSC_Zone	EqDesLev	sauid	dauid	adauid	fsauid	csduid	csdname	cduid	cdname	SAC	eruid	ername	pruid	prname	SS_Region	Sauid_km2
2	16800-RES	-114.9218	50.00402	RES3A-W1	1	108652.5	494972.5	43461	265562.2	0.402242	2.16889	1.289083	RURAL	Residentia	RES	RES3A	Wood	W1	Pre-1973	SSC-2	LC	59001607	59010240	59010004	V0B	5901063	Elkford	5901	East Koote	6	5940	Kootenay	59	British Col	West	0.112932
3	244482-RE	-122.4521	52.97255	RES3A-W1	1	146187	665963	58475	69689	0.647194	3.489671	2.0432	RES-LD	Residentia	RES	RES3A	Wood	W1	1990-2004	SSC-1	LC	59022710	59410280	59410027	V2J	5941019	Cariboo A	5941	Cariboo	3	5950	Cariboo	59	British Col	West	1.380912
4	31783-RES	-119.5725	49.52912	RES3A-W4	1	146187	665963	58475	69689	0.44758	2.413354	1.413017	RES-LD	Residentia	RES	RES3A	Wood	W4	2005-2016	SSC-1	LC	59004822	59070221	59070006	V2A	5907041	Penticton	5907	Okanagan-	3	5930	Thompson	59	British Col	West	3.034177
5	3216-EDU1	-120.2349	55.75344	EDU1-W2-	3	7322175	33356575	6589958	8436892	717.9404	2.200184	361.6017	COMM-INI	Civic	EDU	EDU1	Wood	W2	Pre-1973	SSC-1	PC	59033433	59550150	59550014	V1G	5955014	Dawson Cr	5955	Peace Rive	3	5980	Northeast	59	British Col	West	0.626655
6	11086-GOV	-116.3833	50.92328	GOV1-W2-	1	968544	4412256	871690	919486.3	39.80414	1.49429	21.92747	RURAL	Civic	GOV	GOV1	Wood	W2	Pre-1973	SSC-1	PC	59000153	59010125	59010001	V0A	5901048	East Koote	5901	East Koote	6	5940	Kootenay	59	British Col	West	0.135934
7	11339-RES	-116.0426	50.50177	RES3A-W1	3	325557.5	1484918	130383	209067	1.689674	9.110726	5.334323	RURAL	Residentia	RES	RES3A	Wood	W1	1990-2004	SSC-1	LC	59000179	59010132	59010001	V0A	5901039	Invermere	5901	East Koote	5	5940	Kootenay	59	British Col	West	0.695536
8	31616-COM	-119.591	49.49906	COM1-C2L	1	624466.7	1018867	562020	134933.1	33.88212	0.145368	17.91852	MIXED	Commerci	COM	COM1	Concrete	C2L	1973-1989	SSC-1	PC	59004815	59070214	59070006	V2A	5907041	Penticton	5907	Okanagan-	3	5930	Thompson	59	British Col	West	0.351865
9	22026D-CO	-119.4684	49.87889	COM3-W3	1	221920	362080	199728	220757.7	4.448	0.065567	2.611815	RES-MD	Commerci	COM	COM3	Wood	W3	Pre-1973	SSC-1	PC	59019659	59350049	59350016	V1Y	5935010	Kelowna	5935	Central Ok	1	5930	Thompson	59	British Col	West	0.110385
10	7790-RES1	-120.3001	56.20145	RES1-W1-L	1	81562.5	244687.5	32625	35717.6	0.603454	3.253823	1.905111	COMM-INI	Residentia	RES	RES1	Wood	W1	1990-2004	SSC-0	LC	59034995	59550218	59550001	V0C	5955040	Peace Rive	5955	Peace Rive	5	5980	Northeast	59	British Col	West	0.158854
11	14729-RES	-115.4445	49.40256	RES1-W1-L	1	113906.3	341718.8	45562	136108.2	0.335432	1.808647	1.058961	RES-LD	Residentia	RES	RES1	Wood	W1	Pre-1973	SSC-1	LC	59001065	59010204	59010005	V1C	5901035	East Koote	5901	East Koote	3	5940	Kootenay	59	British Col	West	0.290655
12	11341-RES	-116.0426	50.50177	RES1-W4-L	25	2039063	6117188	815625	892939.9	10.3534	55.82552	32.6858	RURAL	Residentia	RES	RES1	Wood	W4	1990-2004	SSC-1	LC	59000179	59010132	59010001	V0A	5901039	Invermere	5901	East Koote	5	5940	Kootenay	59	British Col	West	0.695536
13	13739-COM	-115.7547	49.49588	COM3-W3	1	221920	362080	199728	57941.88	4.189259	0.059869	2.459886	RES-LD	Commerci	COM	COM3	Wood	W3	2005-2016	SSC-1	LC	59000987	59010176	59010010	V1C	5901022	Cranbrook	5901	East Koote	3	5940	Kootenay	59	British Col	West	0.497933
14	20858B-CO	-120.3561	50.68827	COM1-S5L	1	624466.7	1018867	562020	610125.1	41.79129	0.179302	22.10127	MIXED	Commerci	COM	COM1	Steel	S5L	Pre-1973	SSC-1	PC	59016600	59330063	59330044	V2B	5933042	Kamloops	5933	Thompson	2	5930	Thompson	59	British Col	West	0.144025
15	14743-RES	-115.6023	49.38349	RES1-W1-L	1	113906.3	341718.8	45562	35717.6	0.335432	1.808647	1.058961	RES-LD	Residentia	RES	RES1	Wood	W1	1990-2004	SSC-1	LC	59001070	59010204	59010005	V1C	5901035	East Koote	5901	East Koote	3	5940	Kootenay	59	British Col	West	0.112934
16	27276T-CO	-122.7338	53.9079	COM4-W3	1	1552338	2532762	1397104	240181	24.10549	0	12.39404	RES-LD	Commerci	COM	COM4	Wood	W3	1990-2004	SSC-1	LC	59031060	59530243	59530010	V2L	5953023	Prince Gec	5953	Fraser-For	2	5950	Cariboo	59	British Col	West	0.448601
17	17163-RES	-115.7624	49.59085	RES1-W1-L	4	455625	1366875	182250	142870.4	1.463828	7.892962	4.621323	RES-LD	Residentia	RES	RES1	Wood	W1	1973-1989	SSC-1	LC	59001661	59010245	59010009	V1C	5901022	Cranbrook	5901	East Koote	3	5940	Kootenay	59	British Col	West	0.328971
18	7015-RES1	-121.0249	56.2763	RES1-W1-L	2	227812.5	683437.5	91125	272216.3	0.911771	4.91627	2.878472	RES-LD	Residentia	RES	RES1	Wood	W1	Pre-1973	SSC-1	LC	59034548	59550211	59550008	V0C	5955042	Peace Rive	5955	Peace Rive	3	5980	Northeast	59	British Col	West	0.191104

As shown in Table 4.4, an exposure model consists of several metadata sections with information common to all assets in the portfolio. The metadata section consists of several parameters described below:

The "id" attribute is mandatory and serves as a unique string to identify the asset. It can contain letters (a–z; A–Z), numbers (0–9), dashes (-), and underscores (_), with a maximum of 100 characters. The "taxonomy" attribute is mandatory and specifies the building typology of the asset, which can be user-defined or based on an existing classification scheme (De Bono and Mora 2014a). The "number" attribute represents the number of individual structural units comprising the asset and is mandatory for damage calculations. For risk calculations, it must be defined if costs are provided per structural unit (“OpenQuake Platform” n.d.).

The "location" attribute is mandatory and specifies the longitude (between -180∘ to 180∘) and latitude (between -90∘ to 90∘) of the asset. The occupancies attributes are mandatory for probabilistic or scenario risk calculations with an occupants_vulnerability file. It specifies the number of occupants for the asset during different periods of the day, such as "day", "transit", and "night". The number of occupants is provided as an aggregated value for the asset (TOOLKiT 2015). Next, attention is turned to the section in the file that describes area and cost conversions. The Exposure Model allows defining structural cost, non-structural components cost, contents cost, and business interruption or downtime cost for each asset (Journeay et al. 2022). The valid values for the "name" attribute of the costType element are "structural", "non-structural", "contents", and "business_interruption”.

For each earthquake, damage and risk assessments are carried out for the province/territory in which it occurred and the surrounding provinces/territories near the epicenter. Consequently, multiple provincial/territorial exposure models may be utilized for each earthquake. For earthquakes in the eastern region, risk assessments are performed in Ontario and Quebec. For

earthquakes in the western region, risk assessments are conducted for British Columbia and Yukon. Lastly, for the earthquake in the northern region, assessments are conducted in Alberta, British Columbia, Northwest Territories, and Yukon.

4.4.3. Physical fragility and vulnerability model

In the context of seismic risk, fragility is associated with the structural damage resulting from a seismic event, while vulnerability is associated with the economic or human losses resulting from this damage (Pagani et al. 2023).

4.4.3.1. Fragility model

Seismic fragility represents the probability of an element exposed to seismic hazards sustaining damage due to ground shaking resulting from a seismic event (Hobbs et al. 2022). In risk analysis, fragility model establishes the relationship between the damage ratio and the ground motion intensity (Choi, DesRoches, and Nielson 2004). The damage ratio indicates the percentage of loss and ranges between zero (no loss) and one (complete destruction). The structural attributes of a building, such as construction material, construction system, height, and adherence to design regulations, directly influence its fragility, making it more or less resistant or vulnerable to ground shaking (Nielson and DesRoches 2007). Consequently, structures with higher fragility present a greater seismic risk under the same level of seismic hazard.

Damage states define the extent of damage an exposed element (asset) will experience when specific engineering demand parameters are met. These parameters can include spectral displacement, SA, floor displacement (drift), acceleration between floors, inner story drift, maximum roof displacement, and so on (C. Ventura, Onur, and Finn 2005). A structure is considered to be in a particular damage state, as shown in Figure 4.6.

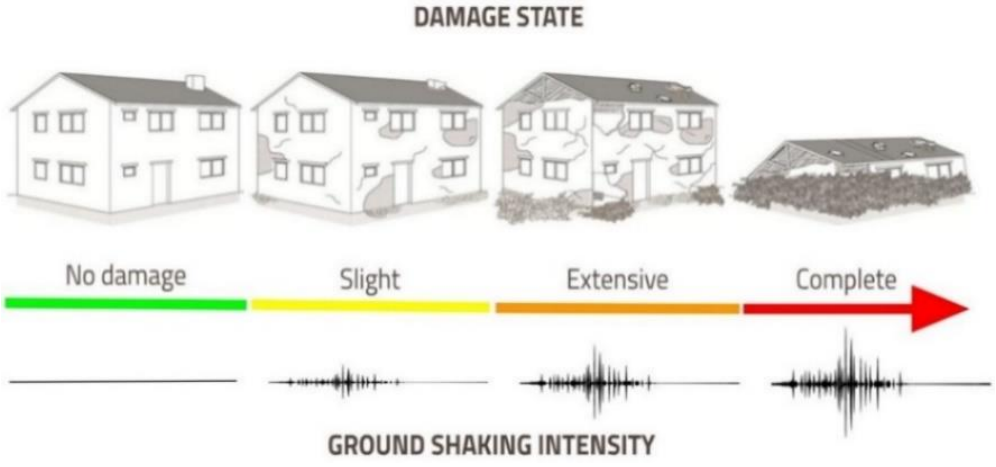

Figure 4.6. Seismic Fragility, demonstrates the correlation between ground movement intensity and the damage level experienced by an exposed element (GEMScienceTools n.d.). No-damage states are observed in the absence of ground movement. As ground motion increases, the level of damage is escalated, and damage states progress from slight to moderate, extensive, and ultimately result in complete or collapse when the building is completely damaged (Rossetto et al. 2014).

If there is no ground movement or lateral load, no damage should occur to the structure. Slight ground shaking will produce visible damage in the form of cracks. The intensity of shaking directly correlates with the extent of observed damage, potentially leading to permanent structural damage or even collapse. Though this process occurs continuously and uniquely for each structure, risk models often categorize it into several damage states: slight, moderate, extensive, complete damage, or collapse.

Developing fragility models requires detailed analyses of the dynamic behavior of structures, and this is a primary focus of many research studies (Rossetto et al. 2014). This relationship can be described within OQ Engine using continuous mathematical functions, which show that the probability of damage increases with higher ground shaking intensity (Pagani et al. 2014). Alternatively, the relationship can be represented using discrete functions (TOOLKiT 2015).

4.4.3.2. Vulnerability model

Seismic vulnerability is the final component needed for estimating losses and damage. It refers to the likelihood of damage or loss experienced by a structure when exposed to seismic activity, specifically ground shaking (Gueguen 2013). Vulnerability models establish a connection between the strength of ground shaking and the extent of damage or loss, such as the number of fatalities, that may occur once a certain level of intensity is reached (Hobbs et al. 2023).

These relationships can be categorized into two types: intensity-based and engineering parameter-based. Intensity-based relationships are often developed based on expert opinions and convey the probability of damage corresponding to earthquake intensity using damage probability matrices (Thibert 2008). In contrast, engineering parameter-based methods frequently employ SA or spectral displacement, represented as demand spectra, to describe input ground motions (Zameeruddin and Sangle 2016). Building characteristics are represented through capacity curves, and building vulnerability is predicted using fragility curves.

Fragility and vulnerability curves specific to each building type are required due to the varied responses of different building types to shaking (McGuire 2004). The fragility and vulnerability functions designed for Canada were created by adapting HAZUS capacity curves from FEMA (Hobbs et al. 2022). Adjustments were made to align with Canadian construction standards, particularly for wood and unreinforced masonry buildings. Hobbs et al. (2022) detailed the use of Monte-Carlo simulations to address variability in building capacity and structural response.

Standard classifications from the HAZUS program, relying on taxonomies, were utilized for construction and occupancy determination. Recent Hobbs's researches (Hobbs et al. 2022) (Tiegan Hobbs et al. 2023) identified additional wood building classes in the Canadian exposure dataset, not considered in HAZUS. Hobbs et al. (2023) highlighted these newly identified classes, prompting the ongoing development of fragility and vulnerability functions. Consequently, to accommodate Canadian wood buildings, a mapping file was employed, incorporating adjustments to wood typologies. The purpose of this mapping file, as outlined by Hobbs et al. (2023), was to link Canadian wood building types to the original HAZUS options.

In summary, the primary objective of this thesis is to validate CanadaSRM1. To achieve this, a methodology has been adopted wherein the Canadian fragility and vulnerability functions derived from CanSRM1 are utilized. This approach was chosen with the intention of comparing the estimated results obtained through CanadaSRM1 with the actual observed data. By employing the established functions from CanadaSRM1, this study aims to assess the accuracy and reliability of CanadaSRM1 in estimating and modeling the structural damage and financial loss caused by potential future earthquakes.

4.5. Uncertainty

The accuracy and reliability of GMMs in predicting intensity are questioned due to observed variability in earthquake ground shaking with similar rupture properties and source-to-site distances (J. J. Bommer and Crowley 2006). Seismic hazard modeling commonly employs truncation levels, like 3 (chosen in this thesis), which accounts for 99.7% of the distribution, as depicted in Figure 4.7, to prevent unrealistically high ground motion values driven by mathematical models rather than actual seismic events.

Intra-event variability refers to variation in ground motion within a single seismic event, arising from differences in ground motions at equidistant locations due to various path effects for a given rupture (Atik et al. 2010). In contrast, inter-event variability encompasses differences in ground motion between multiple seismic events with the same magnitude occurring at the same distance from an observation point (Bostrom, Anselin, and Farris 2008).

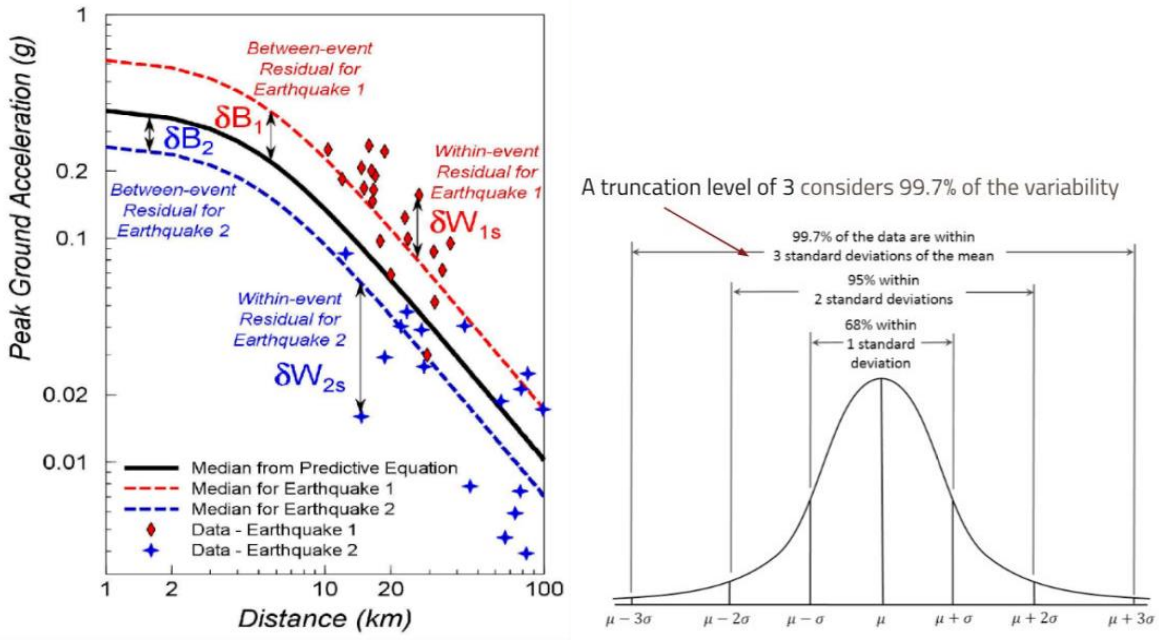

Figure 4.7. GMFs variability. The ground motion intensity has an associated variability, observed in the same event, and in different events, although it is the same type of rupture, magnitude, and distance (Atik et al. 2010).

Uncertainty in risk assessment can manifest in various aspects, such as characterizing the exposure scenario, estimating parameters, and making model predictions (Bostrom, Anselin, and

Farris 2008). Therefore, accounting for uncertainty in seismic hazard analysis is crucial, including aleatoric uncertainty related to the inherent randomness of earthquakes and epistemic uncertainty linked to gaps in our knowledge and data, which is handled using a logic tree (Hobbs et al. 2022).

4.6. Program Executing

The SDC and SRC calculators of the OQ Engine are used to assess building damage and economic loss in the context of seismic events. The overall damage distribution is then characterized by the average and variation (standard deviation) for each building. This information, when combined with the total number or area of buildings, provides the complete picture of building damage (Pagani et al. 2023). In the modeling of seismic scenario in this thesis, in order to deterministic calculation of scenario seismic risk, both kinds of calculators were used.

Starting from version 3.1, the ability to perform scenario risk and scenario damage calculations is enabled by the engine, beginning with the GeoJSON feed for shakemaps (Pagani et al. 2023). In this thesis, all these models were implemented on OQ Engine version 3.11.5 (GEM 2022), which was operated on Amazon Web Services, allowing for the utilization of shakemaps from alternative sources such as the local filesystem or a custom URL. Consequently, the hazard input layer utilized in this study was based on the USGS ID, Table 4.3, provided for each shakemap.

4.6.1. Scenario damage calculator (SDC)

Statistics on the distribution of damages were obtained through the use of the damage scenario calculator. This calculator required three input layers: USGS shakemap as the GMF in the form of ID codes within a configuration file with a .txt format, the national exposure model in .xml format, and the fragility function in .xml format. The propagation of uncertainties was handled in a manner similar to that of a SRC by employing the truncation level 3 (TOOLKiT 2015).

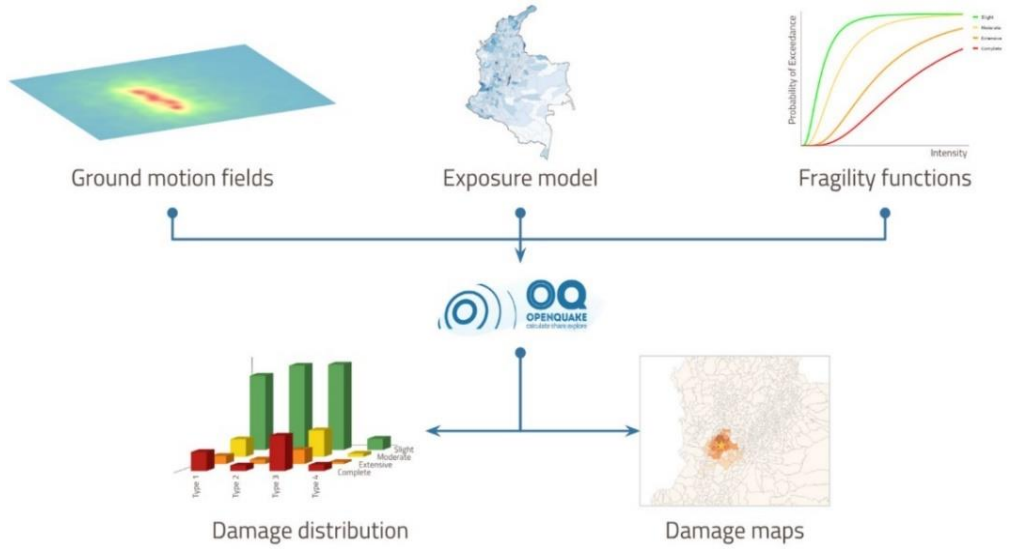

Figure 4.8. SDC, featuring three input layers—GMFs (hazard model), exposure model, and fragility functions. The calculator produces damage maps and distribution, providing a comprehensive analysis of potential impacts. (Global Earthquake Maps | Global Earthquake Model Foundation | Italy n.d.).

As depicted in Figure 4.8, the outputs were generated by this calculator consist of a damage map and a damage distribution chart. The damage map displays the spatial distribution of the number of buildings in a given damage state, taking into account various damage levels such as slight, moderate, extensive, and complete. Meanwhile, the damage distribution, which represents as a bar graph of number of assets in damage states, focuses on statistics per asset, such as moderate damage levels, and aggregates damage distribution statistics by building class and region.

4.6.2. Scenario risk calculator (SRC)

Economic losses can be obtained when the SRC is utilized (Hobbs, Journeay, and Rotheram 2021). The computed loss statistics include the mean and standard deviation of economic losses for each type of loss analyzed (Pagani et al. 2023). The calculator can currently compute loss statistics for four different types: structural losses, non-structural losses, contents losses, and occupant fatalities.

In this thesis, the calculation was performed through the definition of three key models. The hazard model, encompassing a set of pre-computed GMFs, was represented by the USGS shakemap. These GMFs, which were automatically generated minutes after events occurred (Silva and Horspool 2019), were structured in the form of ID codes within a configuration file with a .txt format. Additionally, a national exposure model in .xml format and a physical vulnerability model in .xml format for each loss type were utilized.

The main outcomes of this calculation include loss statistics per asset and mean loss maps. Figure 4.9 illustrates the generated loss maps for each building class or region, and loss statistics were computed for all assets within a specified exposure model for each earthquake rupture, as demonstrated by Hobbs et al. (2023).

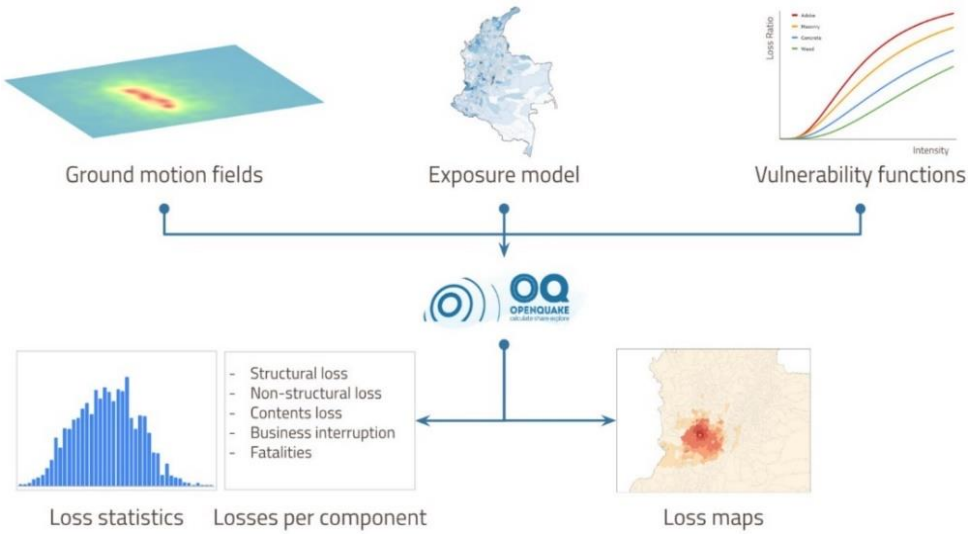

Figure 4.9. SRC, using three input layers: GMFs (representing the hazard model), exposure model, and vulnerability functions. The calculator generates comprehensive outputs in the form of loss maps and loss statistics, providing a robust assessment of potential risks. (Global Earthquake Maps | Global Earthquake Model Foundation | Italy n.d.).

Therefore, the spatial distribution of economic losses was estimated by this deterministic calculator as a loss map in the event of it occurring today in each study area. This map illustrates the distribution of loss ratios for the same event, with loss ratios calculated as the ratio of absolute economic losses to the total replacement costs indicated in the exposure model. The scenario loss ratio map takes the results of the loss map and normalizes them by the exposed value. This map highlights areas with a combination of higher hazard and higher vulnerability.

To execute these calculations and activate these functionalities, a parent calculation was prepared, encompassing the exposure and risk functions for the regions of interest. To achieve this, two ***prepare_job.ini*** files were composed for each area that had been exposed to the examined earthquakes, resembling the following examples which is done for the damage assessment of Val-des-Bois earthquake on Ontario side:

```
# Generated on: 2023-02-14 24:11

[general]
description = Validating CanSRM1 using USGS shakempas from Val-des-Bois earthquakes - Preloading_ON
exposure and vulnerability (damage)
calculation_mode = scenario

[Exposure model]
exposure_file = oqBldgExp_ON.xml

taxonomy_mapping_csv = CanSRM1_TaxMap_b0.csv

[Fragility Functions]
structural_fragility_file = fragility_structural_shakemap.xml

`utput]
 ort_dir = output
```

And for the risk assessment of Val-des-Bois earthquake on Ontario side:

```
# Generated on: 2023-02-14 24:11

[general]
description = Validating CanSRM1 using USGS shakempas from Val-des-Bois earthquakes - Preloading_ON
exposure and vulnerability (loss)
calculation_mode = scenario

[Exposure model]
exposure_file = oqBldgExp_ON.xml

taxonomy_mapping_csv = CanSRM1_TaxMap_b0.csv

[Vulnerability Functions]
structural_vulnerability_file = vulnerability_structural.xml
nonstructural_vulnerability_file = vulnerability_nonstructural.xml
contents_vulnerability_file = vulnerability_contents.xml
occupants_vulnerability_file = vulnerability_occupants.xml

 tput]
  t_dir = output
```

Upon execution of the calculation with the specified command in OQ Engine (Console):

```
$ oq engine --run prepare_job.ini
```

The exposure and risk functions were imported into the datastore.

It should be noted that, when this code is implemented, the shakemap will be downloaded and converted into a format suitable for further processing. Specifically, it will be transformed into a shakemap array with longitude and latitude fields. Subsequently, the shakemap array will be associated with the hazard sites within the region covered by the shakemap.

In the scenario calculators, multiple simulations of GMFs corresponding to the single event should be generated, considering both inter-event variability of ground motions point (Bostrom, Anselin, and Farris 2008) and intra-event residuals obtained from a spatial correlation model for ground motion residuals (Atik et al. 2010). The use of logic trees will allow for uncertainty consideration in the selection of a GMM for the specific tectonic region (Hobbs et al. 2023).

Therefore, ***Job.ini*** files were created based on 100 number of GMFs and truncation level 3 considering a 3-sigma range of uncertainty in the ground motion, for both damage and risk assessments as shown below, which was done for the damage assessment of Val-des-Bois earthquake on Ontario side, And for the risk assessment of Val-des-Bois earthquake on Ontario side:

```
[General]
description = Val-des-Bois - 2010 M5.4 Val-des-Monts earthquake damages_
calculation_mode = scenario_damage

[Calculation Parameters]
number_of_ground_motion_fields = 100
truncation_level = 3

[site_params]
shakemap_id = ld2010062300
spatial_correlation = no
cross_correlation = yes

taxonomy_mapping_csv = CanSRM1_TaxMap_b0.csv

utput]
rt_dir = output
```

```
[General]
description = Val-des-Bois - 2010 M5.4 Val-des-Monts earthquake losse
calculation_mode = scenario_risk

[Calculation Parameters]
number_of_ground_motion_fields = 100
truncation_level = 3

[site_params]
shakemap_id = ld2010062300
spatial_correlation = no
cross_correlation = yes

taxonomy_mapping_csv = CanSRM1_TaxMap_b0.csv

tput]
t_dir = output
```

The calculation ID for the 'pre' calculation was set to 1000. The damage and risk calculations were then initiated, starting from shakemaps, by executing the following command in the OQ Engine Console:

```
$ oq engine --run job.ini --hc 1000
```

After running this command, a set of GMFs conforming to the truncated Gaussian distribution were generated and saved in the datastore, utilizing the parameters truncation_level and number_of_ground_motion_fields. Finally, standard damage and risk calculations were conducted by employing these GMFs and considering the assets situated within the region covered by the shakemap (Hobbs et al. 2023). This approach was in line with the methodology of CanadaSRM1.

Chapter 5 : Results and Outputs

5.1. Introduction

The research findings and estimated outputs, comprising structural and non-structural damage assessment, monetary losses, and casualty estimation resulting from the seismic damage and risk assessment of five earthquakes investigated in the eastern, western, and northern regions of Canada, are presented in this chapter. The data were obtained using the OQ Engine, in alignment with the CanadaSRM1 framework.

By running the calculators, for each GMF, SDC and SRC simulated a damage state and a loss ratio for each building and asset in the exposure model using the provided fragility and the provided probabilistic vulnerability model. The calculators then calculated the mean damage distribution across all realizations. It also provided aggregated damage distribution statistics for the entire portfolio, such as the mean damage fractions for each taxonomy in the exposure model and the mean damage for the entire study regions.

Finally, loss statistics, including the fatalities, mean financial losses, were calculated for each asset. Mean loss maps were also generated, illustrating the mean ground-up losses caused by the scenario events for the different assets in the exposure model. These results are crucial for tasks like emergency planning, raising public awareness of seismic risk, and quickly assessing the impact of seismic events.

5.2. Structural damage from scenario damage assessment

5.2.1. Classification system

The assessment of structural damage resulting from earthquakes involves two primary approaches: engineering parameter-based methodologies such as HAZUS (FEMA, 2021) (Kircher, Whitman, and Holmes 2006), and intensity-based methodologies such as ATC-13 (Thibert 2008) (Rojahn et al. 1986). The former relies on using parameters like SA or spectral displacement to describe ground motions. It then makes use of capacity curves and fragility curves to predict the vulnerability of buildings (Hazus-MH 2003). However, these engineering parameter-based methods may lack accuracy and sufficient data for specific regions (Kircher, Whitman, and Holmes 2006).

There exist five damage states, and each of them is linked to a specific set of damage index and percentage of initial cost. These costs represent the proportion of monetary losses incurred from damages relative to the total replacement value of the building (Hazus-MH 2003). Table 5.1 represents a comprehensive list of the damage states, their descriptions, as well as the corresponding ranges of damage indexes and costs.

In 1988, FEMA-154, a method known as Rapid Visual Screening of Buildings for Potential Seismic Hazards, was developed by the FEMA (Rojahn 1988). This approach has been subsequently updated multiple times with the aim of rapidly assessing seismic vulnerability through visual inspection (Lizundia et al. 2015).

Table 5.1. Damage states (Hazus-MH 2003) (Hill and Rossetto 2023).

	Damage States	Evidence	Description	Damage Index	Cost (% of initial cost)
1	None	None (pre-yield)	No damage	0.0 - 0.14	0.0
2	Slight	Cracking, minor spalling	Limited localized minor damage not requiring repair	0.14 - 0.40	0.5
3	Moderate	Large cracks cover spalled	Significant localized damage of many components requiring repair	0.40 - 0.60	20.0
4	Extensive	Failure of components, bar fracture	Major widespread damage that may result in the facility being destroyed or repaired	0.60 - 1.00	80.0
5	Complete	Partial/total collapse	Total destruction of the majority of the facility	1.0 - ∞	100.0

Buildings were grouped into 15 prototypes by this system, taking into consideration factors such as materials, number of stories, and height, as outlined in Table B.1 with detailed descriptions of residential structures provided in Table B.2. Buildings in this classification were designated as low-rise (one to three stories), mid-rise (four to seven stories), and high-rise (over eight stories) (FEMA 2012).

It is important to note that HAZUS utilized only two wood building classes. However, the exposure dataset for Canada encompasses four wood building classes to better represent the diversity of timber construction in Canada: light frame wood, light frame wood with cripple wall or subfloor, heavy frame wood industrial/commercial, and heavy frame wood residential (Hobbs et al. 2022) (FEMA, 2012). As fragility and vulnerability models have not yet been developed for these new building classes, the Canadian wood building types were reassigned to the original HAZUS options, as modified in Table B.1 (Hobbs et al. 2022).

The distribution of taxonomies within the provinces/territories examined in this thesis is illustrated as pie charts in Figure 5.1. As shown in this figure, the majority of these buildings are comprised of single-family wood-frame structures, constituting approximately 75% of the total in these selected provinces/territories, which aligns with the findings highlighted by Hobbs et al. for the national total. Unreinforced masonry buildings, , known for their vulnerability to seismic shaking in Canada (Fathi-Fazl et al., 2019), make up around 8% of the building stock, with a notable concentration in Ontario and Quebec (Hobbs et al. 2022), and mobile houses show a significant concentration in Alberta. Table 5.2 provides the characteristics of the exposure model for each exposed province/territory.

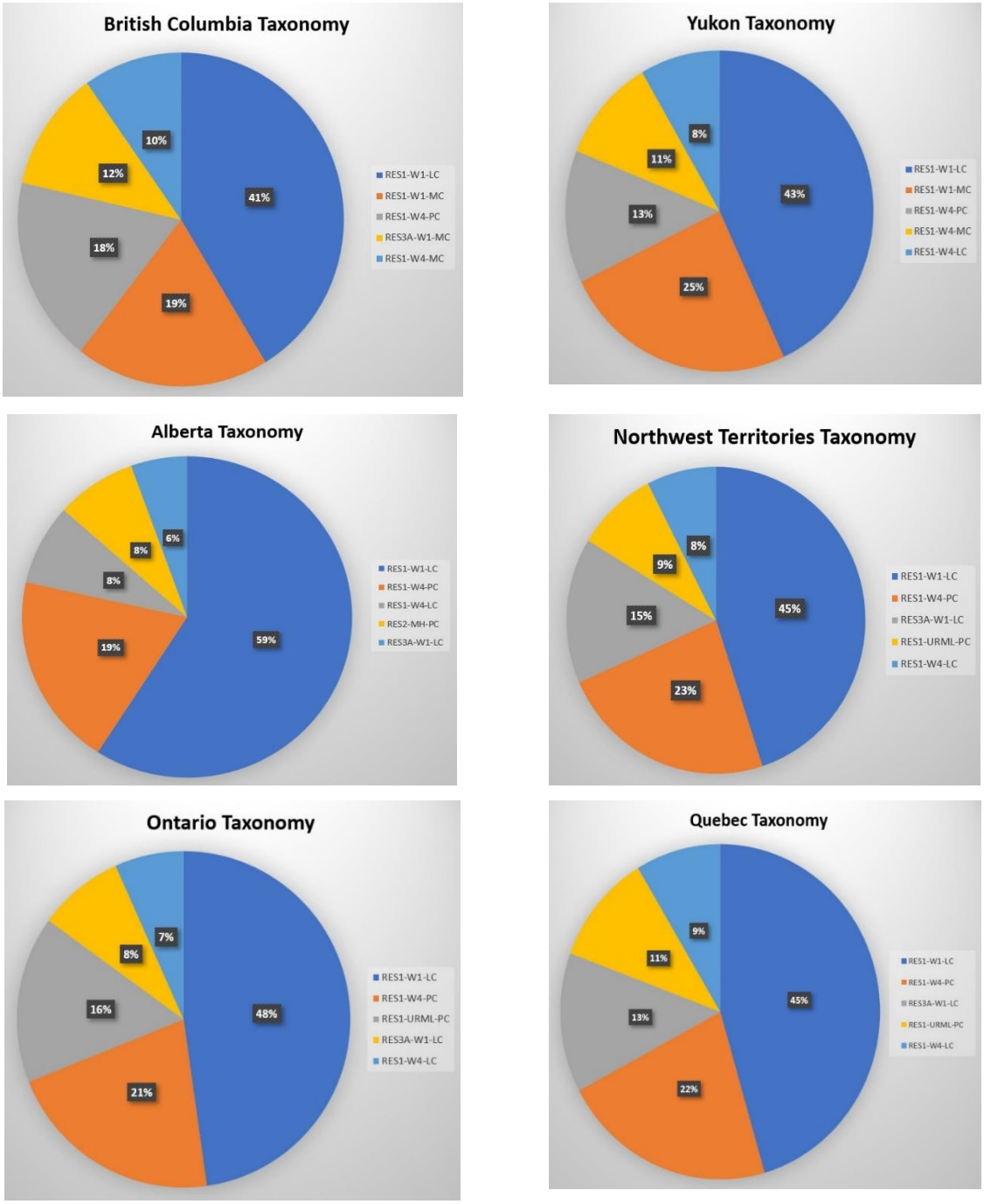

Figure 5.1. Provincial Building Taxonomy for Studied Earthquake. This figure presents a taxonomy of provinc involved in the earthquake analysis explored in this thesis. The pie charts illustrate the predominant building typ and prototypes in each province, as determined by the exposure model obtained for each Canadian province. Detaile explanations for each abbreviation employed in the legends are available in Appendix B. Specifically, W1/W4 denot light/heavy wood frame, URML represents unreinforced masonry, MH stands for mobile home, RES1 corresponds a single-family house, RES2 indicates a mobile house, and RES3A refers to a duplex house.

Table 5.2. Exposure model characteristics.

Province/Territory	Number of Settled Areas (DAUID)	No. of assets
British Columbia	27,344	274,630
Yukon	647	3,916
Alberta	79,639	290,268
NW Territories	253	2,828
Ontario	96,627	733,602
Quebec	54,486	487,210

5.2.2. Damage output

In this thesis, the findings of the scenario damage assessment are encapsulated in various data files. These include:

- ***Excel Spreadsheet Files (.csv):*** Three files with .csv extensions were generated. These files contain:
  - *Selected Events Information:* These files contain information about the 100 selected GMFs used in the study. This information could include details about the events' magnitudes, locations, and other relevant factors.
  - *Aggregate Event Damages:* These files offer insights into the cumulative damage resulting from the selected events. They provide a breakdown of the number of assets in different damage states based on these events.
  - *Asset Damage Distribution:* This part of the Excel files presents data on how damage is distributed among assets in each DAUID. This distribution is categorized into five damage states: no damage, slight damage, moderate damage, extensive damage, and complete damage.
- ***HDF5 Files (.hdf5):*** Two files in the .hdf5 format were created as part of the assessment process for visualization the damage distribution in the form of map.
- ***NPZ File (.npz):*** A single .npz file was generated as well.
- ***Text Files (.rst):*** In addition to the aforementioned files, there are some text files that likely contain supplementary information or descriptions.

By combining the information from these Excel files and the .npz file, a statistical analysis of damage for each asset in each state was conducted. One of the key outcomes of the statistical analysis is the determination of the probability of exceedance for each damage state. In other words, this reveals the likelihood or probability of assets experiencing damage at different severity levels (refer to Table 5.3).

Table 5.3. Structural damage results and statistical analysis for five previous earthquakes.

Damage States	No-damage	Slight	Moderate	Extensive	Complete
Val-des-Bois-ON					
Assets per state	326424.13	127.8	3.53	0.35	0.19
Probability of Exceedance	0.999596	0.000391	0.000011	0.000001	0.000001
Val-des-Bois-QC					
Assets per state	261768.9	86.74	2.76	0.32	0.23
Probability of Exceedance	0.999656	0.000331	0.000011	0.000001	0.000001
Ladysmith-ON					
Assets per state	418059.05	14.42	0.42	0.08	0.03
Probability of Exceedance	0.999964	0.000034	0.000001	0.000000	0.000000
Ladysmith-QC					
Assets per state	139701.5	25.04	1.1	0.21	0.17
Probability of Exceedance	0.999810	0.000179	0.000008	0.000002	0.000001
Mosquito Lake6.2-BC					
Assets per state	56.96	0.04	0	0	0
Probability of Exceedance	0.999298	0.000702	0.000000	0.000000	0.000000
Mosquito Lake6.2-YU					
Assets per state	10159.86	10.7	0.28	0.05	0.01
Probability of Exceedance	0.998915	0.001052	0.000028	0.000005	0.000001
Mosquito Lake6.3-BC					
Assets per state	11.66	0.26	0.04	0.02	0.02
Probability of Exceedance	0.971667	0.021667	0.003333	0.001667	0.001667
Mosquito Lake6.3-YU					
Assets per state	10137.2	5.68	0.12	0	0
Probability of Exceedance	0.999428	0.000560	0.000012	0.000000	0.000000
Nahanni-AB					
Assets per state	5335.28	4.63	0.08	0.01	0
Probability of Exceedance	0.999116	0.000867	0.000015	0.000002	0.000000
Nahanni-BC					
Assets per state	2309.6	1.36	0.04	0	0
Probability of Exceedance	0.999394	0.000588	0.000017	0.000000	0.000000
Nahanni-NWT					
Assets per state	4070.4	4.29	0.22	0.05	0.03
Probability of Exceedance	0.998874	0.001053	0.000054	0.000012	0.000007
Nahanni-YU					
Assets per state	604.72	1.14	0.13	0	0.01
Probability of Exceedance	0.997888	0.001881	0.000215	0.000000	0.000017

To make the results more accessible and understandable, the thesis employs data visualization techniques. In particular, bar charts are used to represent and compare the probability of exceedance for each damage state across all provinces exposed to the five earthquakes being studied. These charts can be found in Figure 5.2 and Figure 5.3.

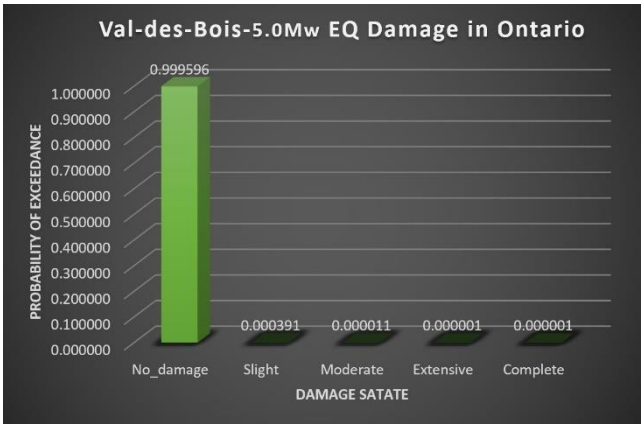

a)

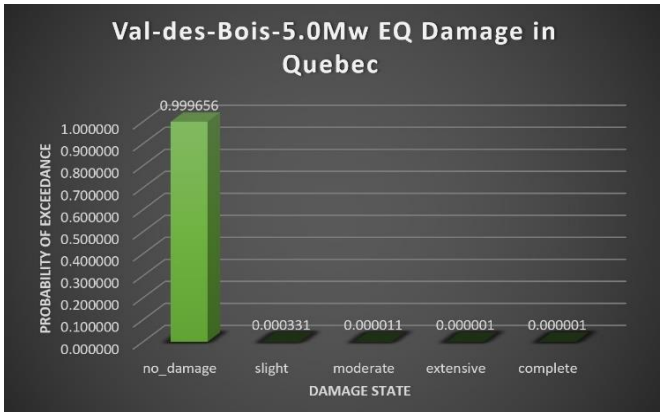

b)

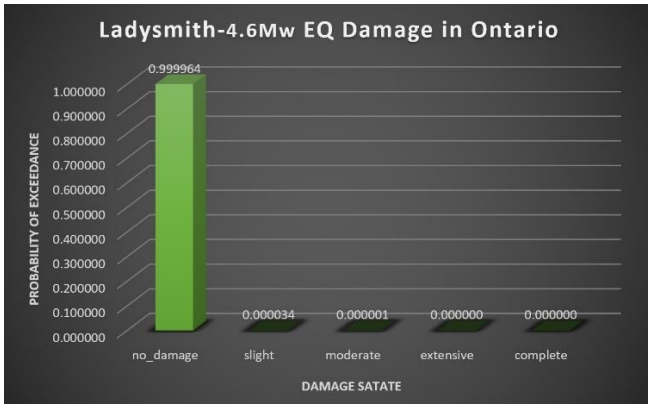

c)

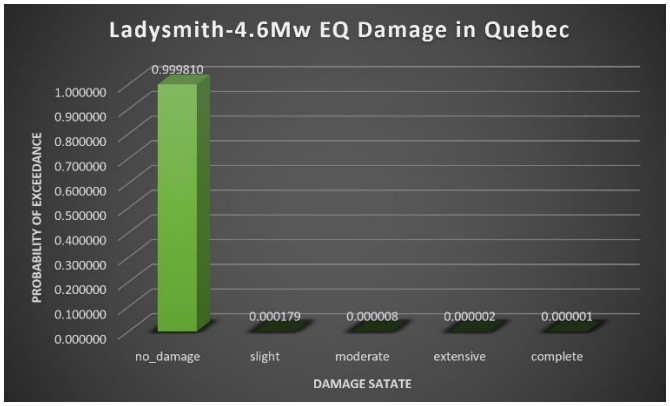

d)

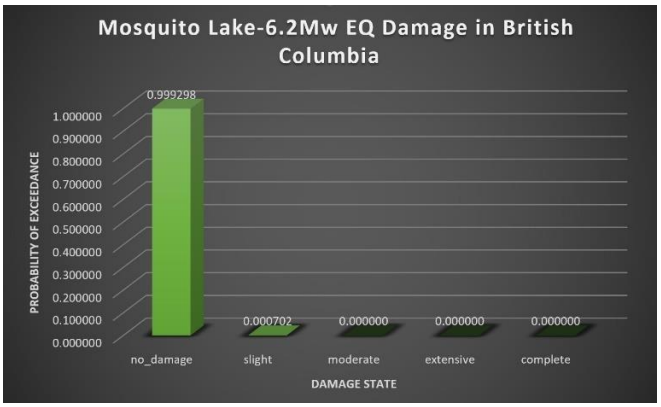

e)

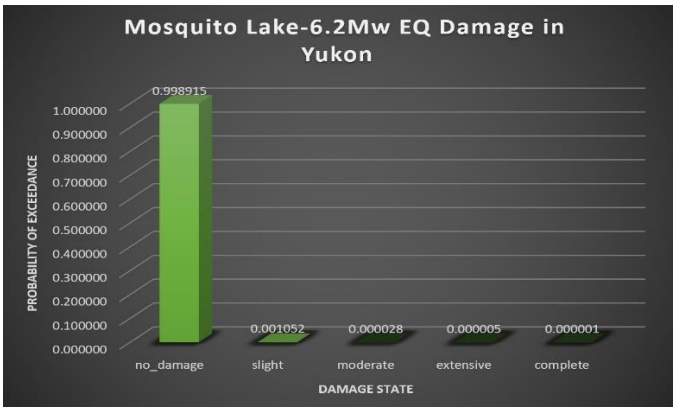

f)

Figure 5.2. The resulted asset damage statistics for a) Val-des-Bois earthquake in Ontario side, b) Val-des-Bois earthquake in Quebec side, c) Ladysmith earthquake in Ontario side, d) Ladysmith earthquake in Quebec side, e) Mosquito Lake-6.2 earthquake in British Columbia side, and f) Mosquito Lake-6.2 earthquake in Yukon side.

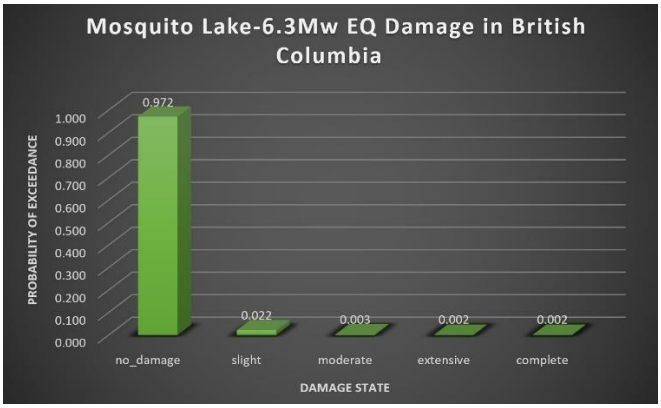

a)

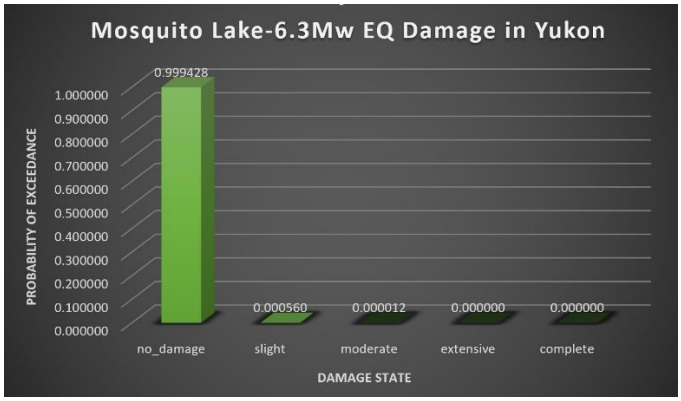

b)

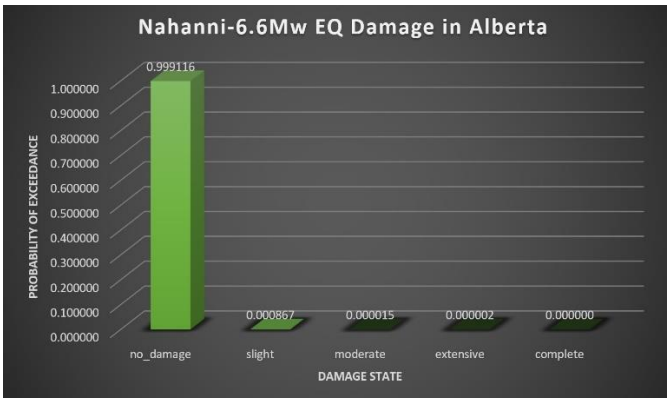

c)

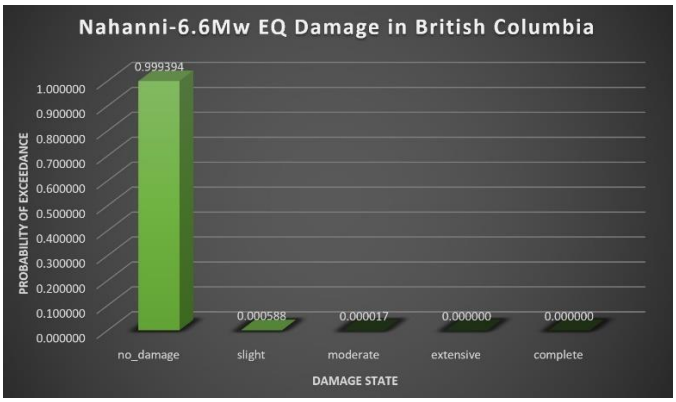

d)

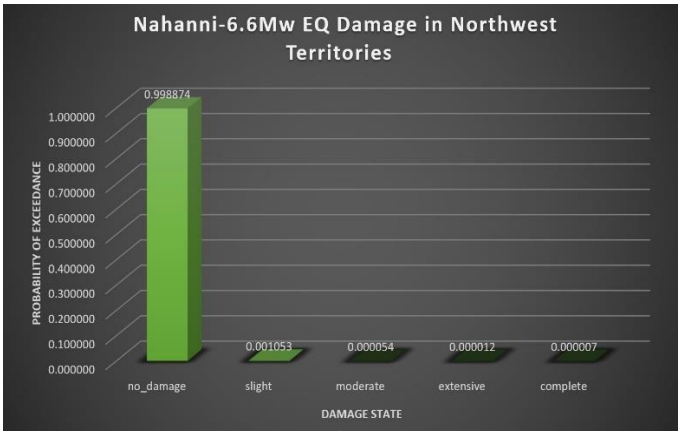

e)

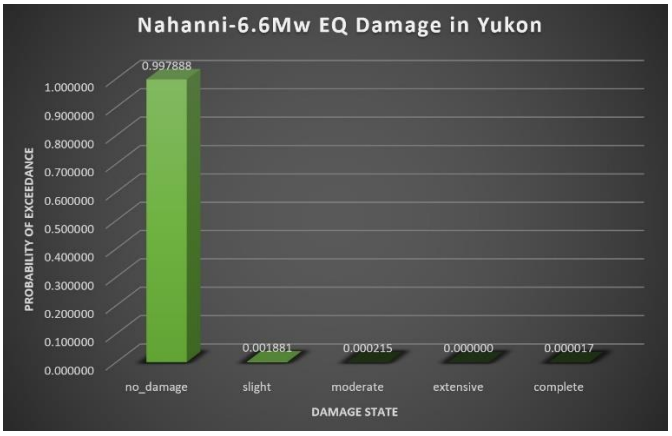

f)

Figure 5.3. The resulted asset damage statistics for a) Mosquito Lake-6.3 earthquake in British Columbia side, b) Mosquito Lake-6.3 earthquake in Yukon side, c) Nahanni earthquake in Alberta side, d) Nahanni earthquake in British Columbia side, e) Nahanni earthquake in Northwest Territories, and f) Nahanni earthquake in Yukon side.

5.3. Mean financial losses and fatalities from scenario risk assessment

5.3.1. Monetary losses

In a seismic risk assessment, estimating losses involves considering three types: monetary loss, human loss, and loss ratio. Monetary losses encompass financial losses resulting from an earthquake and can be direct or indirect (Hallegatte and Przyluski 2010). Direct monetary losses arise from building damage due to ground shaking, while indirect losses result from collateral hazards like tsunamis, landslides, liquefaction, and fire, as well as business interruption (Kircher, Whitman, and Holmes 2006). To calculate these losses, the mean damage factor for each component, which represents the ratio of lost dollars to the replacement value of the building, is multiplied by the corresponding replacement values. The total monetary loss for the building is obtained by summing up the losses from all these components (Cardone et al. 2019).

It's important to note that only direct losses are considered in the study, since calculating indirect losses resulting from collateral hazards, which are associated with business interruption, involves considerable complexity and depends heavily on the estimation of downtime. Additionally, estimating the losses due to business interruption involves assessing the downtime. The time required for repair is just one factor influencing downtime; others include the availability of funds and resources (J. Bommer et al. 2002).

Non-structural damage is determined based on inter-storey drift and floor accelerations but doesn't account for additional issues caused by major structural damage (MDF < 60%). If the structural mean damage factor is greater than or equal to 60%, the monetary losses should be calculated from structural damage only (S. E. Cook 1999). To determine the replacement values for the components, the cost of construction per square meter for a building prototype basis is used.

5.3.2. Casualty estimation

In seismic risk assessment, the main goal is safeguarding human lives. A crucial aspect of this assessment involves estimating the number of casualties resulting from an earthquake. Casualties refer to people who are injured or killed due to the earthquake's impact.

The number of casualties can vary significantly from one earthquake to another, and they can occur through various means. These include structural and non-structural damage, collateral hazards like tsunamis and landslides, heart attacks, car accidents, and other causes. According to Coburn and Spence's book "Earthquake Protection" (2002), building collapse accounts for over 75% of earthquake-related deaths, and if secondary disasters are excluded, building collapse causes almost 90% of such deaths. Secondary disasters refer to collateral hazards (Coburn and Spence 2002). Therefore, it is reasonable to estimate earthquake casualties based on structural damage alone.

To calculate the number of casualties, the population in the building is multiplied by the probability of being in a specific damage state given the earthquake's size and the likelihood of an injury of a certain severity occurring with that damage state (Holzer and Savage 2013). For this purpose, HAZUS defines five damage states: slight, moderate, extensive, complete with collapse,

and complete without collapse (Hazus-MH 2003). These damage states are determined using fragility curves, which express the probability of exceeding a damage state given the spectral displacement or acceleration. The probability of fatalities resulting from these damage states is obtained from casualty rates available in the module (Kircher, Whitman, and Holmes 2006).

To estimate the total number of people killed in the scenario earthquake, the formula considers the probabilities of fatalities for each damage state and the number of occupants in the building at the time of the earthquake. Additionally, the methodology classifies injuries into four severity levels (Kircher, Whitman, and Holmes 2006), which is shown in Table 5.4, ranging from minor injuries requiring medical attention to instantaneous death.

Table 5.4. Injury severity (Kircher, Whitman, and Holmes 2006).

Injury Severity Level	Injury Description
1	Injuries that necessitate simple medical assistance, manageable by non-professionals, usually involving bandages or monitoring. Examples include sprains, deep cuts requiring stitches, minor burns affecting a small area of the body, or non-serious head bumps without loss of consciousness. HAZUS does not provide estimates for injuries of lesser severity that can be self-treated.
2	Injuries that demand extensive medical attention involving advanced medical technologies like x-rays or surgery, yet not anticipated to become life-threatening. Instances include third-degree burns, substantial second-degree burns on significant body areas, head bumps leading to loss of consciousness, fractured bones, severe dehydration, or exposure-related injuries.
3	Injuries with the potential to be immediately life-threatening if not promptly and properly addressed include uncontrolled bleeding, punctured organs, internal injuries, spinal column injuries, and crush syndrome.
4	Immediately killed or fatally wounded.

5.3.3. Loss output

The findings from the scenario risk assessment in this thesis yield the following results:

- ***Excel Spreadsheet Files (.csv):*** Four files with .csv extensions have been generated, containing the following information:
  - *Selected Events Information:* This file contains information identical to that of the scenario damage assessment.
  - *Aggregate Event Losses:* These files provide insights into the four types of losses resulting from the selected events. They offer a breakdown of financial losses in CAD based on these events.
  - *Average Asset Losses:* This Excel file presents data on the monetary loss among assets with different taxonomy in each DAUID. Asset losses are categorized into four types: structural, non-structural, contents, and occupants. It is important to note that the first three mentioned loss types are in CAD, whereas the last type refers to the rate of

fatalities. Fatalities are quantified as the sum of probabilities of death, equating to the expected number of deaths across the study area, rounded to the nearest integer.

- *Average Asset Losses:* This file contains the cumulative financial losses for the entire province, categorized into four types of loss.

- ***HDF5 Files (.hdf5):*** Two files in the .hdf5 format were created as part of the assessment process to visualize economic losses in different ranges of million USD figures in the form of maps.

- ***Text Files (.rst):*** In addition to the aforementioned files, there are text files that contain a comprehensive report of the calculations.

Table 5.5 presents the average results for the five previous earthquake scenarios in terms of total financial losses and fatalities. The data used for these calculations is derived from USGS shakemap and integrated into the CanadaSRM1 model, which was developed in 2016. This means that these acquired results should be adjusted to the date of occurrence and then compared with observed data. This step is explained in detail in Chapter 6.

To make the results more accessible and understandable, the thesis employs data visualization techniques. In particular, bar charts are used to represent and compare the amount of loss for each loss type across all provinces exposed to the five earthquakes being studied. These charts can be found in Figure 5.4 and Figure 5.5.

Table 5.5. Financial loss and Fatality results in USD for loss values, exposed values and loss ratio for five previous earthquakes.

Loss Type	Structural	Non-structural	Contents	Occupants
Val-des-Bois-ON				
Loss Value	405385	2575340	61392	0
Exposed Value	61047600000	171010000000	39098200000	1255170
Loss Ratio	0.000007	0.000015	0.000002	0.000000
Val-des-Bois-QC				
Loss Value	435694	2631990	82971	0
Exposed Value	37102000000	111658000000	21933800000	803915
Loss Ratio	0.000012	0.000024	0.000004	0.000000
Ladysmith-ON				
Loss Value	405385	2575340	61392	0
Exposed Value	61047600000	171010000000	39098200000	1255170
Loss Ratio	0.000007	0.000015	0.000002	0.000000
Ladysmith-QC				
Loss Value	207873	950170	59400	0
Exposed Value	19756000000	60965800000	11354700000	439094
Loss Ratio	0.000011	0.000016	0.000005	0.000000
Mosquito Lake6.2-BC				
Loss Value	2740	6570	327	0
Exposed Value	39000000	109000000	36900000	908
Loss Ratio	0.000070	0.000060	0.000009	0.000000
Mosquito Lake6.2-YU				
Loss Value	16419	108103	2026	0
Exposed Value	2161700000	6109900000	1402600000	28854
Loss Ratio	0.000008	0.000018	0.000001	0.000000
Mosquito Lake6.3-BC				
Loss Value	1790	4120	222	0
Exposed Value	924000	3110000	370000	15
Loss Ratio	0.001940	0.001320	0.000602	0.000000
Mosquito Lake6.3-YU				
Loss Value	4730	36500	579	0
Exposed Value	2160000000	6110000000	1400000000	28900
Loss Ratio	0.000002	0.000006	0.000000	0.000000
Nahanni-AB				
Loss Value	94	459	15	0
Exposed Value	1584070000	3643250000	1364800000	24290
Loss Ratio	0.0000001	0.0000001	0.0000000	0.0000000
Nahanni-BC				
Loss Value	17	333	5	0
Exposed Value	532000000	1420000000	411000000	532276000
Loss Ratio	0.00000003	0.00000023	0.00000001	0.00000000
Nahanni-NWT				
Loss Value	21486	105644	4754	0
Exposed Value	1436130000	3809300000	1121150000	11693
Loss Ratio	0.000015	0.000028	0.000004	0.000000
Nahanni-YU				
Loss Value	218	1831	23	0
Exposed Value	137383000	419564000	92320100	1107
Loss Ratio	0.000002	0.000004	0.000000	0.000000

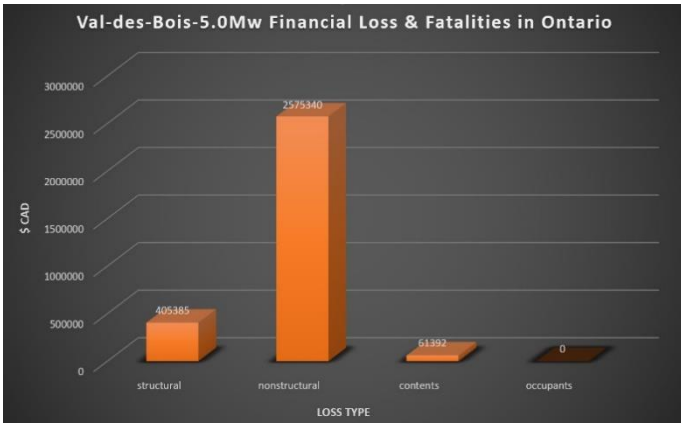

a)

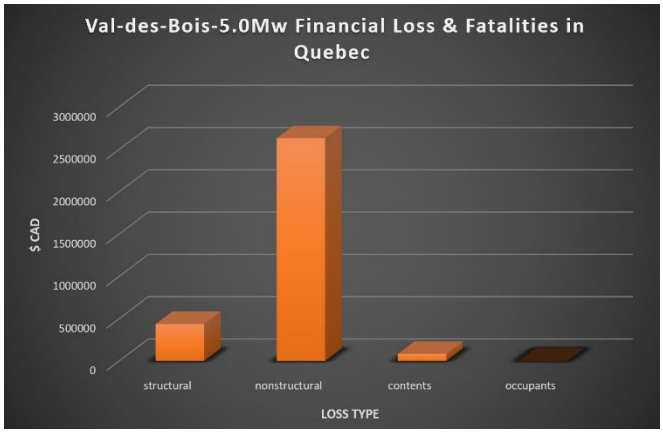

b)

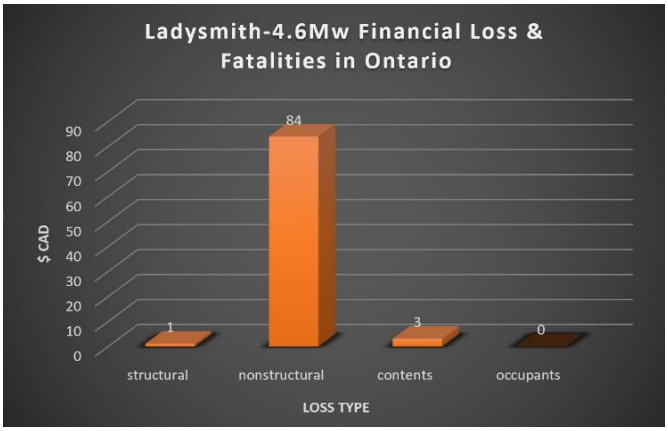

c)

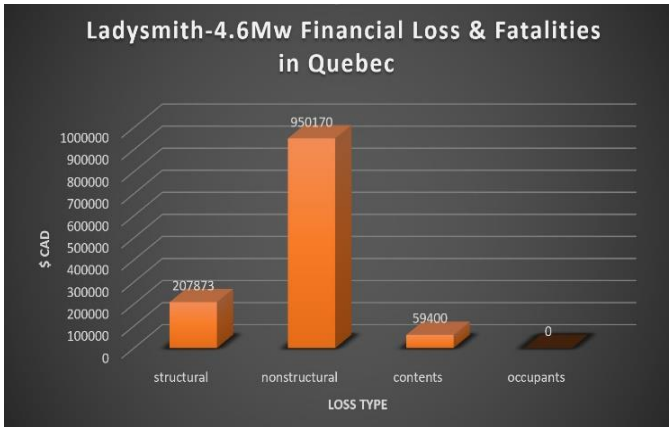

d)

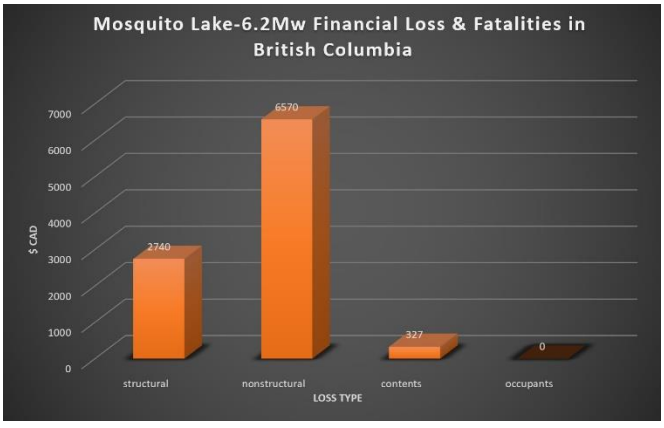

e)

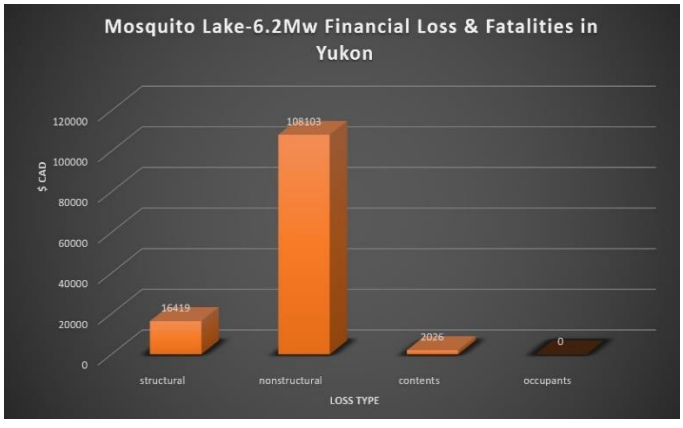

f)

Figure 5.4. The resulted financial losses and fatalities for a) Val-des-Bois earthquake in Ontario side, b) Val-des-Bois earthquake in Quebec side, c) Ladysmith earthquake in Ontario side, d) Ladysmith earthquake in Quebec side, e) Mosquito Lake-6.2 earthquake in British Columbia side, and f) Mosquito Lake-6.2 earthquake in Yukon side.

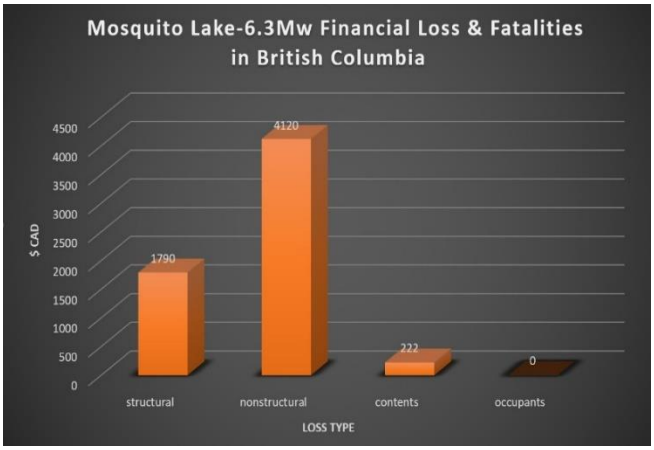

a)

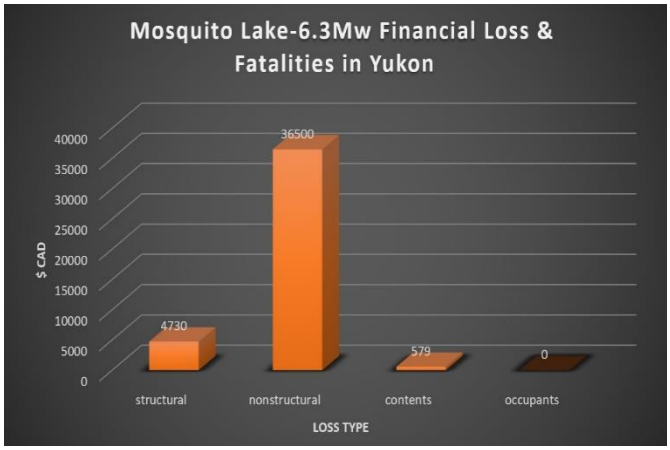

b)

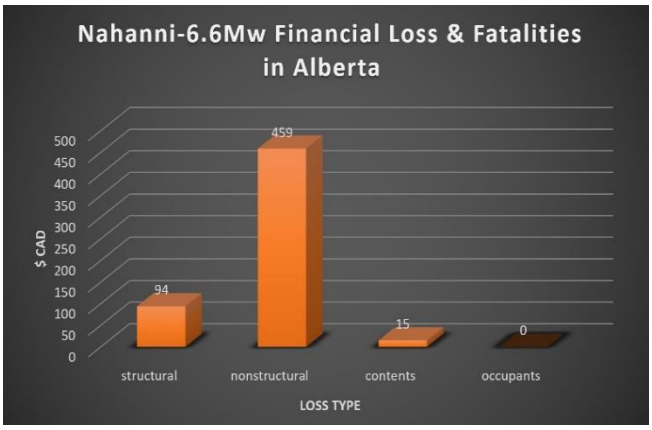

c)

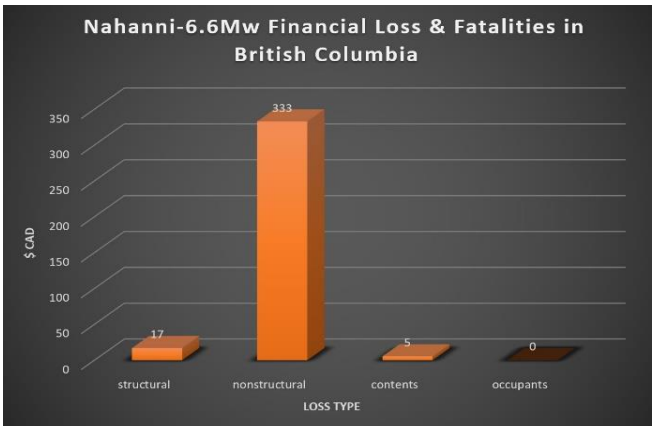

d)

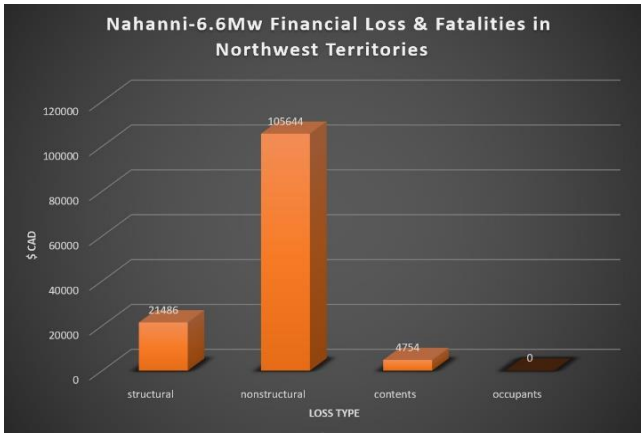

e)

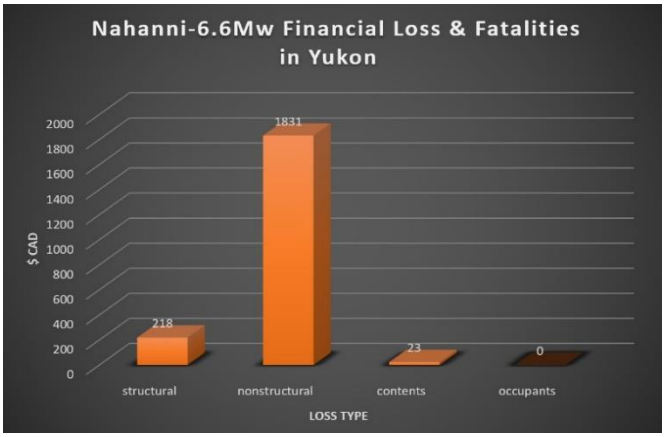

f)

Figure 5.5. The resulted financial losses and fatalities for a) Mosquito Lake-6.3 earthquake in British Columbia side, b) Mosquito Lake-6.3 earthquake in Yukon side, c) Nahanni earthquake in Alberta side, d) Nahanni earthquake in British Columbia side, e) Nahanni earthquake in Northwest Territories, and f) Nahanni earthquake in Yukon side.

Chapter 6 : Discussion and Evaluation

6.1. Introduction

This chapter comprises three key sections: an in-depth discussion of acquired results in the western, eastern, and northern regions of Canada, followed by an account of the processing steps involved in adjusting the estimated outcomes. The final section conducts a comparative analysis, aligning the adjusted results with observed impacts to validate CanadaSRM1, thereby fulfilling the primary objective of this thesis.

6.2. Output discussion

6.2.1. Scenario damage output – damage maps and statistics

Through the application of data visualization techniques, insights can be gleaned regarding the estimated quantities of buildings experiencing varying degrees of damage. This analytical process is underpinned by the utilization of fragility functions, which yield four distinct damage maps for each seismic event, each illustrating diverse levels of structural impairment on a spatial map. Figure 6.1 to Figure 6.5 provide graphical representations of the damage maps obtained through the adept utilization of OQ Plugin, QGIS, and Python. These visualizations elucidate the relative proportions of buildings categorized into four damage states: slight damage, moderate damage, extensive damage, and complete damage, with each figure corresponding to a specific seismic event. It is crucial to emphasize that the extent of damage within each geographical region is not only contingent upon the intensity of ground shaking or the proximity to the epicenter. Instead, it hinges upon various factors, including the nature of the residential structures, their construction materials, the age of the assets, and whether retrofit measures have been implemented.

6.2.1.1. Val-des-Bois earthquake damages

In Figure 6.1, the damage distribution maps resulting from the 2010 Val-des-Bois earthquake portray the effects of this seismic event in Ontario and Quebec. It is important to note that the intensity conveyed by the reddish hues within these maps directly indicates the severity of the damage sustained in the affected regions. This categorization not only facilitates the assessment of immediate impacts but also informs subsequent disaster response and recovery efforts. The distribution of damage from this earthquake is summarized in Table 6.1.

In the case of 'Slight Damage' on the Ontario side, Ottawa, a large and densely populated city, is the most heavily impacted area, with approximately 93 buildings experiencing slight damage. Following Ottawa, Clarence-Rockland, located in close proximity to the epicenter and the nearest urban area in Ontario, has almost 7 affected buildings. Additionally, North Grenville and North Dundas each have almost 1 building suffering from slight damage. In more distant regions, South Stormont and North Glengarry each have almost 2 buildings with damage, while Cornwall, situated in the southern part of the model, experienced slight damage in 4 buildings. Perth, a small area in the southwest of the Ontario model, also experienced minor impact from the earthquake.

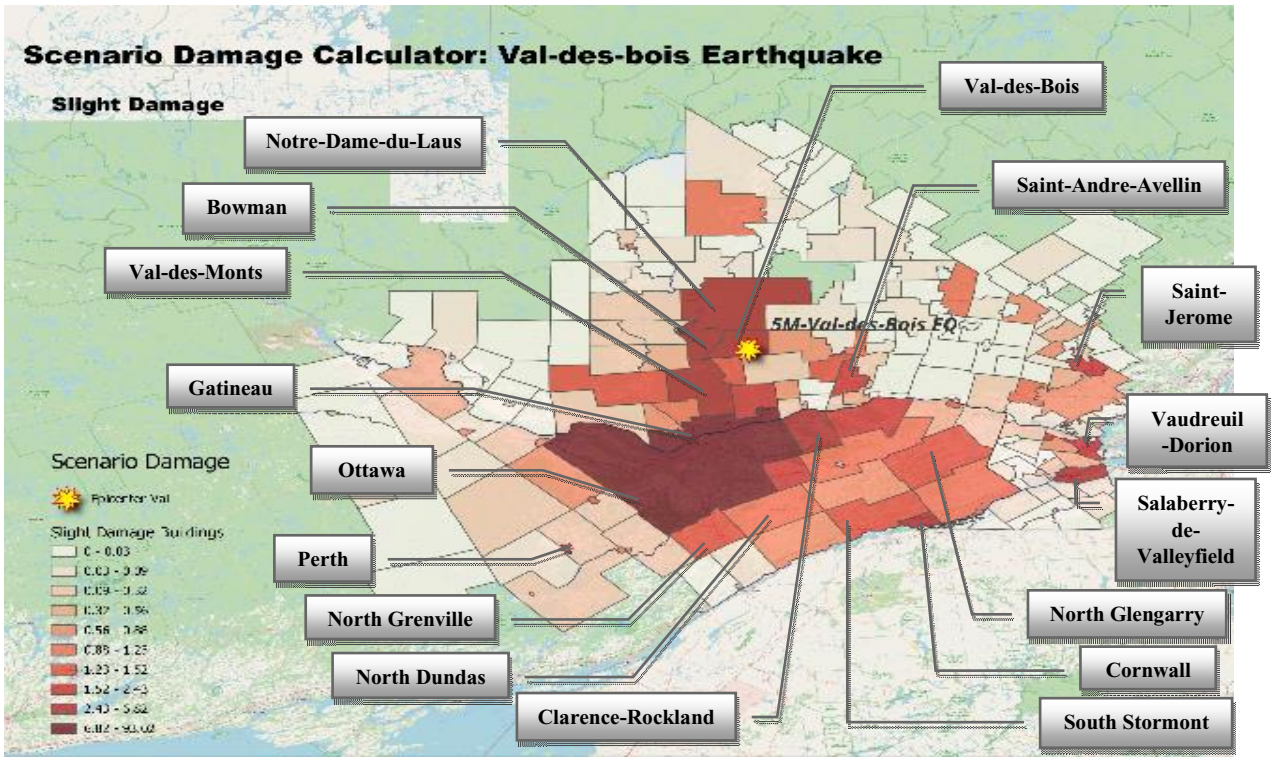
Scenario Damage Calculator: Val-des-bois Earthquake
Slight Damage
Notre-Dame-du-Laus
Bowman
Val-des-Monts
Gatineau
Ottawa
Perth
North Grenville
North Dundas
Clarence-Rockland
Val-des-Bois
Saint-Andre-Avellin
5M-Val-des-Bois EQ
Saint-Jerome
Vaudreuil-Dorion
Salaberry-de-Valleyfield
North Glengarry
Cornwall
South Stormont
Scenario Damage
Epicenter Val
Slight Damage Buildings

a)

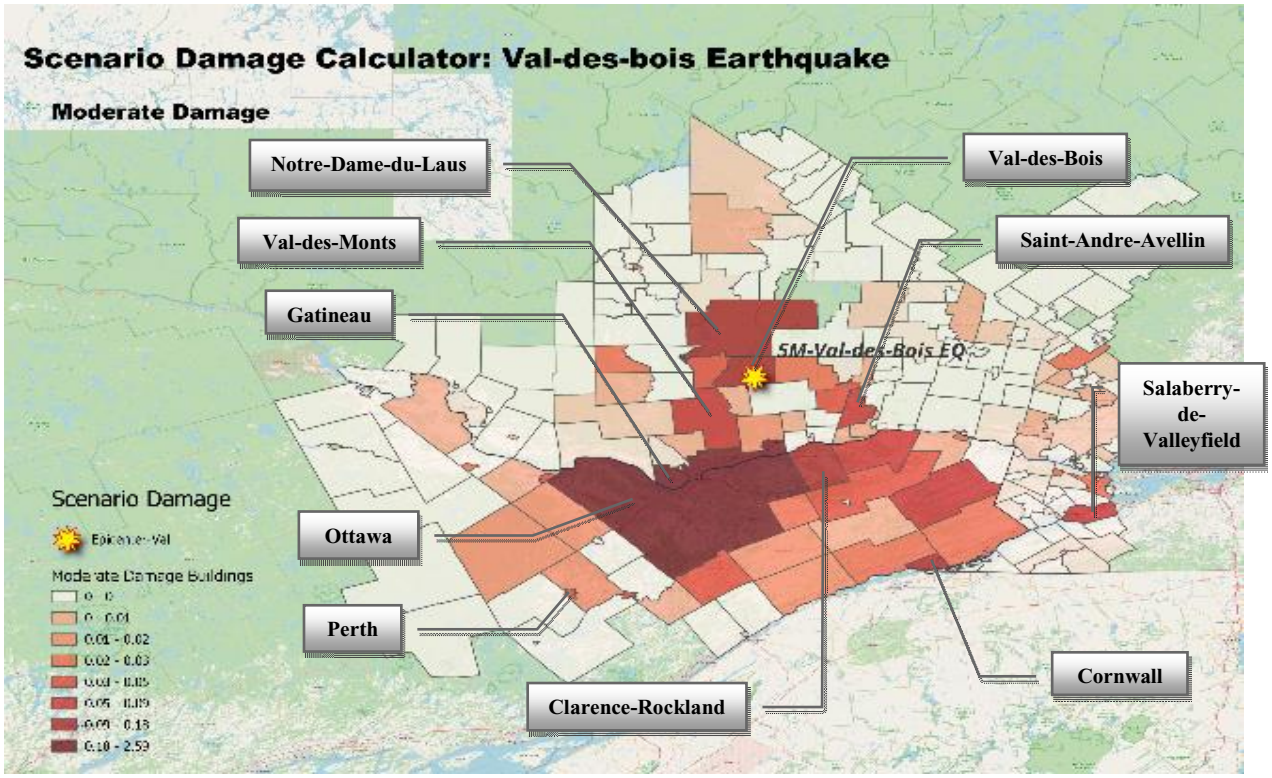
Scenario Damage Calculator: Val-des-bois Earthquake
Moderate Damage
Notre-Dame-du-Laus
Val-des-Monts
Gatineau
Ottawa
Perth
Clarence-Rockland
Val-des-Bois
Saint-Andre-Avellin
5M-Val-des-Bois EQ
Salaberry-de-Valleyfield
Cornwall
Scenario Damage
Moderate Damage Buildings
0.01 - 0.02
0.02 - 0.03
0.10 - 2.59

b)

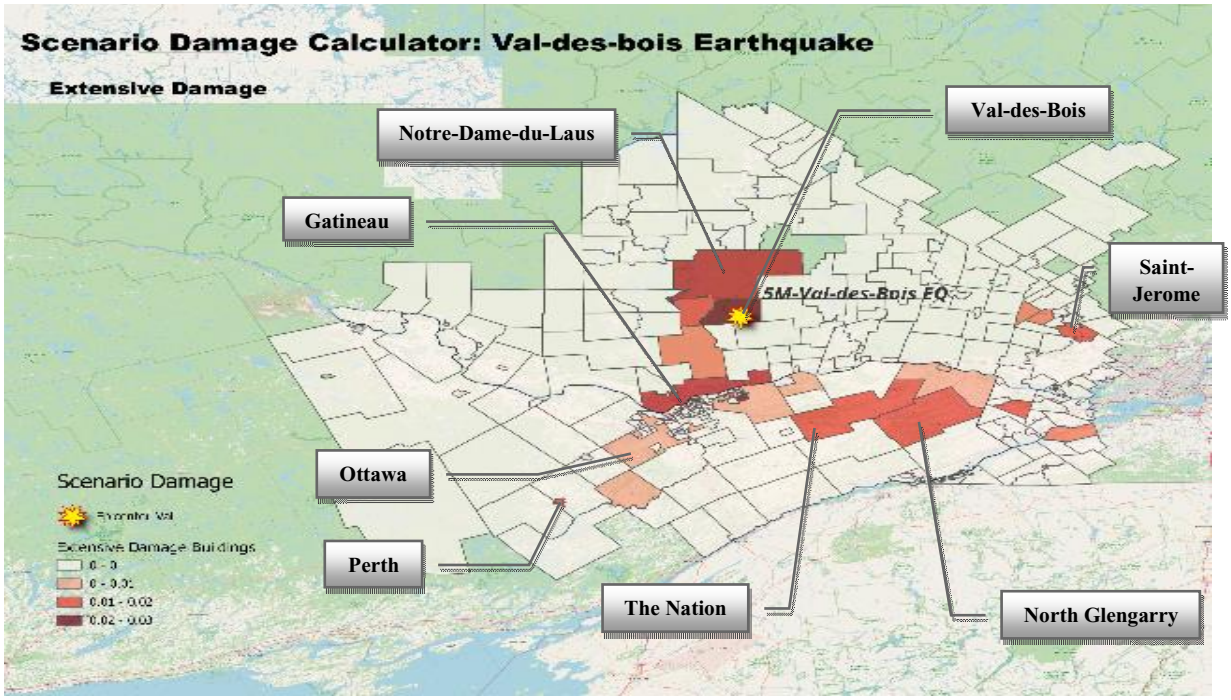

c)

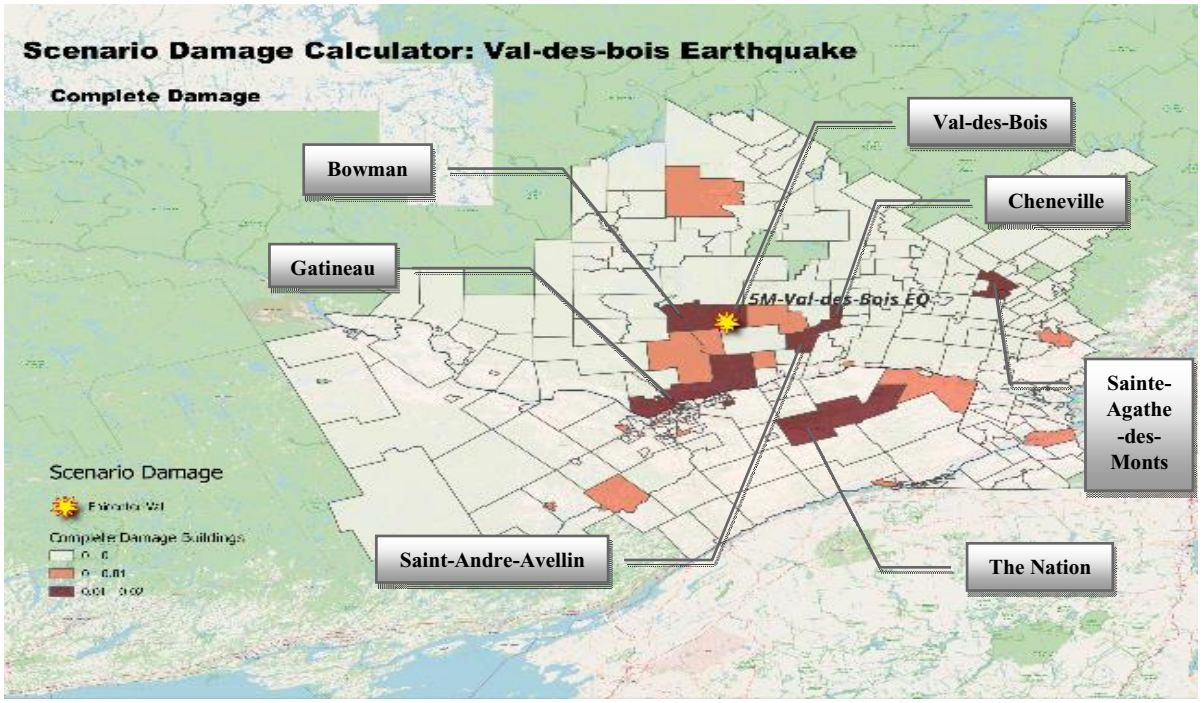

d)

Figure 6.1. Damage distribution maps of Val-des-Bois earthquake. These images are estimated by SDC in 4 different damage states. a) slight damage, b) moderate damage, c) extensive damage, and d) complete damage (collapse). Color scheme, with its varying shades of red, serves as a visual aid in intuitively conveying the severity of the damages incurred, with deeper shades of red indicating more profound damage, and lighter shades signifying less severe impact.

On the Quebec side, the figure reveals that Gatineau, despite being somewhat distant from the epicenter, has 27 affected buildings. Val-des-Bois, the epicenter itself, is expected to have 6 slightly damaged buildings. Bowman to the west, Notre-Dame-du-Laus to the north, and Val-des-Monts to the south of the epicenter each have 4 damaged buildings. Saint-Andre-Avellin, not in close proximity to the epicenter, has 2 damaged buildings. In the southeast of the Quebec model, Salaberry-de-Valleyfield, located far from the epicenter, has 4 damaged buildings. Saint-Jerome, also distant from the epicenter, has 3 damaged buildings, and Vaudreuil-Dorion, also situated far from the epicenter, has 2 damaged buildings.

Table 6.1. Damage distribution summary of 2010 Val-des-Bois earthquake estimated by SDC ("Google Earth" n.d.), (Government of Canada 2022, Canadian census 2011).

`Community Name	Distance-Epicenter (km)	Population	Structural Damages			
			Slight	Moderate	Extensive	Complete
Ontario Provinces/Territories						
Ottawa	89	1,218,000	93	3	3	-
Clarence-Rockland	69	23,185	7	1	-	-
North Grenville	148	15,085	1	-	-	-
North Dundas	147	11,225	1	-	-	-
South Stormont	178	12,617	2	-	-	-
North Glengarry	157	10,251	2	-	< 1	-
Cornwall	191	45,508	4	1	-	-
Perth	173	5,840	< 1	< 1	< 1	-
The Nation	distant	-	-	-	< 1	-
Quebec Provinces/Territories						
Gatineau	67	265,349	27	26	-	< 1
Val-des-Bois	**Epicenter**	938	6	6	2	< 1
Bowman	7	677	4		-	< 1
Notre-Dame-du-Laus	27	1,518	4	4	1	-
Val-des-Monts	39	10,420	4	4	-	-
Saint-Andre-Avellin	87	1,876	2	2	-	< 1
Salaberry-de-Valleyfield	198	38,323	4	4	-	-
Saint-Jerome	173	69,598	3	-	< 1	-
Vaudreuil-Dorion	176	33,305	2	-	-	-
Cheneville	99	792	-	-	-	< 1
Sainte-Agathe-des-Monts	218	6,226	-	-	-	< 1

In the case of 'Moderate Damage', Ottawa has 3 affected buildings, Clarence-Rockland almost 1, Cornwall 1, and Perth has also been somewhat affected on the Ontario side. On the Quebec side, once again, the most affected area is Gatineau, with 26 damaged buildings. Val-des-Bois has 6 damaged buildings, Notre-Dame-du-Laus has 4, Val-des-Monts has 4, and Saint-Andre-Avellin has 2 damaged buildings. In the southeast of the Quebec model, Salaberry-de-Valleyfield has 4 damaged buildings.

Val-des-Bois has 2 damaged buildings, Notre-Dame-du-Laus has one damaged building, and Saint-Jerome has less than one damaged building, all experiencing 'Extensive Damage' on the Quebec side. However, on the Ontario side, Ottawa has 3 damaged buildings. The Nation, North Glengarry, and Perth have also been somewhat affected by extensive damage. Regarding 'Complete Damage', the model estimates no affected areas on the Ontario side. However, areas around the epicenter, such as Val-des-Bois, Bowman, Saint-Andre-Avellin, Gatineau, and Cheneville, along with Sainte-Agathe-des-Monts located far from the epicenter on the Quebec side, are all estimated by the model to have a possibility of less than 1% complete damage.

6.2.1.2. Ladysmith earthquake damages

Figure 6.2 provides an overview of the damage distribution resulting from the 2013 Ladysmith earthquake. In the category of 'Slight Damage' in Ontario, Ottawa, situated to the south of the epicenter, has reported damage in 9 buildings. Russell, located to the east of Ottawa, has 1 building with slight damage. Similarly, Cornwall, positioned far from the epicenter in the southern part of Ontario, has 1 affected building. Other areas around Ottawa, including South Frontenac, North Grenville, and Clarence-Rockland, as well as Mississippi Mills and Rideau Lakes in the southern part of Ontario, have also experienced slight damage. North Glengarry, situated far from the epicenter in the western part of Ontario, reports slight damage as well.

On the Quebec side, the epicenter in Thorne has witnessed slight damage in 5 buildings. Otter Lake, to the north of the epicenter, has 4 affected buildings, while La Pêche, located to the east of the epicenter, has 3 buildings displaying slight damage. Gatineau, situated far from the epicenter but in the vicinity above Ottawa, has 3 affected buildings. Additionally, Clarendon, to the south of the epicenter, has 2 buildings with slight damage, and L'Ile-du-Grand, near the epicenter, reports 1 affected building.

Moving on to the 'Moderate Damage' category, on the Ontario side, Ottawa has experienced damage in 1 building, while Hastings Highlands, located far from the epicenter in the southwest of Ontario, has also reported moderate damage. In Quebec, Thorne has 1 building with moderate damage. La Pêche, Clarendon, and Otter Lake, have also seen moderate damage. For 'Extensive Damage', the Ontario region reports 1 building in Ottawa and 1 building in Cornwall, both situated very far from the epicenter. In Quebec, Thorne has 1 building with extensive damage. Otter Lake, La Pêche, and Kazabazua, have also experienced extensive damage. There are no reported instances of 'Complete Damage' in Ontario, except in Ottawa. In Quebec, neither the epicenter in Thorne nor L'Ile-du-Grand has experienced complete damage. The distribution of damage from this earthquake is summarized in Table 6.2.

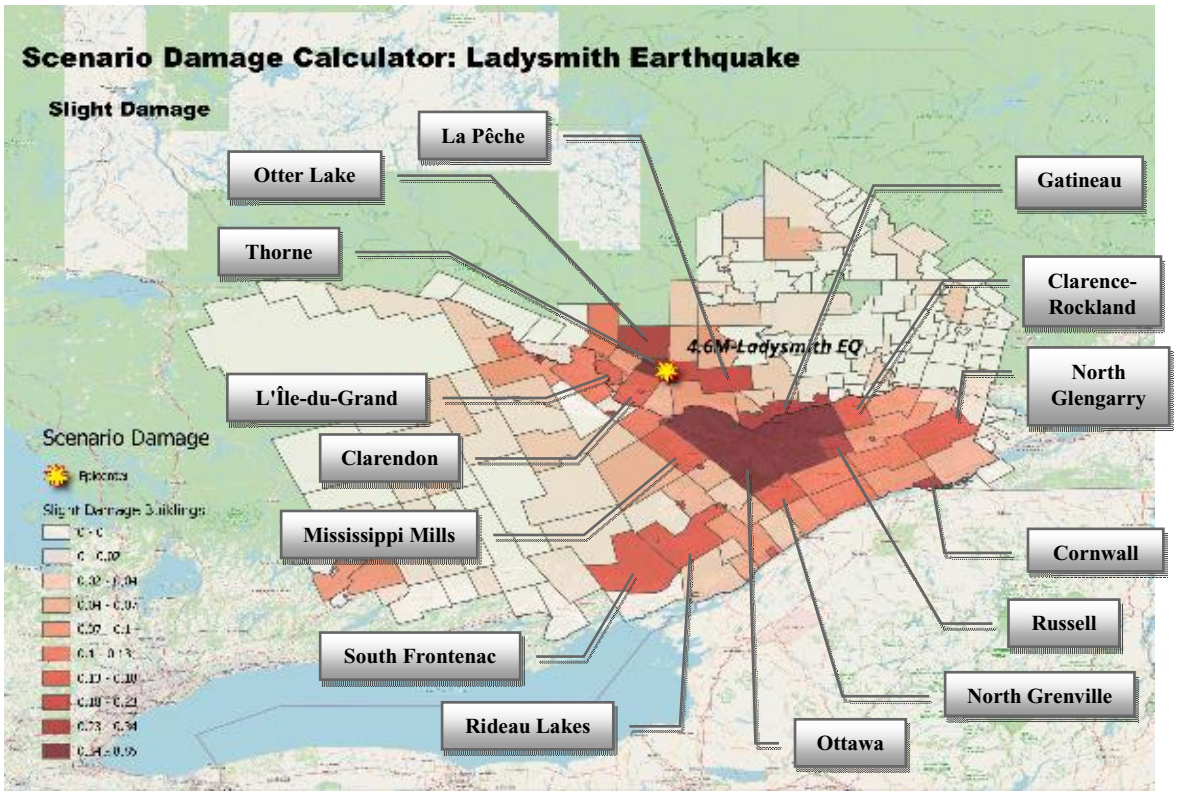
Scenario Damage Calculator: Ladysmith Earthquake
Slight Damage
La Pêche
Otter Lake
Gatineau
Thorne
Clarence-Rockland
4.6M Ladysmith EQ
North Glengarry
L'Île-du-Grand
Scenario Damage
Clarendon
Mississippi Mills
Cornwall
Russell
South Frontenac
North Grenville
Rideau Lakes
Ottawa

a)

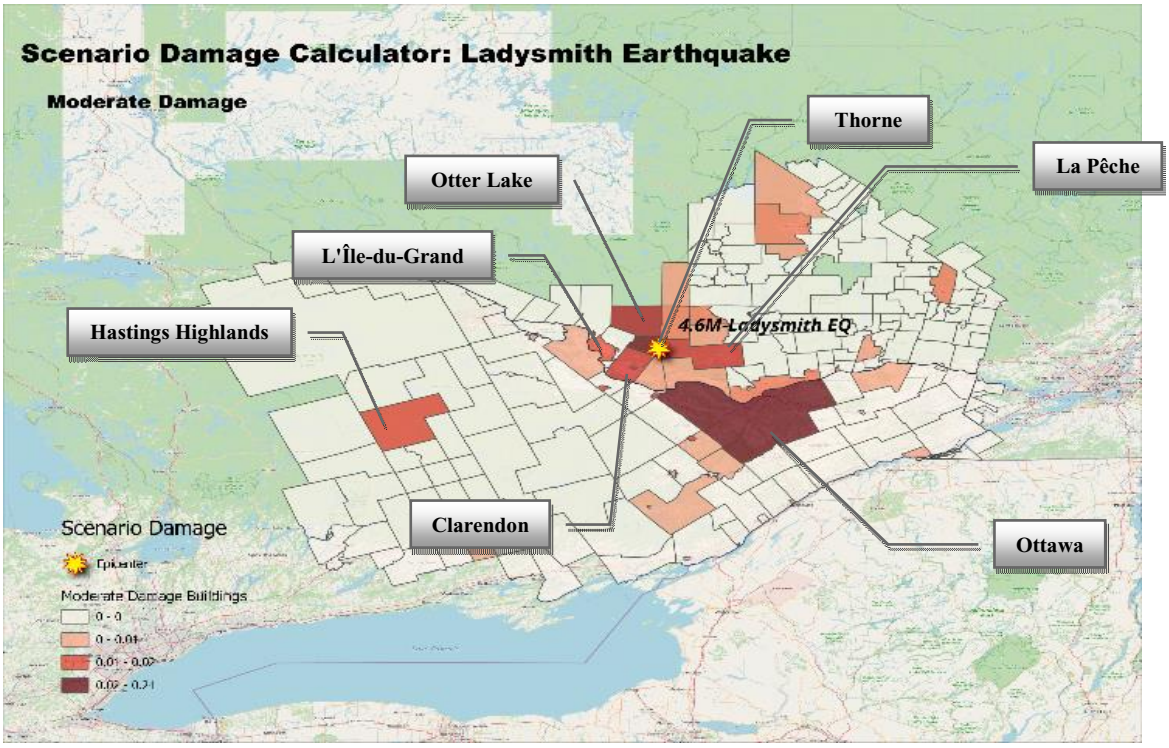
Scenario Damage Calculator: Ladysmith Earthquake
Moderate Damage
Thorne
Otter Lake
La Pêche
L'Île-du-Grand
Hastings Highlands
4.6M Ladysmith EQ
Scenario Damage
Clarendon
Ottawa
Moderate Damage Buildings

b)

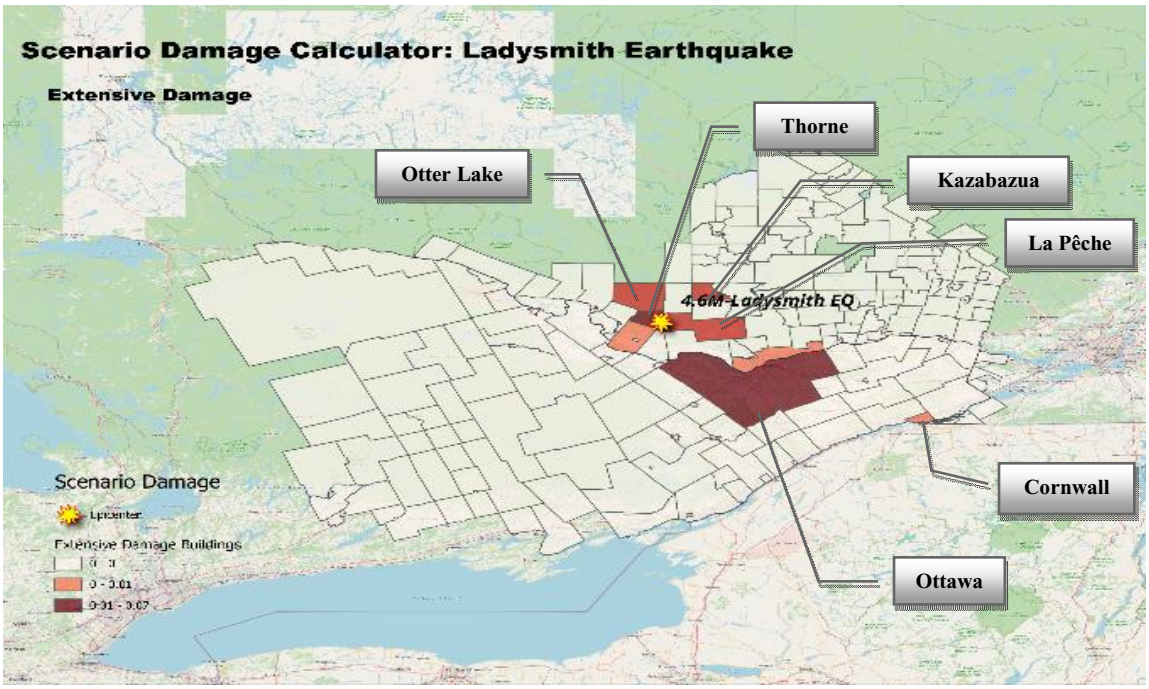

c)

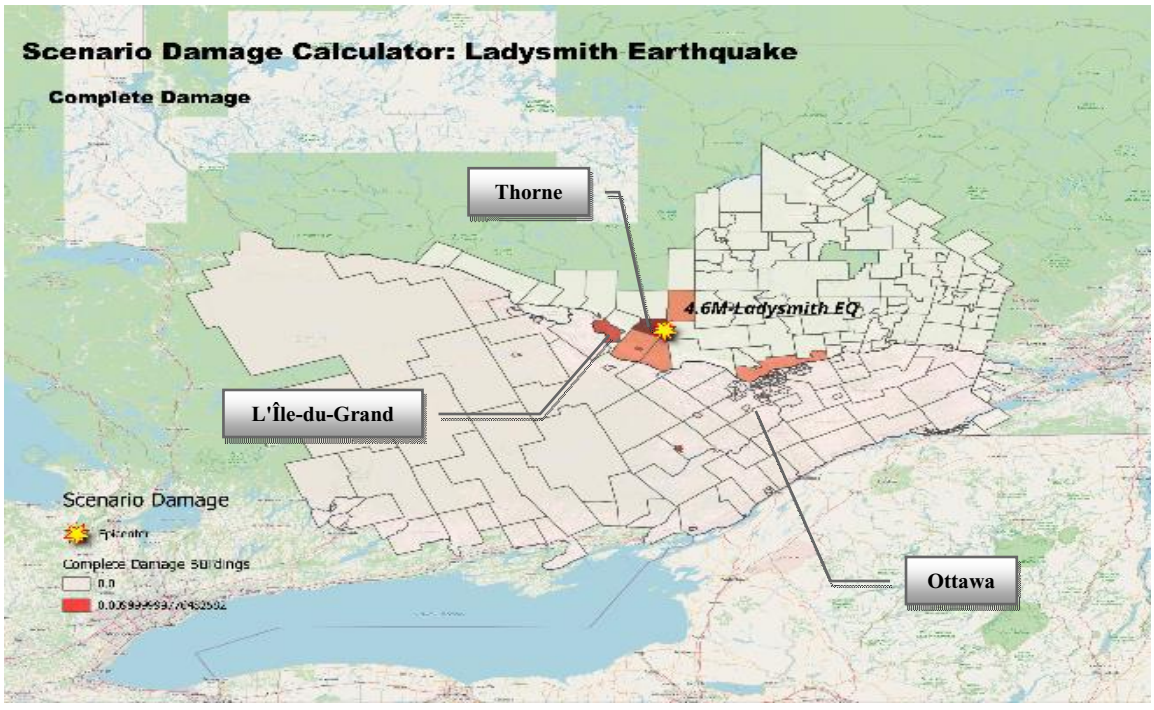

d)

Figure 6.2. Damage distribution maps of Ladysmith earthquake. These images are estimated by SDC in 4 different damage states. a) slight damage, b) moderate damage, c) extensive damage, and d) complete damage (collapse). Color scheme, with its varying shades of red, serves as a visual aid in intuitively conveying the severity of the damages incurred, with deeper shades of red indicating more profound damage, and lighter shades signifying less severe impact.

Table 6.2. Damage distribution summary of 2013 Ladysmith earthquake estimated by SDC ("Google Earth" n.d.), (Government of Canada 2022, Canadian census 2016).

Community Name	Distance-Epicenter (km)	Population	Structural Damages			
			Slight	Moderate	Extensive	Complete
Ontario Provinces/Territories						
Ottawa	79	1,218,000	9	1	1	-
Russell	118	16,520	1	-	-	-
Cornwall	191	45,508	1	-	1	-
South Frontenac	225	18,113	< 1	-	-	-
North Grenville	148	15,085	1	-		-
Clarence-Rockland	69	23,185	7	1	-	-
Mississippi Mills	112	13,163	< 1	-	-	-
Rideau Lakes	184	10,326	< 1	-	-	-
North Glengarry	157	10,251	< 1	-	< 1	-
Hastings Highlands	184	4,078	-	< 1	-	-
Quebec Provinces/Territories						
Thorne	**Epicenter**	448	5	1	1	-
Otter Lake	16	932	4	1	< 1	-
La Pêche	45	7,863	3	1	< 1	-
Gatineau	67	265,349	3	26	-	-
Clarendon	21	1,256	2	< 1	-	-
L'Ile-du-Grand	40	626	1	-	-	-
Kazabazua	52	945	-	-	< 1	-

6.2.1.3. Nahanni earthquake damages

Figure 6.3 presents an overview of the damage distribution resulting from the 1985 Nahanni earthquake. In the category of 'Slight Damage', Grande Prairie in Alberta, situated a considerable distance from the epicenter, has reported damage in one building. Similarly, Peace River, a very small and remote area located far from the epicenter, has one building with slight damage. Athabasca has also been affected in this category. Moving to British Columbia, the Northern Rockies region has experienced slight damage in one building, and Prince George and Bulkley Valley are also included in this category. In the Northwest Territories, the Nahanni National Park Reserve, the epicenter itself, has encountered slight damage in two buildings. Additionally,

Sambaa Lake has reported damage in one building. In the Yukon territory, 4 buildings situated far from the epicenter have sustained slight damage.

In the 'Moderate Damage' category, on the Alberta side, Peace River has experienced moderate damage. In British Columbia, Prince George reports moderate damage. In the Northwest Territories, both the Nahanni National Park Reserve and Sambaa Lake have sustained moderate damage. There are no reported instances of moderate damage in the Yukon region. For 'Extensive Damage', on the Alberta side, Grande Prairie, has reported extensive damage. However, in British Columbia, there are no areas reporting extensive damage. In the Northwest Territories, the Nahanni National Park Reserve has experienced extensive damage in one building, and Sambaa Lake has also reported extensive damage in one building. There are no reported instances of extensive damage in the Yukon region. In the 'Complete Damage' category, there are no estimated reports of complete damage in Alberta, British Columbia, Northwest Territories, or the Yukon region. The distribution of damage from this earthquake is summarized in Table 6.3.

Table 6.3. Damage distribution summary of 1985 Nahanni earthquake estimated by SDC ("Google Earth" n.d.), (Government of Canada 2022, Canadian census 1986).

Community Name	Distance-Epicenter (km)	Population	Structural Damages			
			Slight	Moderate	Extensive	Complete
Alberta Provinces/Territories						
Grande Prairie	904	26,471	1	-	< 1	-
Peace River	953	6,355	1	< 1	-	-
Athabasca	1,288	2,990	< 1	-	-	-
British Columbia Provinces/Territories						
Northern Rockies	312	5,856	1	-	-	-
Prince George	1,127	67,621	1	< 1	-	-
Bulkley Valley	1,496	5,256	1	-	-	-
Northwest-Territories Provinces/Territories						
Nahanni National Park Reserve	**Epicenter**	775	2	< 1	1	-
Sambaa Lake	281	54	1	< 1	1	-
Yukon Provinces/Territories						
North of Yukon	1,625		4	-	-	-

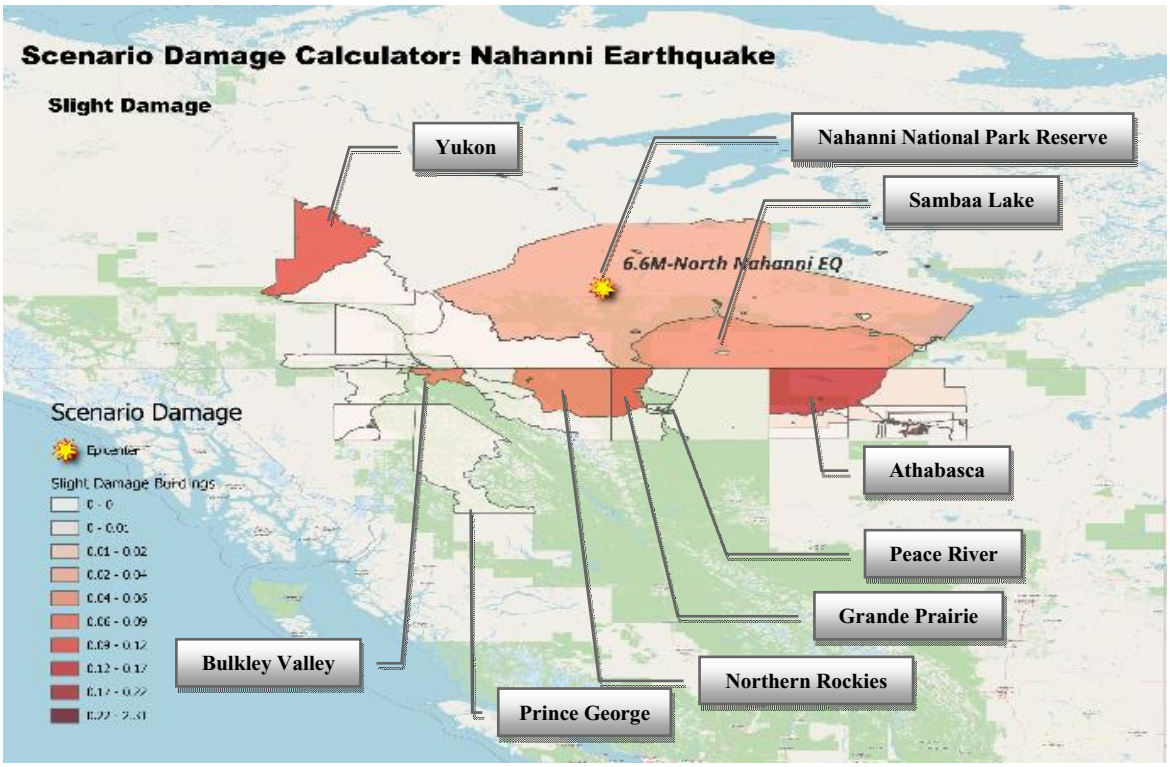
Scenario Damage Calculator: Nahanni Earthquake
Slight Damage
Yukon
Nahanni National Park Reserve
Sambaa Lake
6.6M-North Nahanni EQ
Scenario Damage
Epicenter
Slight Damage Buildings
Athabasca
Peace River
Grande Prairie
Bulkley Valley
Northern Rockies
Prince George

a)

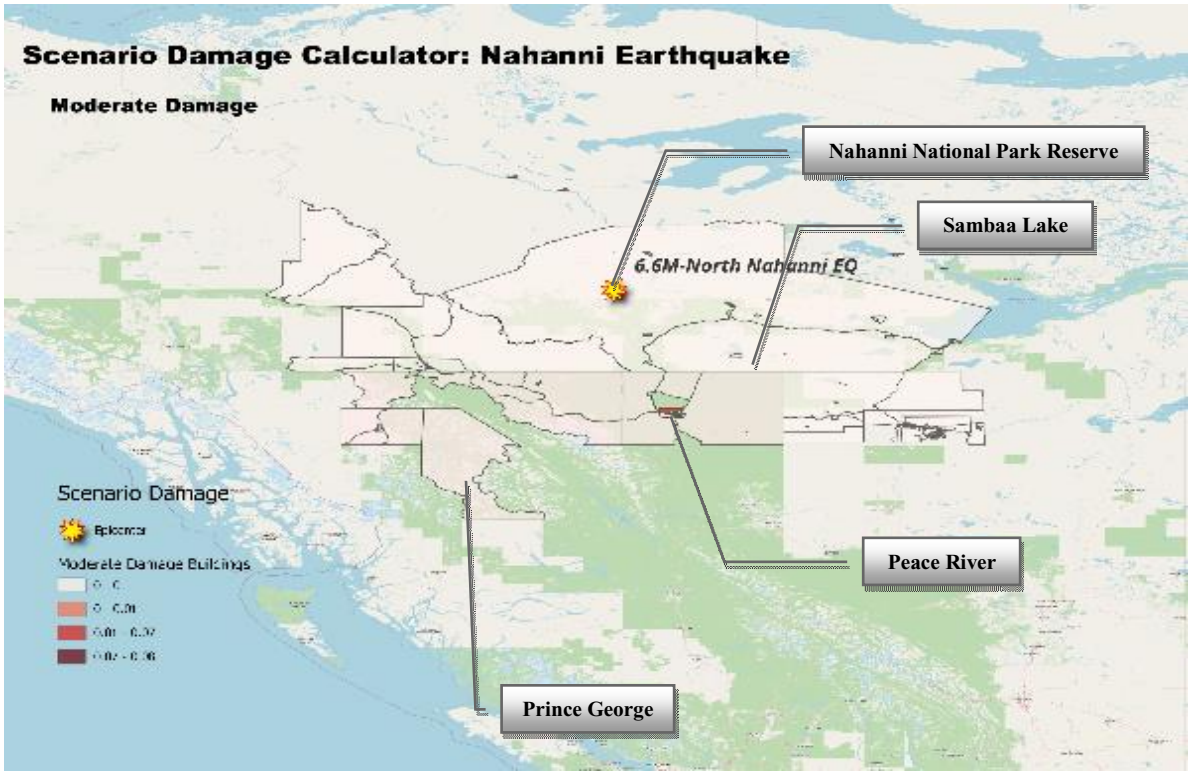
Scenario Damage Calculator: Nahanni Earthquake
Moderate Damage
Nahanni National Park Reserve
Sambaa Lake
6.6M-North Nahanni EQ
Scenario Damage
Peace River
Prince George

b)

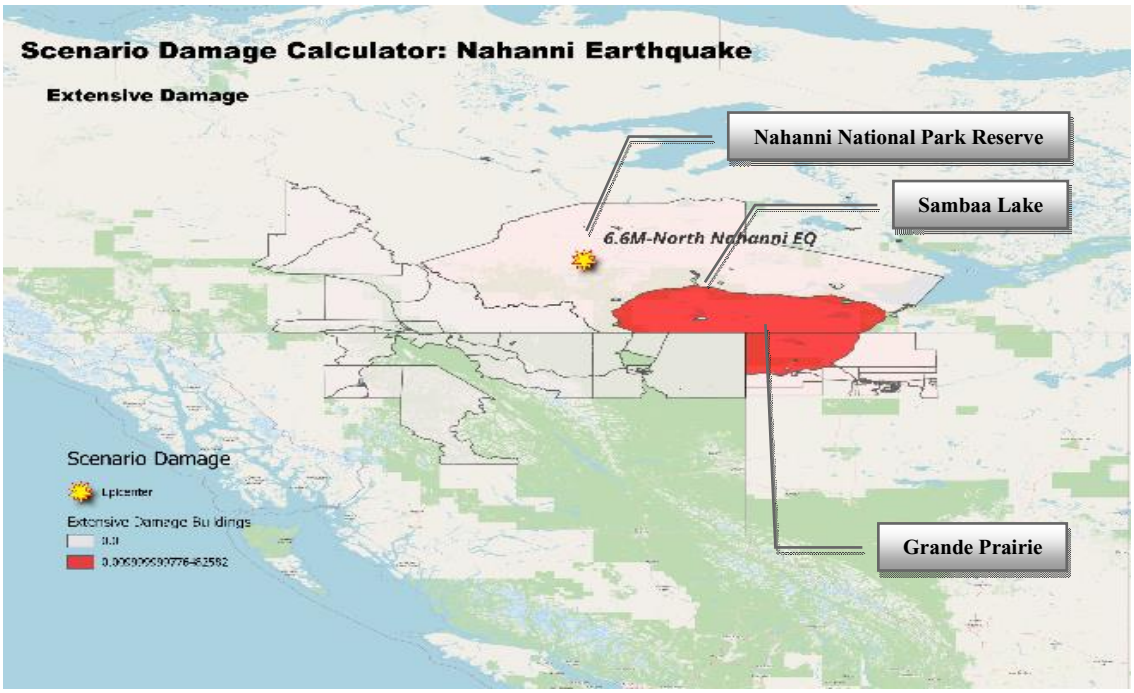

c)

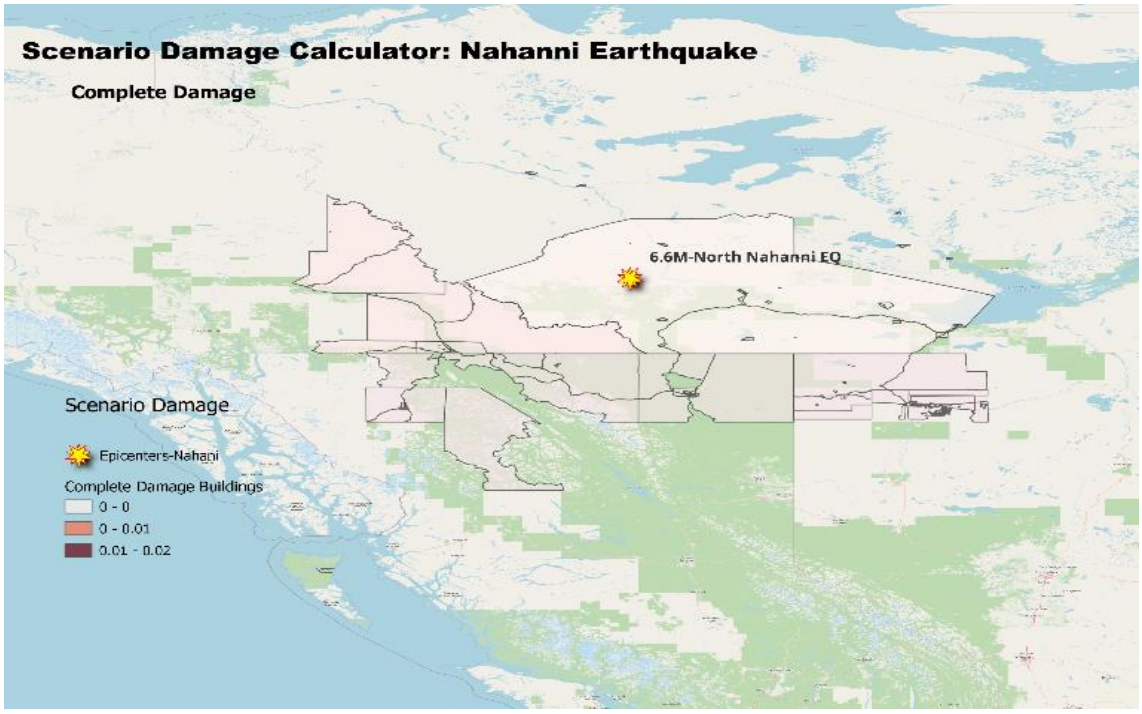

d)

Figure 6.3. Damage distribution maps of Nahanni earthquake. These images are estimated by SDC in 4 different damage states. a) slight damage, b) moderate damage, c) extensive damage, and d) complete damage (collapse). Color scheme, with its varying shades of red, serves as a visual aid in intuitively conveying the severity of the damages incurred, with deeper shades of red indicating more profound damage, and lighter shades signifying less severe impact.

6.2.1.4. Mosquito-Lake-M6.2 earthquake damages

Figure 6.4 provides an overview of the damage distribution resulting from the 2017 Mosquito-Lake earthquake with a magnitude of 6.2. In the 'Slight Damage' category in British Columbia, we observe that the British Columbia-Nechako epicenter has experienced slight damage in one building. Additionally, the Bulkley Valley region in BC is included in this category. In the Yukon region, there is a very small area located southwest of Yukon where 2 buildings, situated far from the epicenter, have sustained slight damage. Furthermore, there are small areas in Macpherson, Whitehorse, and Tagish that are far from the epicenter and have reported slight damage.

Moving on to the 'Moderate Damage' category, in BC, the British Columbia-Nechako epicenter is the sole location experiencing moderate damage. In Yukon, all areas except Whitehorse and Macpherson have reported zero instances of moderate damage. Additionally, there is a very small area to the east of the epicenter in Tagish, and it has reported moderate damage.

Regarding 'Extensive Damage,' in BC, the British Columbia-Nechako epicenter is the only area with reports of extensive damage. In the Yukon region, all areas except for Yukon-Whitehorse, located far from the epicenter in a very small area northeast of Yukon, have reported zero instances of extensive damage. In the 'Complete Damage' category, in BC, the British Columbia-Nechako epicenter is the sole location with reports of complete damage. In the Yukon region, all areas except for Yukon-Whitehorse, have reported zero instances of complete damage, with a very low probability in this specific area. The distribution of damage from this earthquake is summarized in Table 6.4.

Table 6.4. Damage distribution summary of 2017 Mosquito Lake earthquake-M6.2 estimated by SDC ("Google Earth" n.d.), (Government of Canada 2022, Canadian census 2016).

Community Name	Distance-Epicenter (km)	Population	Structural Damages			
			Slight	Moderate	Extensive	Complete
British Columbia Provinces/Territories						
Nechako	**Epicenter**	38,636	1	< 1	< 1	< 1
Bulkley Valley	820	5,256	1	-	-	-
Yukon Provinces/Territories						
SW- Yukon	1,375	-	2	-	-	-
Macpherson	174	1,225	1	< 1	-	-
Whitehorse	173	25,085	1	< 1	< 1	< 1
Tagish	200	249	1	< 1	-	-

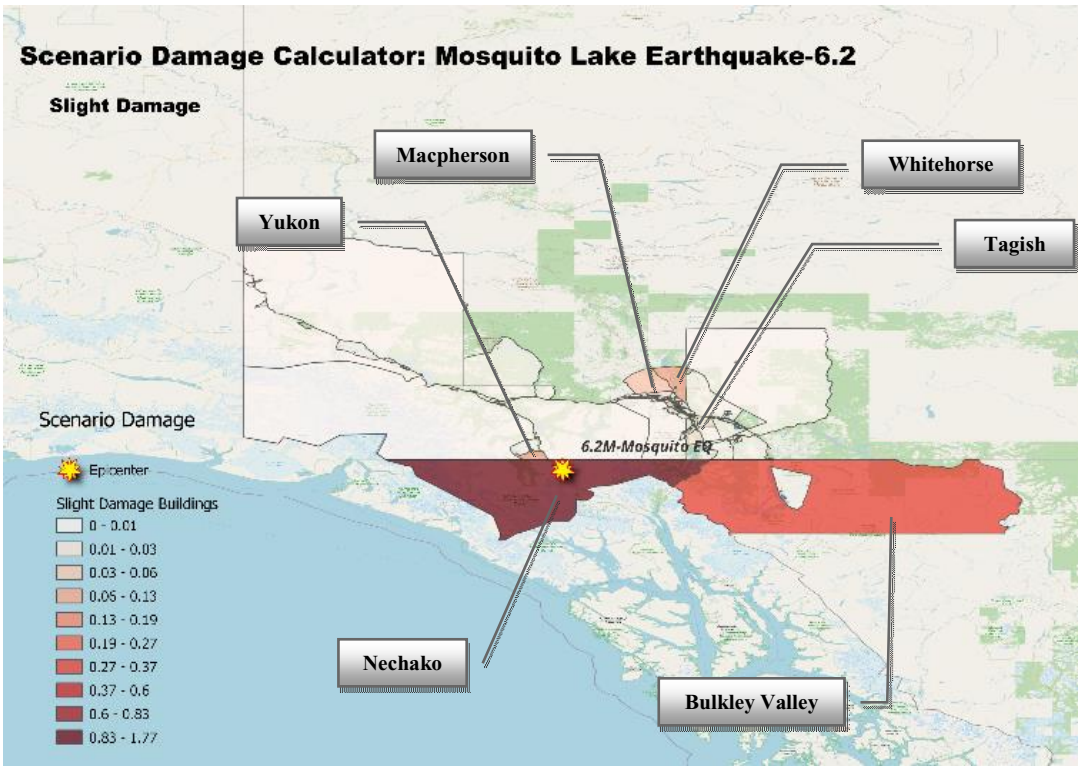
Scenario Damage Calculator: Mosquito Lake Earthquake-6.2
Slight Damage
Macpherson
Whitehorse
Yukon
Tagish
6.2M-Mosquito EQ
Scenario Damage
Epicenter
Slight Damage Buildings
0 - 0.01
0.01 - 0.03
0.03 - 0.06
0.06 - 0.13
0.13 - 0.19
0.19 - 0.27
0.27 - 0.37
0.37 - 0.6
0.6 - 0.83
0.83 - 1.77
Nechako
Bulkley Valley

a)

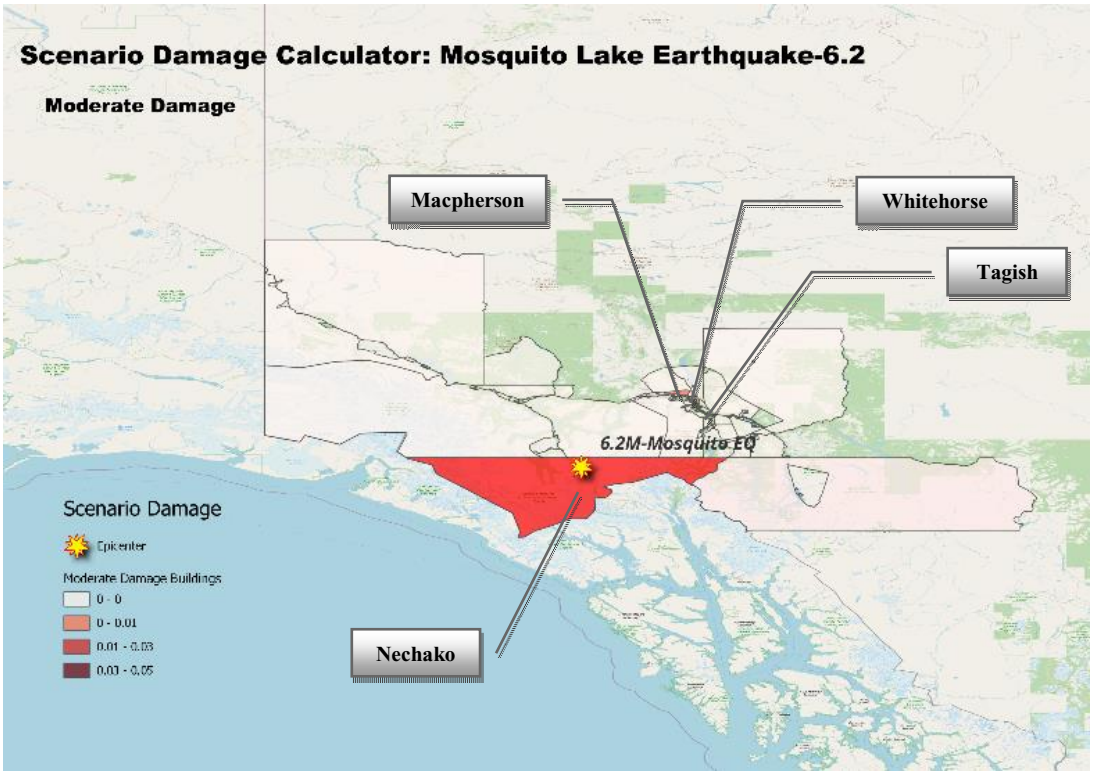
Scenario Damage Calculator: Mosquito Lake Earthquake-6.2
Moderate Damage
Macpherson
Whitehorse
Tagish
6.2M-Mosquito EQ
Scenario Damage
Epicenter
Moderate Damage Buildings
0 - 0
0 - 0.01
0.01 - 0.03
0.03 - 0.05
Nechako

b)

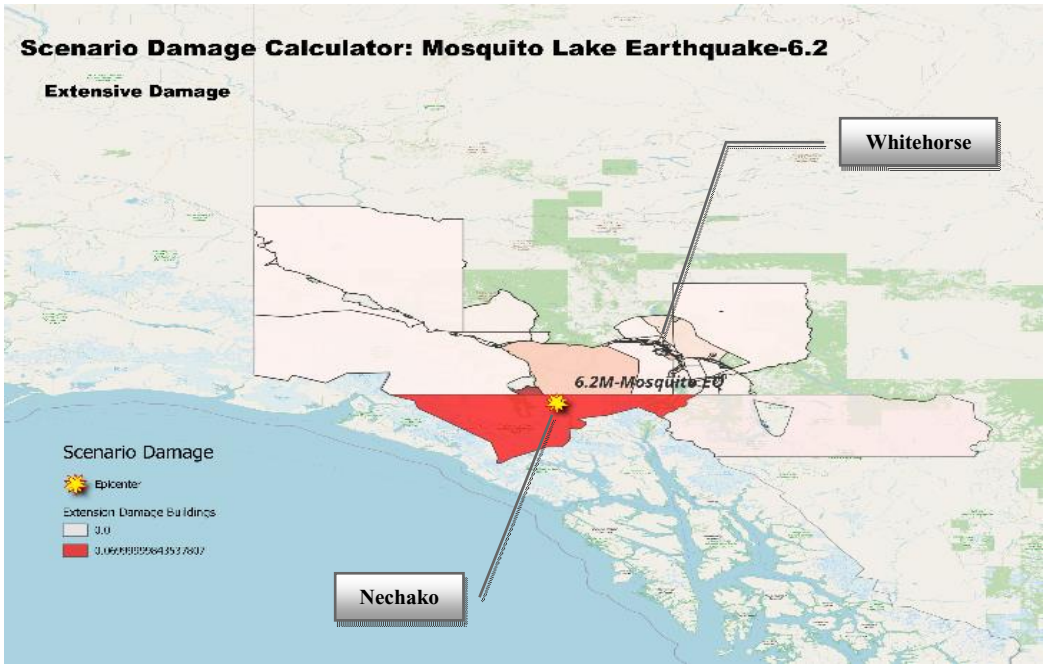

c)

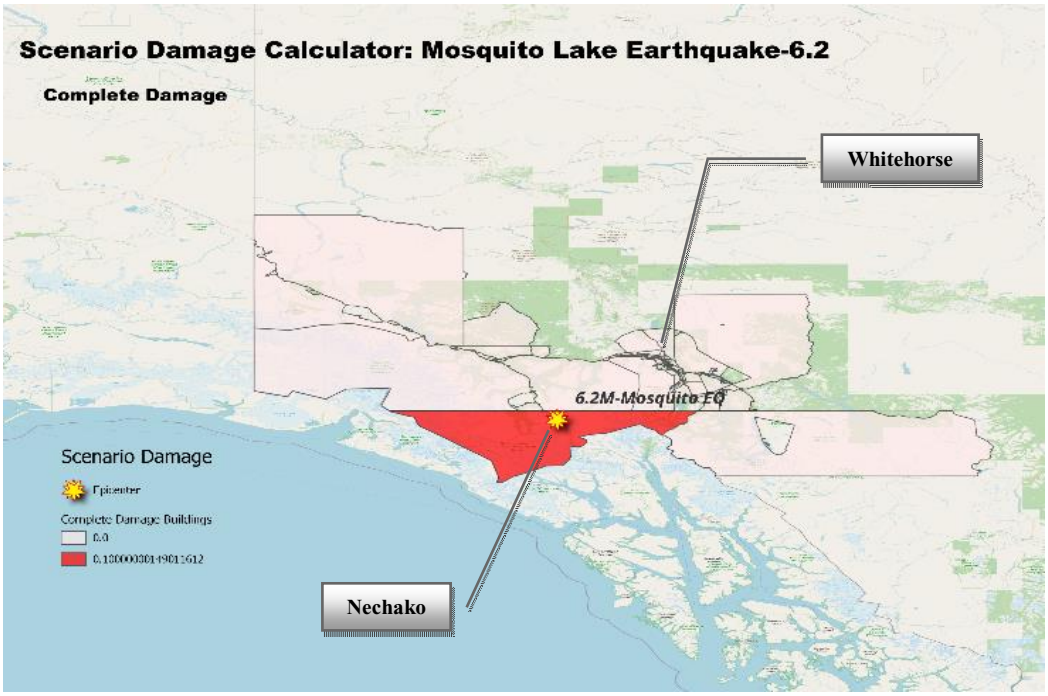

d)

Figure 6.4. Damage distribution maps of Mosquito Lake earthquake-M6.2. These images are estimated by SDC in 4 different damage states. a) slight damage, b) moderate damage, c) extensive damage, and d) complete damage (collapse). Color scheme, with its varying shades of red, serves as a visual aid in intuitively conveying the severity of the damages incurred, with deeper shades of red indicating more profound damage, and lighter shades signifying less severe impact.

6.2.1.5. Mosquito-Lake-M6.3 earthquake damages

Figure 6.5 presents a comprehensive overview of the damage distribution resulting from the 2017 Mosquito-Lake earthquake, which had a magnitude of 6.3. In the category of 'Slight Damage', it is observed that within British Columbia, specifically at the Nechako epicenter, only one building has reported damage. Additionally, the Bulkley Valley region also falls into this category. Moving to the Yukon region, Whitehorse, located a considerable distance from the epicenter in a small area to the northeast of Yukon, has one building displaying slight damage. Tagish and Macpherson also report one building with slight damage.

Transitioning to the 'Moderate Damage' category, British Columbia-Nechako, the epicenter itself, reports moderate damage in British Columbia. In the Yukon region, all areas except for Whitehorse and Macpherson, both located far from the epicenter, have experienced no incidents of moderate damage. Tagish has reported one building with moderate damage.

In terms of 'Extensive Damage', British Columbia-Nechako, is the sole reporting area in British Columbia. In the Yukon region, all areas except for Whitehorse, have encountered no instances of extensive damage. In the 'Complete Damage' category, British Columbia-Nechako, is the only reporting area in British Columbia. In the Yukon region, all areas except for Whitehorse, which is positioned at a distance from the epicenter in a small area to the northeast of Yukon, report a very low probability of complete damage. The distribution of damage from this earthquake is summarized in Table 6.5.

Table 6.5. Damage distribution summary of 2017 Mosquito Lake earthquake-M6.3 estimated by SDC ("Google Earth" n.d.), (Government of Canada 2022, Canadian census 2016).

Community Name	Distance-Epicenter (km)	Population	Structural Damages			
			Slight	Moderate	Extensive	Complete
British Columbia Provinces/Territories						
Nechako	**Epicenter**	38,636	1	< 1	< 1	< 1
Bulkley Valley	820	5,256	1	-	-	-
Yukon Provinces/Territories						
Macpherson	174	1,225	1	< 1	-	-
Whitehorse	173	25,085	1	< 1	< 1	< 1
Tagish	200	249	1	1	-	-

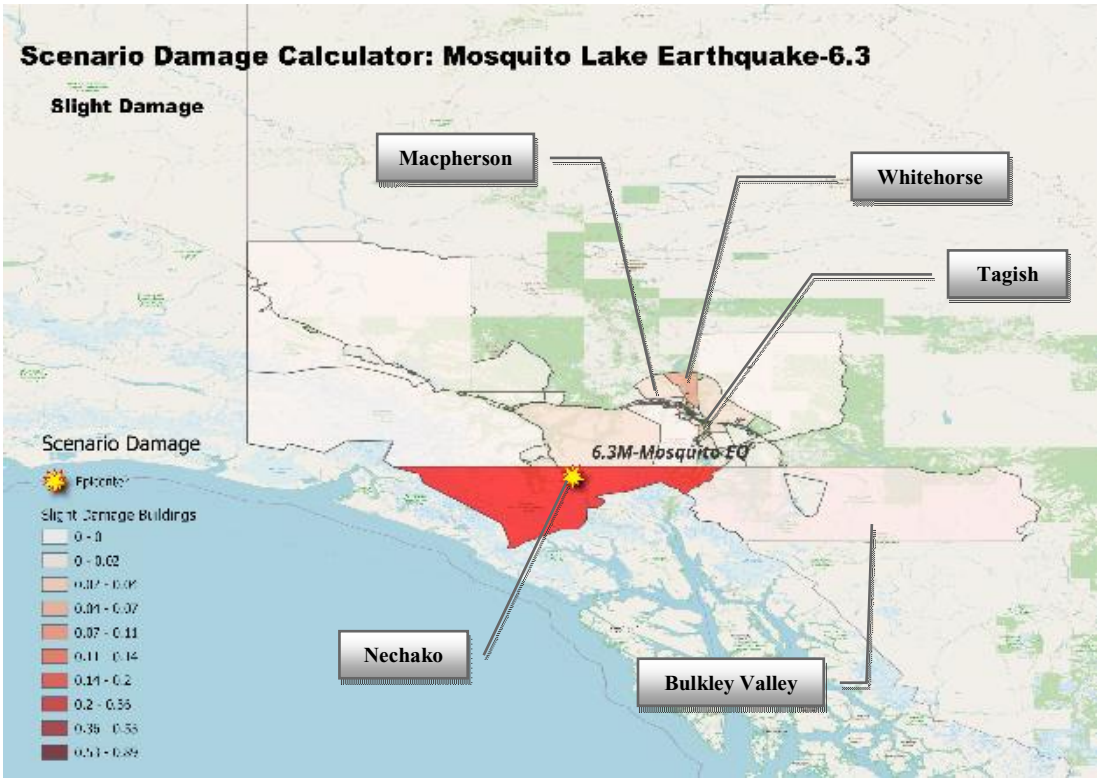
Scenario Damage Calculator: Mosquito Lake Earthquake-6.3
Slight Damage
Macpherson
Whitehorse
Tagish
6.3M-Mosquito EQ
Scenario Damage
Epicenter
Slight Damage Buildings
Nechako
Bulkley Valley

a)

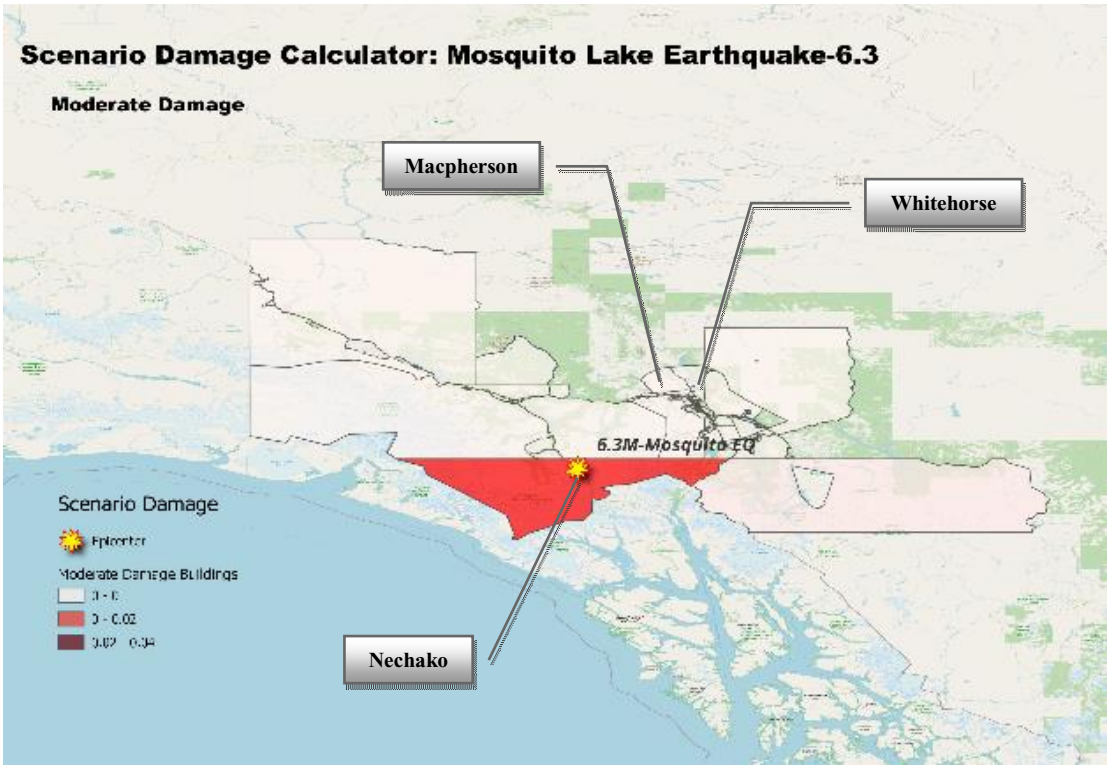
Scenario Damage Calculator: Mosquito Lake Earthquake-6.3
Moderate Damage
Macpherson
Whitehorse
6.3M-Mosquito EQ
Scenario Damage
Epicenter
Moderate Damage Buildings
Nechako

b)

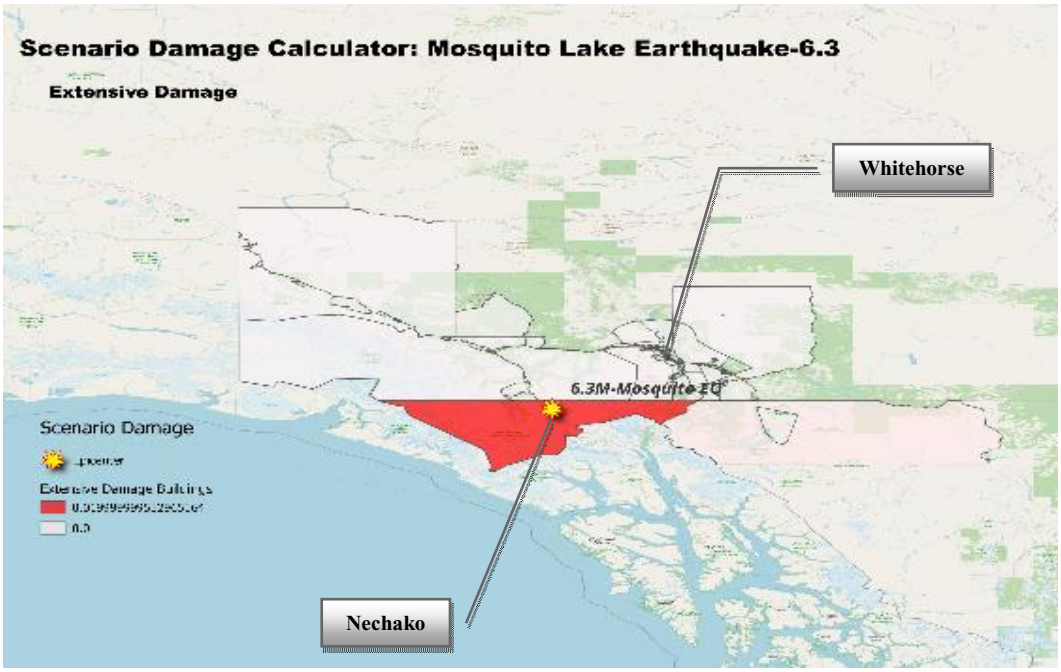

c)

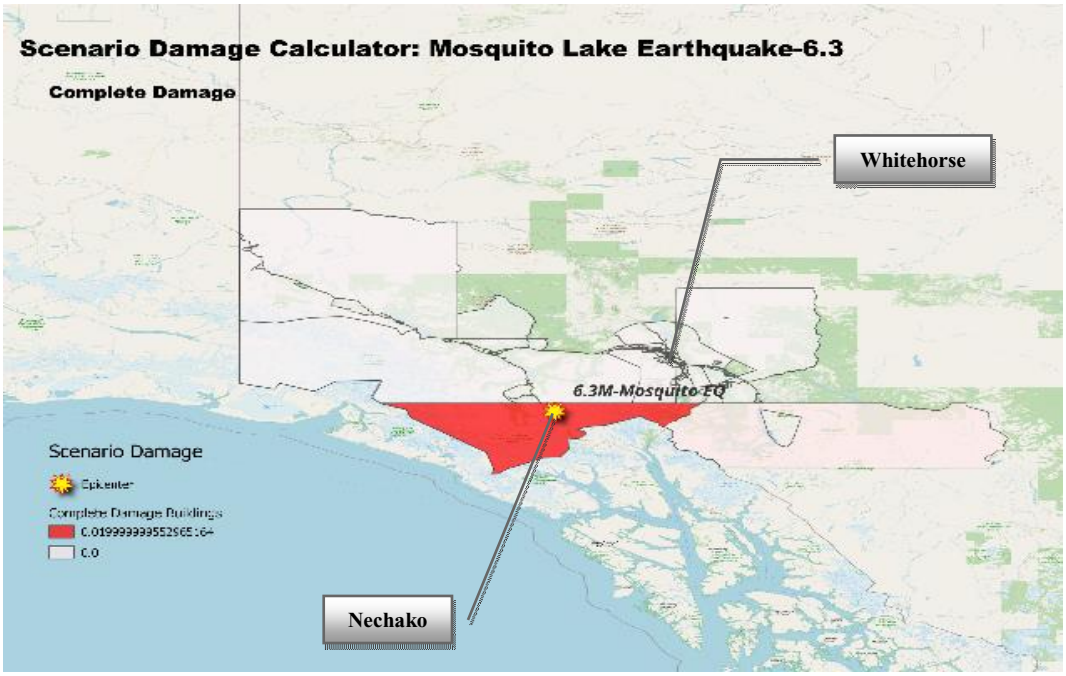

d)

Figure 6.5.Damage distribution maps of Mosquito Lake earthquake-M6.3. These images are estimated by SDC in 4 different damage states. a) slight damage, b) moderate damage, c) extensive damage, and d) complete damage (collapse). Color scheme, with its varying shades of red, serves as a visual aid in intuitively conveying the severity of the damages incurred, with deeper shades of red indicating more profound damage, and lighter shades signifying less severe impact.

6.2.2. Scenario damage output – summary of aggregated damages

In light of the preceding discussions, an attempt was made to depict the cumulative damages incurred by all events through the utilization of a bar chart, as presented in Figure 6.6. It is readily apparent that these earthquakes did not manifest as catastrophic events, characterized by dramatic structural impacts. Consequently, a substantial proportion of the bars within the chart are attributed to the state of no damage. To enhance the clarity of discerning the comparatively minor proportions, the no-damage state was excluded, and the bar chart was subsequently constructed based solely on the categories of slight, moderate, extensive, and complete damage, as illustrated in Figure 6.7.

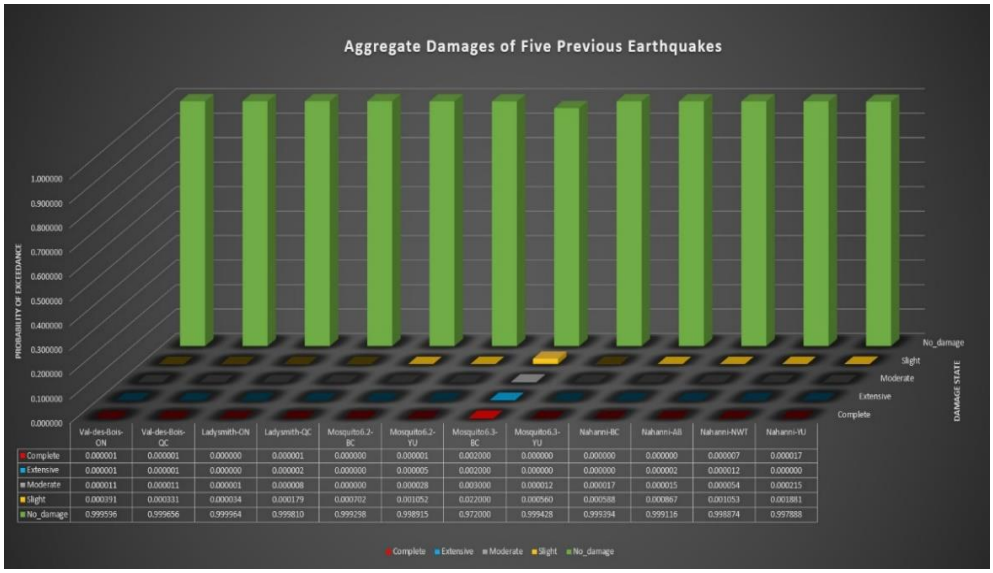

	Val-des-Bois-ON	Val-des-Bois-QC	Ladysmith-ON	Ladysmith-QC	Mosquito6.2-BC	Mosquito6.2-YU	Mosquito6.3-BC	Mosquito6.3-YU	Nahanni-BC	Nahanni-AB	Nahanni-NWT	Nahanni-YU
Complete	0.000001	0.000001	0.000000	0.000001	0.000000	0.000001	0.002000	0.000000	0.000000	0.000000	0.000007	0.000017
Extensive	0.000001	0.000001	0.000000	0.000002	0.000000	0.000005	0.002000	0.000000	0.000000	0.000002	0.000012	0.000000
Moderate	0.000011	0.000011	0.000001	0.000008	0.000000	0.000028	0.003000	0.000012	0.000017	0.000015	0.000054	0.000215
Slight	0.000391	0.000331	0.000034	0.000179	0.000702	0.001052	0.022000	0.000560	0.000588	0.000867	0.001053	0.001881
No_damage	0.999596	0.999656	0.999964	0.999810	0.999298	0.998915	0.972000	0.999428	0.999394	0.999116	0.998874	0.997888

Figure 6.6. The aggregated damages for five examined events based on 5 damage states.

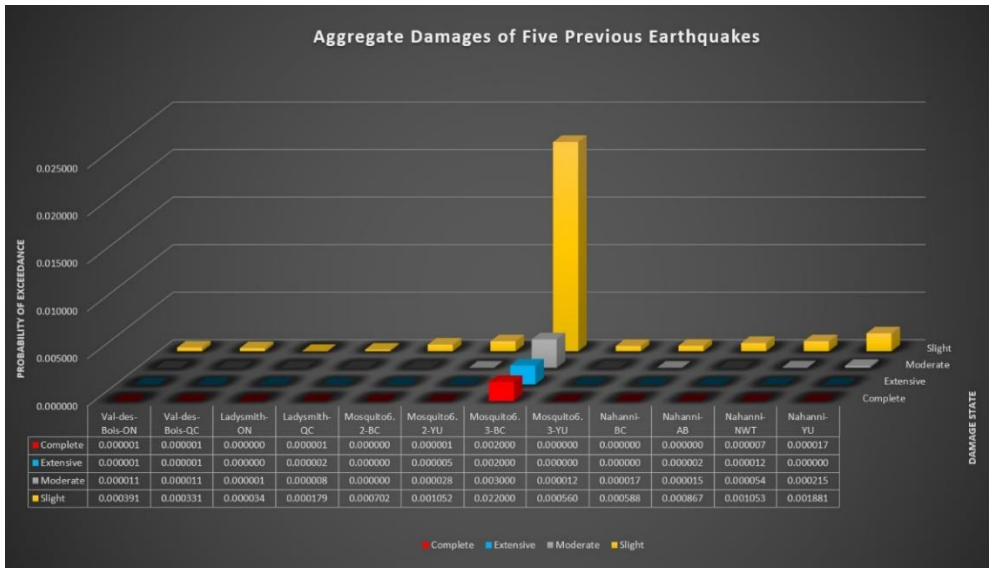

	Val-des-Bois-ON	Val-des-Bois-QC	Ladysmith-ON	Ladysmith-QC	Mosquito6.2-BC	Mosquito6.2-YU	Mosquito6.3-BC	Mosquito6.3-YU	Nahanni-BC	Nahanni-AB	Nahanni-NWT	Nahanni-YU
Complete	0.000001	0.000001	0.000000	0.000001	0.000000	0.000001	0.002000	0.000000	0.000000	0.000000	0.000007	0.000017
Extensive	0.000001	0.000001	0.000000	0.000002	0.000000	0.000005	0.002000	0.000000	0.000000	0.000002	0.000012	0.000000
Moderate	0.000011	0.000011	0.000001	0.000008	0.000000	0.000028	0.003000	0.000012	0.000017	0.000015	0.000054	0.000215
Slight	0.000391	0.000331	0.000034	0.000179	0.000702	0.001052	0.022000	0.000560	0.000588	0.000867	0.001053	0.001881

Figure 6.7. The aggregated damages for five examined events based on 4 damage states, with no-damage state excluded.

As is evident from this figure, the most probable type of damage in the area, aside from no damage, is slight damage. As the severity of damage escalates, progressing from moderate to extensive or complete, the corresponding probabilities exhibit a decreasing trend. An additional point of interest pertains to the Mosquito Lake earthquake, characterized by a magnitude of 6.3. The probability of damage in British Columbia, for all states, particularly slight damage, is notably higher in comparison to the other events.

6.2.3. Scenario risk output – monetary losses

The SRC outputs are acquired as loss maps pertaining to financial losses and fatalities, and loss statistics encompassing comprehensive statistical data related to the aggregated losses experienced across all sites. Figure 6.8 depicts the financial loss distribution maps resulting from the examination of the five earthquakes. It is important to note that the losses have been rounded to the nearest integer to facilitate processing and interpretation.

6.2.3.1. Val-des-Bois earthquake losses

It is clear that the 2010 Val-des-Bois earthquake caused minimal structural losses, primarily in the city of Ottawa, totaling approximately $330,786. Additionally, neighboring areas such as Clarence-Rockland, Russell, and Cornwall suffered structural losses of nearly $27,079, $6,264, and $7,642, respectively. Furthermore, Alfred and Plantagenet on the Ontario side experienced structural losses amounting to $5,035. Moreover, this earthquake resulted in significant non-structural losses, with Ottawa bearing the highest burden at $2,027,380. Clarence-Rockland, Cornwall, Alfred and Plantagenet, North Grenville, and Russell also incurred non-structural losses totaling $179,635, $61,516, $33,102, $20,222, and $4,409, respectively. Regarding content losses, Ottawa once again emerged as the most affected area, recording losses of $49,067. Clarence-Rockland, Russell, Cornwall, and Alfred and Plantagenet also experienced content losses amounting to $4,319, $1,126, $1,053, and $758, respectively.

On the Quebec side, the Val-des-Bois earthquake caused comparatively lower structural losses, with Gatineau incurring approximately $152,213. Val-des-Bois itself, the epicenter area, experienced $50,518 in structural losses, and Val-des-Monts, Notre-Dame-du-Laus, Bowman, Notre-Dame-de-la-Salette, L'Ange-Gardien, and even regions far from the epicenter in the southeast of the Quebec model reported structural losses of $35,180, $24,676, $23,827, $18,638, $14,303, $5,555, and $3,115, respectively. The Val-des-Bois earthquake also resulted in noteworthy non-structural losses on the Quebec side, with Gatineau bearing the highest burden at $1,060,146. Val-des-Bois, Val-des-Monts, Bowman, Notre-Dame-du-Laus, and areas far from the epicenter, such as Salaberry-de-Valleyfield, Saint-Jérôme, and Vaudreuil-Dorion, incurred non-structural losses totaling $212,328, $190,422, $109,084, $105,495, $48,497, $28,704, and $22,476, respectively. Content losses were also observed in select areas on the Quebec side, with Gatineau leading the way with losses amounting to $19,457. Val-des-Bois, Val-des-Monts, Notre-Dame-du-Laus, and Bowman reported content losses of $12,543, $7,572, $6,181, and $6,821, respectively. An overview of the financial losses caused by this earthquake is summarized in Table 6.6.To calculate the total financial losses resulting from each individual event, the aggregate losses

of structure, non-structure, and contents must be summed, and the total loss for each side of the exposed area likely affected by that particular earthquake should be calculated.

Table 6.6. Financial loss summary caused by 2010 Val-des-Bois earthquake estimated by SRC ("Google Earth" n.d.), (Government of Canada 2022, Canadian census 2011).

Community Name	Distance-Epicenter (km)	Population	Financial Losses (CAD)		
			Structural	Non-structural	Content
Ontario Provinces/Territories					
Ottawa	89	1,218,000	330,786	2,027,380	49,067
Clarence-Rockland	69	23,185	27,079	179,635	4,319
Russell	118	16,520	6,264	4,409	1,126
Cornwall	191	45,508	7,642	61,516	1,053
Alfred & Plantagenet	87	9,196	5,035	33,102	758
North Grenville	148	15,085	-	20,222	-
Aggregated Losses			**405,385**	**2,575,340**	**61,392**
Loss per Province	**3,042,117**				
Quebec Provinces/Territories					
Gatineau	67	265,349	152,213	1,060,146	19,457
Val-des-Bois	**Epicenter**	938	50,518	212,328	12,543
Val-des-Monts	39	10,420	35,180	190,422	7,572
Notre-Dame-du-Laus	27	1,518	24,676	105,495	6,181
Bowman	7	677	23,827	109,084	6,821
Notre-Dame-de-la-Salette	18.9	757	18,638	-	-
L'Ange-Gardien	57.1	3634	14,303	-	-
Salaberry-de-Valleyfield	198	38,323	-	48,497	-
Saint-Jerome	173	69,598	-	28,704	-
Vaudreuil-Dorion	176	33,305	-	22,476	-
Aggregated Losses			**435,694**	**2,631,990**	**3,150,655**
Loss per Province	**6,218,339**				
Total Loss	**$9,260,456**				

For the 2010 Val-des-Bois earthquake on the Quebec side, the combined losses for contents, non-structural, and structural components amounted to $3,150,655, $2,631,990, and $435,694, respectively, resulting in a total loss of $6,218,339 for the province of Quebec. On the Ontario side, the combined losses for contents, non-structural, and structural components totaled $61,392, $2,575,340, and $405,385, respectively, resulting in a total loss of $3,042,117 for the province of Ontario. Therefore, the combined losses for Quebec and Ontario yield a total financial loss of $9,260,456 caused by this earthquake.

This information provides valuable insight into the potential economic impact, indicating that if the 2010 Val-des-Bois earthquake had occurred in approximately 2016 (the year to which the model is conditioned), CanSRM1 estimates that it would have resulted in nearly **$9,260,456** in losses for Canada. This may seem like a large value to some, but in terms of an earthquake in a major metropolitan area, it is actually quite small. Much of this damage, as documented in Section 6.1.1.1, is slight. Therefore, this figure is almost exclusively from small levels of damage to many buildings. This level of damage is unlikely to be reported or possibly even repaired, meaning it won't be measured by engineers or insurers.

6.2.3.2. Ladysmith earthquake losses

In the context of the 2013 Ladysmith earthquake, an analysis was conducted to assess the financial loss distribution, considering both structural and non-structural components, as well as content losses on both the Ontario and Quebec sides. On the Ontario side, minor financial losses were observed. Shifting our focus to the Quebec side, the epicenter, Thorne, experienced substantial structural losses totaling $58,389. Additional structural losses were incurred by Otter Lake located in the north of epicenter at $29,933, La Pêche (East) at $25,101, Clarendon (South) at $19,615, Gatineau at $7,762, and L'Île-du-Grand at $8,650. Non-structural losses on the Quebec side were noteworthy, with Thorne registering $234,265, Otter Lake at $125,823, La Pêche at $110,378, La Pêche at $82,799, Gatineau at $69,575, and L'Île-du-Grand-Calumet at $31,619. Moreover, content losses in Quebec were observed in various regions, including Thorne at $22,235, Otter Lake at $9,662, La Pêche at $5,788, Clarendon at $5,923, Gatineau at $3,423, and L'Île-du-Grand-Calumet at $1,828.

An overview of the financial losses caused by this earthquake is summarized in Table 6.7. This figure was derived by calculating the total loss on the Quebec side, which includes content, non-structural, and structural losses, resulting in $1,217,443. When combined with the minimal losses on the Ontario side ($88), the total loss reached $1,217,531. This information sheds light on the potential economic impact, illustrating that if the 2013 Ladysmith earthquake had occurred in approximately 2016, it would have caused a total loss of **$1,217,531** in Canada.

Table 6.7. Financial loss summary caused by 2013 Ladysmith earthquake estimated by SRC ("Google Earth" n.d.), (Government of Canada 2022, Canadian census 2016).

Community Name	Distance-Epicenter (km)	Population	Financial Losses (CAD)		
			Structural	Non-structural	Content
Ontario Provinces/Territories					
Loss per Province	**Minor Financial Losses**				
Quebec Provinces/Territories					
Thorne	**Epicenter**	448	58,389	234,265	22,235
Otter Lake	16	932	29,933	125,823	9,662
Clarendon	21	1,256	19,615	110,378	5,923
Gatineau	67	265,349	7,762	69,575	3,423
L'Île-du-Grand	40	626	8,650	31,619	1,828
La Pêche	45	7,863	25,101	82,799	5,788
Loss per Province	**1,217,443**				
Total Loss	**$1,217,531**				

6.2.3.3. Mosquito-Lake-M6.2 earthquake losses

In the context of the 2017 Mosquito-Lake-M6.2 earthquake, various regions were impacted, including both the British Columbia and Yukon sides. On the British Columbia side, structural losses were incurred primarily in the vicinity of the epicenter, British Columbia-Nechako epicenter, totaling $2,694. Additionally, a nominal sum of $100 in structural losses was observed in the British Columbia-Bulkley Valley region. Non-structural losses were reported within the British Columbia-Nechako epicenter area, amounting to $6,049, while the British Columbia-Bulkley Valley recorded non-structural losses of $300. In terms of contents, British Columbia-Nechako epicenter experienced a minimal loss of $317.

Turning to the Yukon side, structural losses were noted both near the epicenter and in areas farther away. Specifically, within the vicinity of the epicenter, a significant sum of $1,068 was observed in a small area located in the southwest of Yukon, while Macpherson recorded structural losses of $230. Furthermore, in the Yukon-Whitehorse region, located at a distance from the epicenter reported structural losses amounting to $118. Non-structural losses on the Yukon side were concentrated near the epicenter, with the small area in the southwest of Yukon registering $5,146 and Macpherson recording losses of $1,065. Similarly, the Yukon-Whitehorse region, experienced minimal non-structural losses, totaling $12. In terms of contents, the small area in the southwest of Yukon reported losses of $112, while Macpherson experienced losses amounting to $11. Table 6.8 summarizes an overview of the financial losses caused by this earthquake.

All in all, on the British Columbia side, the total loss was computed by summing the contents, non-structural, and structural losses, resulting in $9,631. Conversely, on the Yukon side, the total loss was estimated at $126,549. When combining the losses on the British Columbia side and the Yukon side, the total financial loss of $136,180 emerges. This analysis enables us to appreciate that if the 2017 Mosquito-Lake-M6.2 earthquake had occurred approximately in 2016, it would have resulted in financial losses totaling **$136,180** in Canada.

Table 6.8. Financial loss summary caused by 2017 Mosquito-Lake-M6.2 earthquake estimated by SRC ("Google Earth" n.d.), (Government of Canada 2022, Canadian census 2016).

Community Name	Distance-Epicenter (km)	Population	Financial Losses (CAD)		
			Structural	Non-structural	Content
British Columbia Provinces/Territories					
Nechako	**Epicenter**	38,636	2,694	6,049	317
Bulkley Valley	820	5,256	100	300	
Loss per Province	**9,631**				
Yukon Provinces/Territories					
SW- Yukon	1,375	-	1,068	5,146	112
Macpherson	174	1,225	230	1,065	11
Whitehorse	173	25,085	118	12	
Loss per Province	**126,549**				
Total Loss	**$136,180**				

6.2.3.4. Mosquito-Lake-M6.3 earthquake losses

The 2017 Mosquito-Lake-M6.3 earthquake is the other focal point of our analysis. On the British Columbia side, the Nechako epicenter bore minor structural losses totaling $1,794. Similarly, non-structural losses were observed in these areas, with Nechako epicenter reporting losses of $4,115. In terms of contents, the Nechako epicenter suffered losses of $222.

On the Yukon side, structural losses were distributed as follows: Whitehorse incurred minimal losses in very small areas in the northeast of the Yukon model, amounting to $410. Near the epicenter, Yukon experienced structural losses in both Macpherson, and the small area in southwest Yukon, with losses of $97 and $78, respectively. Non-structural losses were also observed in these areas, with losses of $1,046 in southwest Yukon and $306 in Macpherson. Whitehorse reported non-structural losses, totaling $2,455. Contents losses were noted in Yukon near the epicenter, with losses of $45 in southwest of Yukon and $5 in Macpherson. Whitehorse, reported contents losses, amounting to $29.

To calculate the total losses on the British Columbia side, the sum of contents, non-structural, and structural losses is computed, resulting in a total loss of $6,133. Similarly, on the Yukon side,

the total loss is calculated by adding contents, non-structural, and structural losses, resulting in a total loss of $41,814. When the losses on the British Columbia side are combined with the losses on the Yukon side, the total financial loss caused by the 2017 Mosquito-Lake-M6.3 earthquake is calculated as $47,947. This analysis allows us to understand that if the 2017 Nahanni earthquake had occurred around 2016 (in alignment with the year of model development), it would have resulted in losses amounting to approximately **$47,947** in Canada. An overview of the financial losses caused by this earthquake is summarized in Table 6.9.

Table 6.9. Financial loss summary caused by 2017 Mosquito-Lake-M6.3 earthquake estimated by SRC ("Google Earth" n.d.), (Government of Canada 2022, Canadian census 2016).

Community Name	Distance-Epicenter (km)	Population	Financial Losses (CAD)		
			Structural	Non-structural	Content
British Columbia Provinces/Territories					
Nechako	**Epicenter**	38,636	1,794	4,115	222
Loss per Province	**6,133**				
Yukon Provinces/Territories					
SW- Yukon	1,375	-	578	1,046	45
Macpherson	174	1,225	97	306	5
Whitehorse	173	25,085	410	2,455	29
Loss per Province	**41,814**				
Total Loss	**$47,947**				

6.2.3.5. Nahanni earthquake losses

The 1985 Nahanni earthquake, spanning various regions, provides an insightful examination of seismic repercussions. On the Alberta side, structural losses were noted in Grande Prairie registering the structural loss at $90. Non-structural losses also affected these remote areas, including Grande Prairie with $432. Furthermore, contents suffered losses in Grande Prairie at $12. Turning to the British Columbia side, structural losses were observed in the Northern Rockies at $20 and Prince George at $11. Non-structural losses afflicted the Northern Rockies at $85, Prince George at $15, and Bulkley Valley at $20.

Moving to the Northwest Territories side, structural losses were concentrated in the epicenter area of Nahanni National, amounting to $211, and in Sambaa Lake, totaling $26. Non-structural losses were pronounced in the epicenter area of Nahanni National at $495 and in Sambaa Lake at $135. Contents also experienced losses in the epicenter area of Nahanni National at $17 and in Sambaa Lake at $4. Across the Yukon side, structural losses were discerned in northern Yukon region1 at $5. Non-structural losses affected this area at $48.

To ascertain the total financial loss stemming from this earthquake, calculations were performed for each affected region. On the Northwest Territories side, the total loss was determined by summing contents, non-structural, and structural losses, resulting in a total of $131,884. The Yukon side's total loss amounted to $2,072, while the Alberta side faced a combined loss of $567, and the British Columbia side confronted a total loss of $355. Combining the losses from the Northwest Territories, Yukon, Alberta, and British Columbia yields a comprehensive total financial loss of $134,878. This analysis underscores that had the 1985 Nahanni earthquake occurred around 2016 (the year on which the model is founded), it would have resulted in an estimated **$134,878** in losses for Canada.

It is imperative to acknowledge that, due to certain data limitations such as the municipality shapefile in the eastern region, the results may not be entirely reliable in high precision projects. However, considering that the primary aim of this study is to validate a national model based on total losses, these obtained results remain dependable.

Table 6.10. Financial loss summary caused by 1985 Nahanni earthquake estimated by SRC ("Google Earth" n.d.), (Government of Canada 2022, Canadian census 2016).

Community Name	Distance-Epicenter (km)	Population	Financial Losses (CAD)		
			Structural	Non-structural	Content
Alberta Provinces/Territories					
Grande Prairie	904	26,471	**90**	**432**	**12**
Loss per Province	**567**				
British Columbia Provinces/Territories					
Northern Rockies	312	5,856	20	185	
Prince George	1,127	67,621	11	115	
Bulkley Valley	1,496	5,256		2o	
Loss per Province	**355**				
Northwest-Territories Provinces/Territories					
Nahanni National Park Reserve	**Epicenter**	775	211	495	17
Sambaa Lake	281	54	26	135	4
Loss per Province	**131,884**				
Yukon Provinces/Territories					
North of Yukon	1,625	-	5	48	
Loss per Province	**2,072**				
Total Loss	**$134,878**				

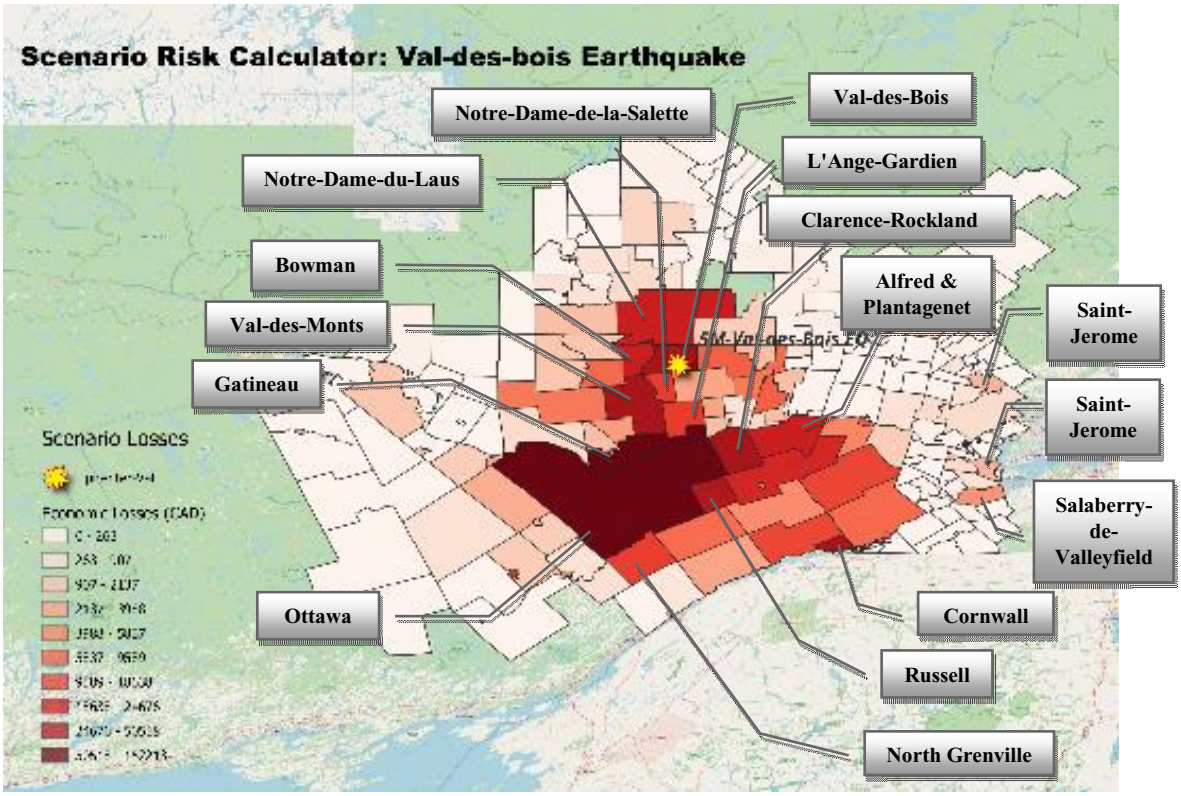
Scenario Risk Calculator: Val-des-bois Earthquake
Notre-Dame-de-la-Salette
Val-des-Bois
L'Ange-Gardien
Notre-Dame-du-Laus
Clarence-Rockland
Bowman
Alfred & Plantagenet
Saint-Jerome
Val-des-Monts
Gatineau
Saint-Jerome
Salaberry-de-Valleyfield
Ottawa
Cornwall
Russell
North Grenville
Scenario Losses

a)

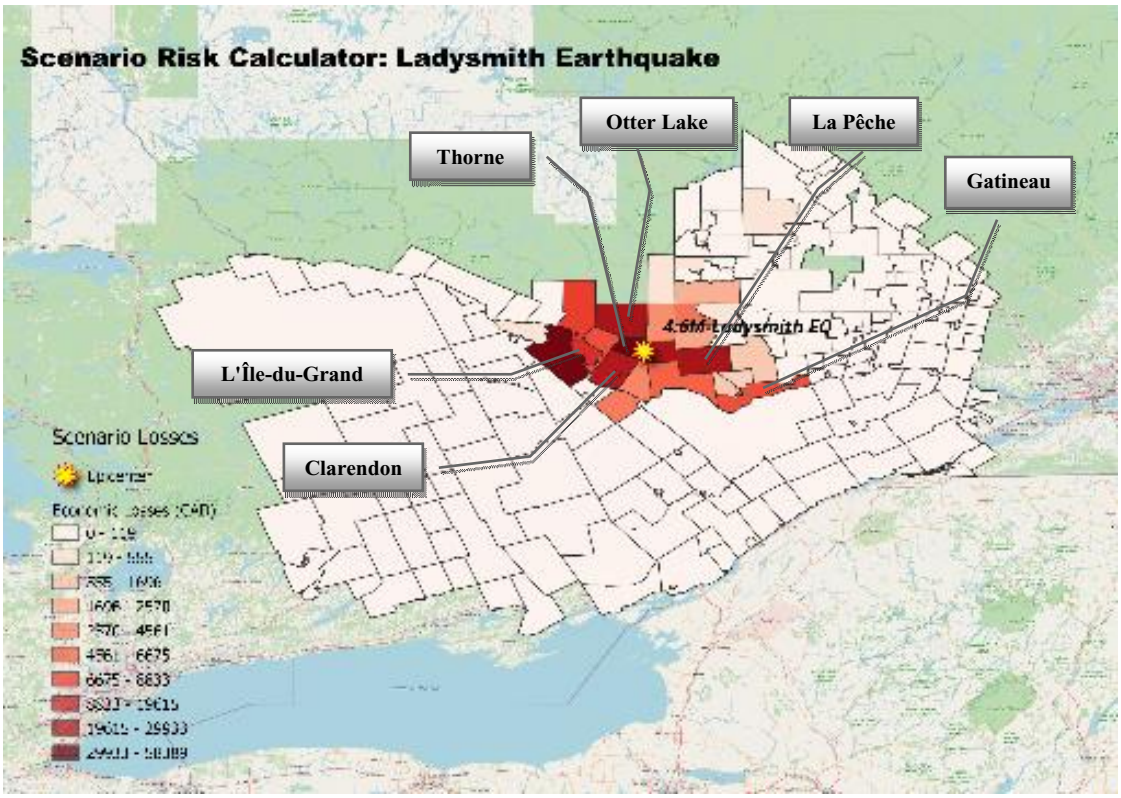
Scenario Risk Calculator: Ladysmith Earthquake
Otter Lake
La Pêche
Thorne
Gatineau
L'Île-du-Grand
Clarendon
Scenario Losses

b)

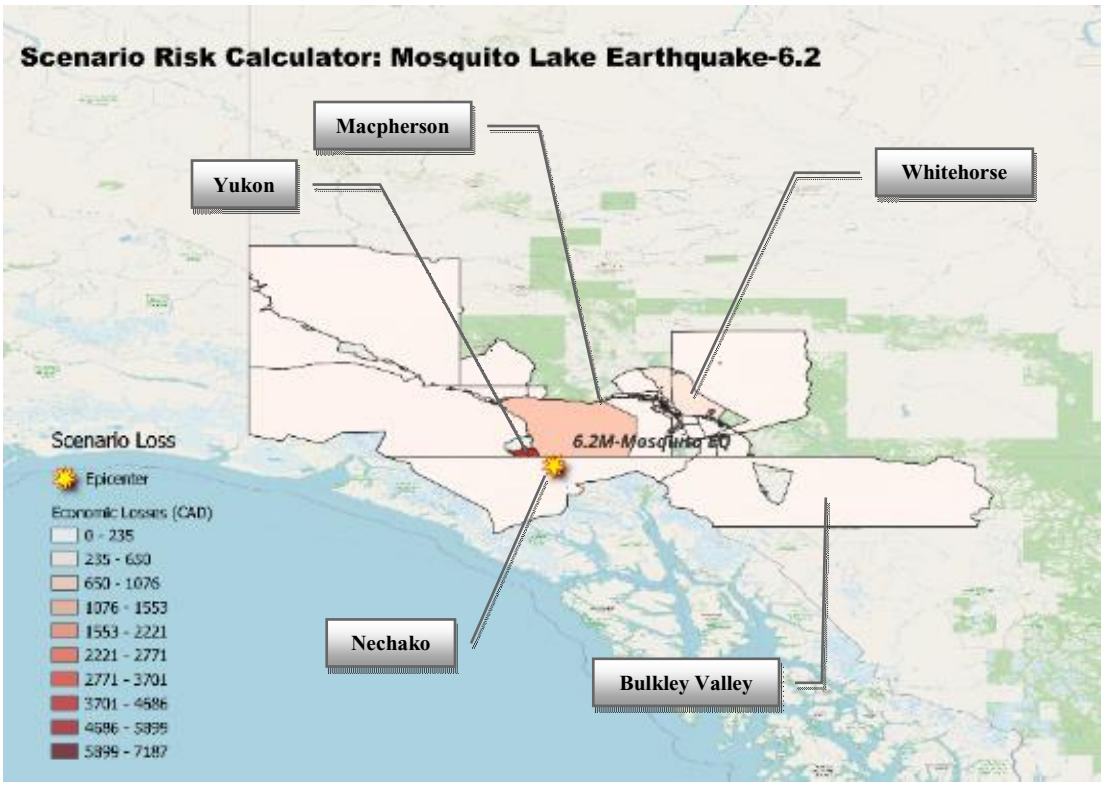
Scenario Risk Calculator: Mosquito Lake Earthquake-6.2
Macpherson
Yukon
Whitehorse
Nechako
Bulkley Valley
Scenario Loss
Epicenter
Economic Losses (CAD)
0 - 235
235 - 650
650 - 1076
1076 - 1553
1553 - 2221
2221 - 2771
2771 - 3701
3701 - 4686
4686 - 5899
5899 - 7187

c)

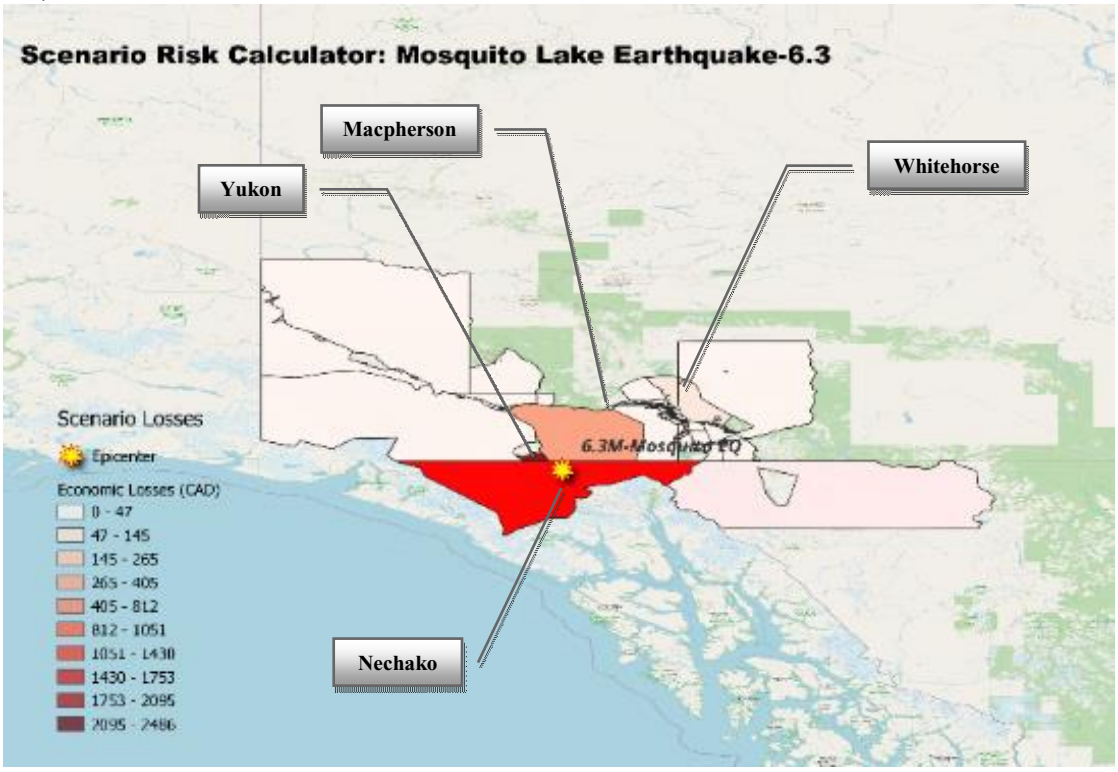
Scenario Risk Calculator: Mosquito Lake Earthquake-6.3
Macpherson
Yukon
Whitehorse
Nechako
Scenario Losses
Epicenter
Economic Losses (CAD)
0 - 47
47 - 145
145 - 265
265 - 405
405 - 812
812 - 1051
1051 - 1430
1430 - 1753
1753 - 2095
2095 - 2486

d)

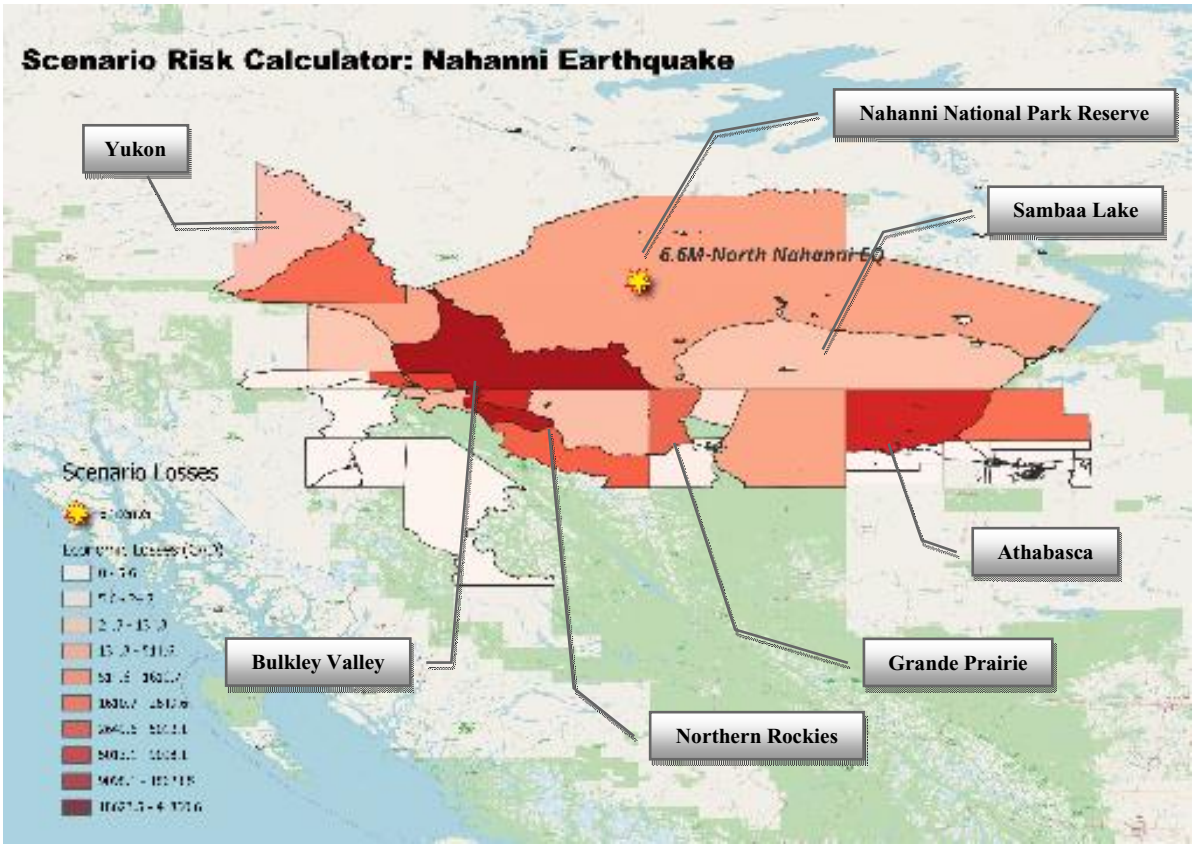

e)

Figure 6.8. Mean loss maps, showing financial loss distribution maps of eastern, western, and northern Canada. These images are estimated by SRC for 5 examined earthquakes. a) 2010 Val-des-Bois earthquake, b) 2013 Ladysmith earthquake, c) 2017 Mosquito Lake earthquake-M6.2, d) 2017 Mosquito Lake earthquake-M6.3, and e) 1985 Nahanni earthquake. Color scheme, with its varying shades of red, serves as a visual aid in intuitively conveying the severity of the damages incurred, with deeper shades of red indicating more profound damage, and lighter shades signifying less severe impact.

6.2.4. Scenario risk output – human losses

As mentioned earlier, the second category of information obtained from SRA relates to the number of lives lost in a particular earthquake. The process of acquiring fatalities for each specific event mirrors that of calculating total economic losses. In this procedure, the number of fatalities gathered from each exposed area affected by the event is totaled and then rounded to the nearest whole number. It is essential to emphasize that no occupant losses were estimated in connection with these five examined events, and the total estimated fatalities for all cases remained at zero.

6.2.5. Scenario risk output – summary of aggregated losses

Table 6.11 presents a summary of the final results, which have been estimated by the scenario seismic risk model and are aligned with the utilization of CanadaSRM1. Figure 6.9 provides a bar chart of the acquired results. Aggregate losses for five distinct events under study are presented in Figure 6.10 .

Table 6.11. Scenario risk outputs of five studied earthquakes.

Earthquakes	Financial loss in 2016	Fatalities in 2016
Val-des-Bois	$9,260,456	0
Ladysmith	$1,217,531	0
Nahanni	$134,878	0
Mosquito-Lake-M6.2	$136,180	0
Mosquito-Lake-M6.3	$47,947	0

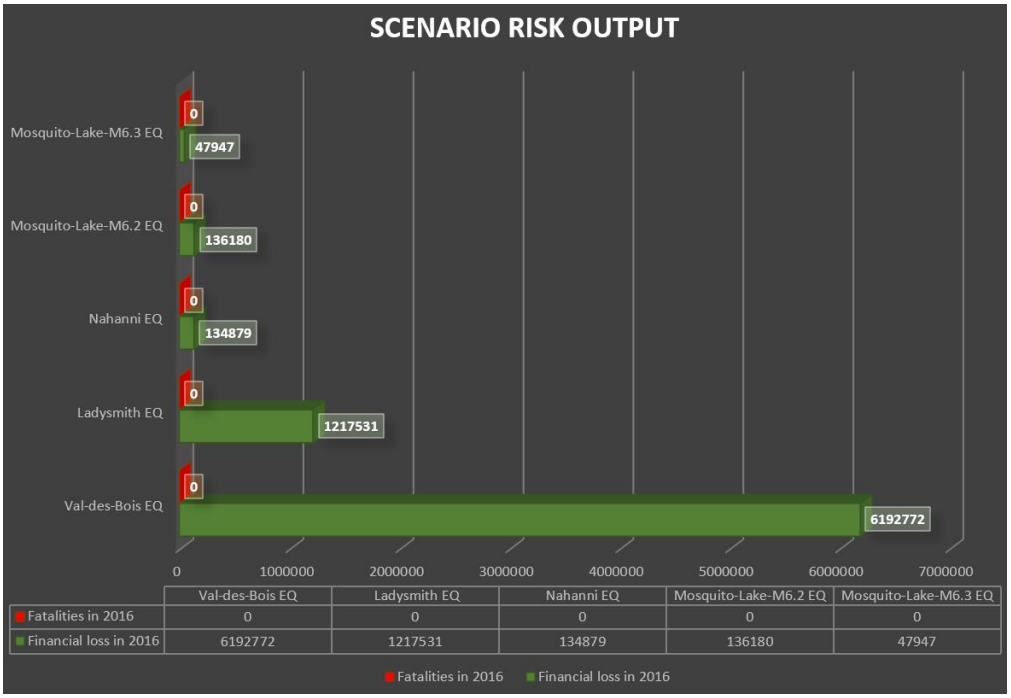

Figure 6.9. Scenario risk outputs of five studied earthquakes.

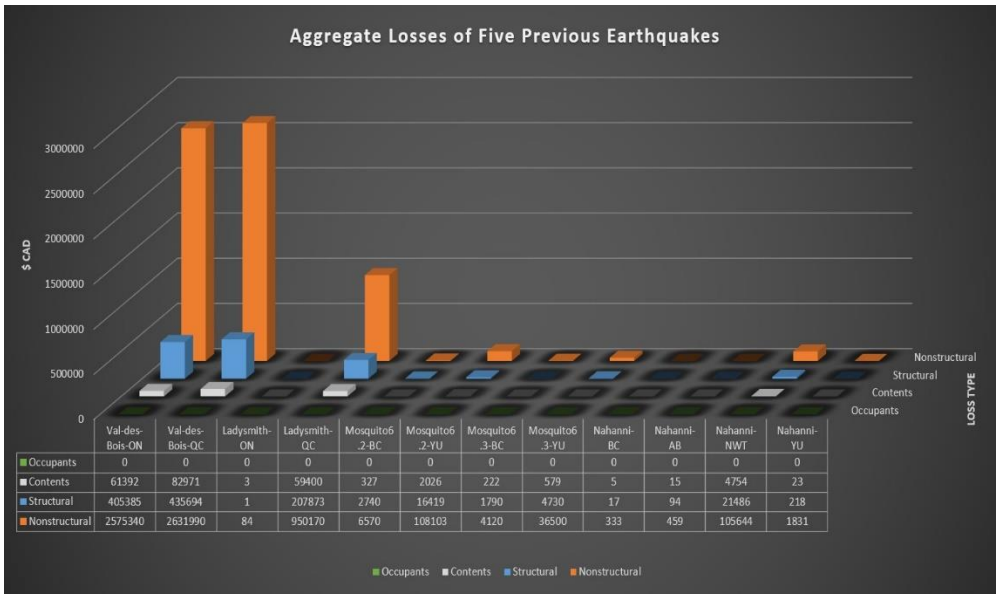

Figure 6.10. Aggregate losses for five distinct events under study.

6.3. Data processing and adjustments

It is noteworthy that CanSRM1 was developed in the year 2016, aligning its calculations inherently with the temporal context of that specific year. Therefore, before the estimated impacts generated by the CanadaSRM1 model can be meaningfully compared with the actual observed impacts of these earthquakes, there arises a compelling necessity to account for the overarching influences of both population growth and inflation. This, in turn, requires a conversion of the total financial loss figures, originally expressed in 2016 dollars, into the currency values prevailing at the time of each earthquake occurrence under consideration.

6.3.1. Financial loss adjustment

The losses reported are specific to damage incurred by Canadian buildings and their contents, converted from 2016 Canadian Dollars. For this purpose, Statistics Canada data was employed, with Statistics Canada being the national agency responsible for the provision of essential statistical information to Canadians (Statistics Canada 2023a). Data and insights pertaining to Canada's economy, society, and environment, including various surveys and a Census conducted every five years, are generated by them.

The data in question encompasses the Consumer Price Index, which undergoes monthly adjustments. To compute the coefficient employed in the adjustment for each year, the total dollar values of the year of occurrence are multiplied by 100 and then divided by the dollar values in the all-items column of 2016, as depicted in Equation (4-2). Subsequently, the adjustment coefficient is determined as a percentage, relying on Bank of Canada inflation tables, which draw upon Statistics Canada (2023) data. This coefficient, denoted as i_{coeff}, is calculated using the following formula:

$$\boldsymbol{i_{coeff} = \frac{CAD_{occ} \times 100}{CAD_{2016}}} \qquad (6\text{-}1)$$

where CAD_{occ} represents the total dollar value for the year of occurrence (Statistics Canada 2023a), CAD_{2016} represents the total dollar value for February 2016 (Statistics Canada 2023a), and i_{coeff} signifies the adjustment coefficient that reflects the rate of inflation during that period.

Finally, by multiplying the total losses, obtained from the risk assessment for each earthquake, by this coefficient and subsequently dividing by 100, as presented in Equation6-2), the total corresponding losses in the year of occurrence can be estimated. The formula for estimating the total losses adjusted for the year of event occurrence, denoted as $Loss_{occ}$, is as follows:

$$\boldsymbol{Loss_{occ} = \frac{Loss_{2016} \times i_{coeff}}{100}} \qquad 6\text{-}2)$$

where $Loss_{2016}$ signifies the total losses estimated by the model for the year 2016, and $Loss_{occ}$ represents the total losses adjusted for the year of event occurrence.

Due to inflation, when considering earthquakes that took place before 2016, it is observed that the resulting value will be reduced compared to its 2016 counterpart. Conversely, when examining

earthquakes that occurred after 2016, it becomes apparent that the resulting value will be elevated in comparison to the corresponding 2016 figure. Table 6.12 serves as an illustrative depiction of the adjustment coefficients, i_{coeff}, corresponding to fluctuations in the rate of inflation, which pertain to each of the five earthquakes, considered individually and in isolation.

Table 6.12. The adjustment coefficient based on inflation rate from the year of occurrence to 2016.

Earthquake	CAD_{2016}	CAD_{2010}	CAD_{2013}	CAD_{1985}	CAD_{2017}	i_{coeff}
Val-des-Bois EQ	127.1	116.2	-	-	-	91.4
Ladysmith EQ	127.1	-	123.0	-	-	96.77
Nahanni EQ	127.1	-	-	64.1	-	50.4
Mosquito-Lake-M6.2 EQ	127.1	-	-	-	130.5	102.7
Mosquito-Lake-M6.3 EQ	127.1	-	-	-	130.5	102.7

6.3.1.1. Val-des-Bois earthquake

According to Statistics Canada, the composite consumer price index for February 2016 was recorded at $127.10, while the corresponding figure for June 2010, the month of the 2010 Val-des-Bois earthquake, stood at $116.20. To render the economic findings compatible and to maintain consistency across the time frame, adjustments were made to account for inflation, using the Bank of Canada's inflation tables spanning the period from 2010 to 2016, which, in turn, relied on data sourced from Statistics Canada. This rigorous procedure was implemented to express the results in terms of constant 2010 dollars. Consequently, the total estimated losses, originally denoted at $9,260,456for 2016, were recalibrated to $8,464,057 to represent the equivalent losses in 2010.

6.3.1.2. Ladysmith earthquake

A similar procedure was employed for the analysis of the Ladysmith earthquake of 2013. In May 2013, the total consumer price was recorded at $123.0. Consequently, adjustments were carried out by applying a factor of 96.77%. Thus, the total losses, initially estimated at $1,217,531 for 2016, were recalibrated to reflect the equivalent total losses in 2010, resulting in a figure of $1,178,204.

6.3.1.3. Nahanni earthquake

In the case of the Nahanni earthquake results, due consideration was given to the fact that this seismic event transpired in the year 1985. Drawing from the records provided by Statistics Canada, the corresponding figure for December 1985 was significantly lower than for February 2016, approximately $64.10. This correction amounted to 50.4% and was executed in alignment with the Bank of Canada's inflation tables spanning the years from 1985 to 2016. As a result of this process, the total estimated losses, which had amounted to $134,878,915 for the year 2016, were transformed into the equivalent figure of $67,978,973 when measured in 1985 dollars.

6.3.1.4. Mosquito-Lake-M6.2 earthquake

The results of the Mosquito-Lake earthquake, which had a magnitude of 6.2, needed to be accounted for in light of the fact that this seismic event occurred in the year 2017. According to Statistics Canada, the total consumer price index for February 2016 stood at $127.10. In contrast, by May 2017, the total consumer price index had risen to $130.50. Consequently, in order to accurately adjust the economic results for the Mosquito-Lake earthquake, we applied an inflation factor of 102.7% based on the Bank of Canada's inflation tables spanning the years 2016 to 2017. As a result of this adjustment, the total estimated losses, initially calculated at $136,179,553 for the year 2016, were revised to $139,856,401 to reflect the total losses in the year 2017.

6.3.1.5. Mosquito-Lake-M6.3 earthquake

A similar procedure was employed in the case of the M6.3 Mosquito-Lake earthquake of 2017. According to Statistics Canada, the total consumer price index for February 2016 stood at $127.10, while in May 2017, it had risen to $130.50. In order to reconcile the economic findings, a currency adjustment was performed, whereby the dollar values were modified by $102.7% in accordance with the Bank of Canada's inflation tables for the years 2016 through 2017. Consequently, the total estimated losses, which amounted to $47,947 for 2016, were converted to $49,241 to represent the total losses in 2017.

In Table 6.13, an exhaustive summary of all computations, encompassing the resultant adjustments, is presented. The tabular representation also includes the outcomes of recalculated total financial losses and fatalities from the year 2016 through the year of occurrence for each of the aforementioned five seismic events.

Table 6.13. The estimated results for the studied earthquakes and the adjusted results after processing.

Earthquakes	Financial Loss in 2016 (CAD)	Financial Loss in Occurrence Date	Fatalities
2010 Val-des-Bois	$9,260,456	$8,464,057	0
2013 Ladysmith	$1,217,531	$1,178,204	0
1985 Nahanni	$134,879	$67,979	0
2017 Mosquito-Lake-M6.2	$136,180	$139,856	0
2017 Mosquito-Lake-M6.3	$47,947	$49,242	0

6.4. Comparison and model validation

The validation of CanadaSRM1 is an intricate process, ideally conducted through the utilization of observations garnered from previous earthquakes and the cumulative losses incurred over the relevant time frames. However, it should be underscored that in the Canadian context, there exists a notable deficiency of pertinent events that can be considered for this validation purpose. Within the annals of disaster databases, such as EM-DAT and the CDD, records dating back to the year 1900 are maintained. Their categorization of a disaster is explicitly defined as an event that involves the occurrence of 10 or more fatalities, the impact of 100 or more individuals through

injuries, evacuations, homelessness, or the initiation of a national or international assistance appeal (Tiegan E Hobbs et al. 2023). It is also noteworthy that the CDD's tracking extends to events that possess historical significance or that inflict substantial damage, thereby impeding the autonomous recovery of affected communities.

In the specific context of Canada, it is imperative to recognize that EM-DAT has not registered any occurrences of earthquakes. Conversely, the CDD has managed to document a total of nine such seismic events. Among these nine events, it is worth highlighting that only two have resulted in casualties: the 1946 surface-wave Magnitude (Ms) 7.2 Vancouver Island earthquake (Rogers and Hasegawa 1978) and the 1925 magnitude 6.7 Charlevoix-Kamouraska earthquake (Maurice Lamontagne 2002; M Lamontagne et al. 2018). Furthermore, when considering injuries, only one event, namely the 1944 Mw 5.8 Cornwall earthquake (John F. Cassidy and Bent 1993), has documented injuries. Adding to this, it is essential to note that the sole event with a recorded financial impact is the 1988 Ms 5.7 Saguenay earthquake (Mitchell, Tinawi, and Law 1990).

Given the scarcity of historical earthquake data that encompasses significant losses, this study necessitates adherence to a stringent threshold. Each earthquake subjected to scrutiny within this study is categorically deemed a disastrous event only when the model estimates a number of fatalities exceeding 10 people, thereby aligning with the data recorded by Disaster Databases. When delving into the CatIQ, which is entrusted with the arduous task of aggregating data from the insurance industry pertaining to all events in Canada that have engendered insured losses exceeding $30 million since 2008, a contrast emerges. Notably, CatIQ has not documented any earthquake events within its purview. Consequently, if the model's estimation of the total financial losses inflicted by earthquakes consistently falls below the $30 million threshold, it can be asserted that the model's estimation is reliable and aligned with the observed.

In the examination of the five selected earthquakes that have been subjected to scrutiny within this thesis, it becomes evident that these seismic events remain conspicuously absent from the Disaster Databases as recognized disaster events. Furthermore, they are expected by CanSRM1 to have caused modest damage in eastern, western, and northern Canada and their estimated impacts, whether assessed in terms of financial losses or numbers of fatalities, fall significantly below the established threshold for reporting in a disaster database. This is therefore a successful attempt at validating the reliability of the first generation of Canadian seismic risk model as a potent tool for the estimation of the impact of future earthquakes. This predictive capacity assumes paramount significance within the realm of geohazard management and risk reduction, where it serves as a proactive means to mitigate potential human losses and economic ramifications stemming from future earthquakes.

Table 6.14 provides a comprehensive summary of the final result comparison and validation test outcomes for all five examined events. The table includes information on Canadian building and contents damage, converted to the CAD of the occurrence year, rounded to the nearest million, and fatalities expressed as the cumulative probability of death, rounded to the nearest integer.

Table 6.14. Effects of the 5 examined earthquakes, utilizing USGS shakemap data as input for the CanadaSRM1 model.

Earthquakes	Val-des-Bois	Ladysmith	Nahanni	Mosquito-Lake-M6.2	Mosquito-Lake-M6.3
Year of occurrence	2010	2013	1985	2017	2017
Adjusted Financial losses	$8,464,057	$1,178,204	$67,979	$139,856	$49,242
Rounded Financial losses	$8 million	$1 million	Bellow $1 million	Bellow $1 million	Bellow $1 million
Adjusted Fatalities	0	0	0	0	0
Economic loss threshold	> $30 million				
Human loss threshold	> 10 deaths				
Comparison	Below threshold	Below threshold	Below threshold	Below threshold	Below threshold
Validation	**Validated**	**Validated**	**Validated**	**Validated**	**Validated**

Chapter 7 : Conclusion and Future Works

7.1. Introduction

This chapter serves as the concluding section of the thesis. It not only presents the final conclusions drawn from the research but also highlights certain limitations associated with the methods and software employed throughout the study. Additionally, it offers valuable recommendations for potential avenues of future research, which are tailored to the specific scope of this study.

7.2. Conclusions

SRA is a vital area of study, especially when dealing with densely populated urban areas. One of the most formidable challenges in this field is ensuring the reliability of the tools and models used to predict the impact of earthquakes. The crux of the matter lies in validating these tools against actual earthquake data and observations. However, this task is often complex due to the limited availability of such data.

This study focuses on a specific aspect of seismic risk assessment, namely, the validation of Canada's first-generation seismic risk model, known as CanadaSRM1. This model plays a crucial role in estimating the potential consequences of earthquakes in Canada, which is particularly important in a country prone to seismic activity. To ensure the model's accuracy, it needs to be rigorously validated using real-world earthquake events.

To achieve this, the researchers turn to previous earthquake events that have occurred in various regions of Canada. These actual events serve as benchmarks against which the model's predictions are compared. Among these benchmark scenarios are events like the Mosquito Lake 2017 pair earthquakes, Val-des-Bois 2010 earthquake, Ladysmith 2013 earthquake, and Nahanni 1985 earthquake. By analyzing how well the model aligns with the outcomes of these events, the researchers can assess its reliability.

The methodology employed in this research is reliable. It involves the use of specialized tools like the OQ Engine and a comprehensive national exposure dataset. These tools enable the researchers to estimate critical factors such as building damage, economic losses, and potential fatalities that might occur during the benchmark earthquake scenarios. Importantly, the research methodology adheres closely to the established framework of the CanadaSRM1.

What makes this study particularly significant are the results it produces. Despite the inherent complexities and simplifications that come with assessing seismic risk, the outcomes reveal a remarkable alignment between the model's predictions and the actual losses and fatalities recorded by disaster databases during previous earthquakes. This alignment is a substantial achievement, indicating that CanadaSRM1 is indeed a reliable tool for understanding the potential impacts of earthquakes in Canada.

The implications of this successful validation are far-reaching. It means that CanadaSRM1 can now be confidently applied to simulate and forecast the potential consequences of future earthquakes across the country. This is of paramount importance for disaster preparedness and

management. The insights generated by this model extend their influence on various sectors, including construction, urban planning, and infrastructure development.

Furthermore, the study highlights that the validation of the deterministic (scenario-based) component of CanadaSRM1 strengthens confidence in the probabilistic component of the model. Both components share critical inputs and parameters, collectively reinforcing the overall reliability of the entire risk assessment framework.

In summary, this study's achievement in successfully validating CanadaSRM1 using actual earthquake data is a significant milestone in the field of seismic risk assessment. It equips decision-makers, emergency responders, and planners with a powerful and dependable tool for anticipating and mitigating the potential impact of future seismic events in Canada. This is of paramount importance in a nation susceptible to seismic activity, where effective disaster risk reduction is crucial for protecting lives, infrastructure, and communities.

7.3. Limitations

Despite the success in model validation, several limitations come to light that need consideration. First and foremost is the challenge posed by the quality and availability of earthquake data. The study heavily relies on historical earthquake records, which may have gaps or inaccuracies. These data limitations can potentially affect the precision of the model validation process.

Furthermore, like many modeling endeavors, this research relies on certain assumptions and simplifications. While these are necessary for computational feasibility, they may not capture the full complexity of real-world seismic events and their consequences. This introduces an element of uncertainty, particularly regarding ground motion estimations. Another limitation arises from the geographical diversity within Canada. The country spans vast regions, and seismic characteristics can vary significantly from one area to another. The research may not comprehensively account for all regional variations, potentially limiting its applicability in specific locales.

Temporal factors are also worth noting. While the study focuses on historical earthquake events, it may not fully encompass the temporal changes in various influencing factors. This includes changes in building codes, infrastructure development, population growth, and land use patterns over time, all of which can have an impact on seismic risk. Moreover, on a local scale, variations in building construction practices, soil conditions, and vulnerability might not be adequately addressed by the research. These local factors are crucial in assessing seismic risk but can be challenging to incorporate comprehensively. The complexity of the model itself is another aspect to consider. To make it computationally manageable, certain simplifications may be necessary. While these simplifications enhance efficiency, they can also influence the model's precision, particularly when dealing with nuanced factors.

Additionally, while the model excels in simulating past earthquakes, predicting future events is inherently uncertain. The validation primarily focuses on historical events, and extrapolating this accuracy to foresee unobserved future events introduces challenges.

External factors that influence seismic risk, such as government policies, disaster preparedness measures, and socioeconomic conditions, might not be fully considered in the study. These external dynamics can significantly affect the real-world outcomes of seismic events. It's also essential to clarify the distinction between model verification and validation. The research validates the model against historical events, but it does not provide absolute confirmation of the model's correctness. Instead, it assesses its performance within a specific context.

7.4. Future works

To overcome the limitations and enhance the accuracy of the methodology used in this thesis for validating the seismic risk model, here are some future work suggestions:

7.4.1. Incorporate In-Situ Data

To improve the validation process, consider incorporating in-situ data from seismic monitoring stations and ground sensors. These real-time measurements can provide valuable information for validating model predictions. Additionally, the use of high-quality ground motion data can enhance the accuracy of ground motion modeling.

7.4.2. Leverage Remote Sensing

Utilize high-resolution satellite imagery and remote sensing data to assess the physical damage caused by earthquakes. Remote sensing can provide detailed and up-to-date information on infrastructure damage, which can be compared with model predictions for validation.

7.4.3. Harness AI and Machine Learning Techniques

Apply unsupervised clustering techniques like the K-means algorithm to identify patterns and clusters within the data. This can help refine exposure models by grouping similar regions with comparable characteristics, allowing for more accurate risk assessments. Explore the use of machine learning models, such as random forests or neural networks, to enhance the predictive accuracy of the seismic risk model. These models can capture complex relationships within the data and improve predictions.

7.4.4. Expand the Earthquake Dataset

To increase the robustness of the validation process, examine a more extensive dataset of earthquakes. By considering a broader range of historical events, the model's performance can be assessed across various magnitudes, depths, and locations, providing a more comprehensive validation.

7.4.5. Utilize Alternative Disaster Databases

Incorporate other disaster databases like AIR Worldwide to cross-reference and validate the estimated results. Comparing model outputs with multiple data sources can help assess the model's accuracy and reliability further.

7.4.6. Comprehensive Damage Assessment

In addition to estimating structural damages, consider expanding the assessment to encompass non-structural damage and other types of damage. Non-structural components within buildings, such as contents, equipment, and utilities, can also incur significant losses during earthquakes. By incorporating non-structural damage assessments, the model can provide a more comprehensive and accurate picture of the overall impact.

7.4.7. Incorporate Secondary Hazards and Site Conditions

Extend the methodology beyond the consideration of direct seismic risk to include secondary hazards and indirect damage factors. Earthquakes can trigger secondary hazards like tsunamis, fires, and floods, which can greatly amplify the overall damage sustained by buildings. Additionally, site-specific conditions, such as soil amplification, liquefaction susceptibility, landslide potential, and surface rupture risk, should be factored into the assessment. Accounting for these factors will lead to a more realistic estimation of earthquake-induced damage and risk.

7.4.8. Utilize High-Performance Computing (HPC)

To mitigate aleatoric uncertainty and significantly increase the precision of the seismic risk calculations, consider leveraging high-performance computing (HPC) resources, such as supercomputers. By utilizing HPC capabilities, you can substantially increase the number of GMF simulations beyond the limitations of personal computers. This allows for a more extensive and finer-grained analysis of ground motion scenarios, reducing uncertainties and providing a more accurate assessment of seismic risk. The increased computational power and speed of supercomputers can expedite the modeling process, making it possible to explore a broader range of scenarios and parameters, ultimately improving the reliability of the seismic risk model.

7.4.9. Temporal Analysis

Investigate the temporal dynamics of seismic risk by examining changes over time. Consider how factors such as urban development, building code revisions, and population growth impact seismic risk. This longitudinal analysis can provide insights into the evolving nature of seismic risk.

7.4.10. Sensitivity Analysis

Perform sensitivity analyses to understand how variations in model inputs and assumptions affect the model's outcomes. Identifying the most influential parameters can guide efforts to refine the model and improve its accuracy.

7.4.11. Real-Time Validation

Develop a system for real-time validation of the model by continuously comparing model predictions with observed earthquake impacts as new data becomes available. This ongoing validation can enhance the model's adaptability and reliability.

7.4.12. Collaborative Research

Collaborate with experts in fields such as seismology, geology, and disaster management to gain insights and expertise in specific aspects of seismic risk assessment. Interdisciplinary research can lead to more accurate and comprehensive models.

These suggestions for future work are intended to tackle the limitations of the current methodology and harness advanced technologies and data sources to improve the accuracy and reliability of the validation process for seismic risk models. Consequently, the methodology can evolve to offer a more thorough and precise assessment of seismic risk, taking into account a broader spectrum of potential impacts and hazards. By integrating these methods, researchers can contribute to more efficient disaster preparedness and risk reduction endeavors. This all-encompassing approach will aid in making better-informed decisions and formulating more effective disaster preparedness and mitigation strategies.

Appendix A : Important Canadian Earthquakes

Table A.1. An overview of important earthquakes in Canada from 1663 to 2012 (Geological Survey of Canada).

Year	Day	Latitude	Longitude	Mw	Location	Comment
1663	Feb 5	47.60	-70.10	7.0	Charlevoix-Kamouraska Region	
1700	Jan 26	48.50	-125.00	9.0	Cascadia Subduction Zone	Largest quake in Canada, one of the world's greatest quakes
1732	Sep 16	45.50	-73.60	5.8	Western Quebec Seismic Zone, Montreal Region	
1791	Dec 6	47.40	-70.50	6.0	Région Charlevoix-Kamouraska	
1860	Oct 17	47.50	-70.10	6.0	Région Charlevoix-Kamouraska	
1870	Oct 20	47.40	-70.50	6.5	Charlevoix-Kamouraska Region	
1872	Dec 15	48.60	-121.40	7.4	Washington-B.C. Border	Widely felt in B.C.
1899	Sep 4	60.00	-140.00	8.0	Yukon-Alaska Border	Widely felt in north-western B.C.
1918	Dec 6	49.62	-125.92	7.0	Vancouver Island, BC	Widely felt, minor damage
1925	Mar 1	47.80	-69.80	6.2	Charlevoix-Kamouraska region	
1929	May 26	51.51	-130.74	7.0	South of Haida Gwaii (formerly Queen Charlotte Islands), BC	Widely felt, minor damage
1929	Nov 18	44.50	-56.30	7.2	Atlantic Ocean, south of Newfoundland	
1933	Nov 20	73.00	-70.75	7.3	Baffin Bay, Northwest Territories	
1935	Nov 1	46.78	-79.07	6.1	Quebec - Ontario Border, Temiscamingue region	
1944	Sep 5	44.97	-74.90	5.8	Cornwall region, Ontario-New York border	
1946	Jun 23	49.76	-125.34	7.3	Vancouver Island, BC	Widely felt, most damaging quake in western Canada
1949	Aug 22	53.62	-133.27	8.1	Offshore Haida Gwaii (formerly Queen Charlotte Islands), BC	Largest quake in Canada, one of the world's greatest quakes
1949				7.0	Washington	Much damage in Washington and felt in southwestern B.C.
1958	Jul 10	58.60	-137.10	7.9	near the British Columbia-Alaska Border	Damage in Alaska, widely felt in northwestern B.C.
1964				9.0	Alaska	Tsunami damage on Vancouver Island
1970	Jun 24	51.77	-130.76	7.4	South of Haida Gwaii (formerly Queen Charlotte Islands), BC	Widely felt
1979	Feb 28	60.59	-141.47	7.2	Southern Yukon-Alaska Border	
1982	Jan 9	47.00	-66.60	5.7	Miramichi, New Brunswick	
1982	Jan 11	47.00	-66.60	5.4	Miramichi, New Brunswick	
1985	Oct 5	62.21	-124.22	6.6	Nahanni region, Northwest Territories	
1985	Dec 23	62.19	-124.24	6.9	Nahanni region, Northwest Territories	
1988	Nov 25	48.12	-71.18	5.9	Saguenay region	
1989	Dec 25	60.12	-73.60	6.3	Ungava region	
2012	Oct 28	52.55	-132.24	7.7	Offshore Haida Gwaii	

Appendix B : Taxonomy and Occupancy Terms

Table B.1. Building taxonomies, Adapted from Table 3 from (Hobbs et al. 2022), Table 3.2 from HAZUS (FEMA 2012).

Code	Building Prototype	Class	Height	Stories
W1	Small Wood Frame	Wood Light Frame Residential		1-2
W2		Wood, Heavy Frame Residential		3-6
W3	Large Wood Frame	Wood, Heavy Frame Commercial & Industrial		All
W4		Wood, Light Frame with Cripple Wall or Subfloor		1-2
S1L	Steel Moment Frame	Steel Moment Frame Low Rise	Low-Rise	1-3
S1M		Steel Moment Frame Medium Rise	Mid-Rise	4-7
S1H		Steel Moment Frame High Rise	High-Rise	8+
S2L	Steel Braced Frame	Steel Braced Frame Low Rise	Low-Rise	1-3
S2M		Steel Braced Frame Medium Rise	Mid-Rise	4-7
S2H		Steel Braced Frame High Rise	High-Rise	8+
S3	Light Metal Frame	Light Metal Frame		All
S4L	Steel Frame Concrete Wall	Steel Frame with Cast-in-Place Concrete Shear Walls Low Rise	Low-Rise	1-3
S4M		Steel Frame with Cast-in-Place Concrete Shear Walls Med Rise	Mid-Rise	4-7
S4H		Steel Frame with Cast-in-Place Concrete Shear Walls High Rise	High-Rise	8+
S5L	Steel Frame Infill Wall	Steel Frame with Unreinforced Masonry Infill Walls Low Rise	Low-Rise	1-3
S5M		Steel Frame with Unreinforced Masonry Infill Walls Med Rise	Mid-Rise	4-7
S5H		Steel Frame with Unreinforced Masonry Infill Walls High Rise	High-Rise	8+
C1L	Concrete Moment Frame	Reinforced Concrete Moment Frame Low Rise	Low-Rise	1-3
C1M		Reinforced Concrete Moment Frame Medium Rise	Mid-Rise	4-7
C1H		Reinforced Concrete Moment Frame High Rise	High-Rise	8+
C2L	Concrete Shear Wall	Concrete Frame with Concrete Walls Low Rise	Low-Rise	1-3
C2M		Concrete Frame with Concrete Walls Medium Rise	Mid-Rise	4-7
C2H		Concrete Frame with Concrete Walls High Rise	High-Rise	8+
C3L	Concrete Frame Infill Wall	Concrete Frame with Unreinforced Masonry Infill Walls Low Rise	Low-Rise	1-3
C3M		Concrete Frame with Unreinforced Masonry Infill Walls Med Rise	Mid-Rise	4-7
C3H		Concrete Frame with Unreinforced Masonry Infill Walls High Rise	High-Rise	8+
PC1	Tilt Up	Precast Concrete Tilt-Up Walls		All
PC2L	Precast Concrete Frame	Precast Concrete Frames with Concrete Shear Walls Low Rise	Low-Rise	1-3
PC2M		Precast Concrete Frames with Concrete Shear Walls Med Rise	Mid-Rise	4-7
PC2H		Precast Concrete Frames with Concrete Shear Walls High Rise	High-Rise	8+
RM1L	Reinforced Masonry Flexible Diaphragm	Reinforced Masonry Bearing Walls with Wood or Metal Deck Diaphragms Low Rise	Low-Rise	1-3
RM1M		Reinforced Masonry Bearing Walls with Wood or Metal Deck Diaphragms Medium Rise	Mid-Rise	4+
RM2L	Reinforced Masonry Rigid Diaphragm	Reinforced Masonry Bearing Walls with Precast Concrete	Low-Rise	1-3
RM2M		Reinforced Masonry Bearing Walls with Precast Concrete	Mid-Rise	4-7
RM2H		Reinforced Masonry Bearing Walls with Precast Concrete	High-Rise	8+
URML	Unreinforced Masonry	Unreinforced Masonry Bearing Wall Low Rise	Low-Rise	1-2
URMM		Unreinforced Masonry Bearing Wall Medium Rise	Mid-Rise	3+
MH	Mobile Home	Mobile Homes		All

Table B.2. Occupancy Classifications, reprinted from (Hobbs et al. 2022), originally featured in FEMA's Methodology for Estimating Disaster-Related Potential Losses (HAZUS) Table 3.3 (FEMA, 2012).

Label	Occupancy Class	Example Descriptions
Residential		
RES1	Single Family Dwelling	House
RES2	Mobile Home	Mobile Home
RES3	Multi Family Dwelling RES3A RES3B RES3C RES3D RES3E RES3F	Apartment/Condominium Duplex 3-4 Units 5-9 Units 10-19 Units 20-49 Units 50+ Units
RES4	Temporary Lodging	Hotel/Motel
RES5	Institutional Dormitory	Group Housing (military, college), Jails
RES6	Nursing Home	
Commercial		
COM1	Retail Trade	Store
COM2	Wholesale Trade	Warehouse
COM3	Personal and Repair Services	Service Station/Shop
COM4	Professional/Technical Services	Offices
COM5	Banks	
COM6	Hospital	
COM7	Medical Office/Clinic	
COM8	Entertainment & Recreation	Restaurants/Bars
COM9	Theaters	Theaters
COM10	Parking	Garages
Industrial		
IND1	Heavy	Factory
IND2	Light	Factory
IND3	Food/Drugs/Chemicals	Factory
IND4	Metals/Minerals Processing	Factory
IND5	High Technology	Factory
IND6	Construction	Office
Agriculture		
AGR1	Agriculture	
Religion/Non/Profit		
REL1	Church/Non-Profit	
Government		
GOV1	General Services	Office
GOV2	Emergency Response	Police/Fire Station/EOC
Education		
EDU1	Grade Schools	
EDU2	Colleges/Universities	Does not include group housing

Appendix C : Executed Code

The following scripts introduce a selection of Python code snippets that are instrumental in the visualization process within the scope of this thesis.

```
# Function to read a dataset from an HDF5 file
    def read_hdf5_dataset(file_path, dataset_name):
        with h5py.File(file_path, 'r') as f:
            return f[dataset_name][()]

# Function to plot a map with given longitudes and latitudes
    def plot_map(lon, lat, title, marker_style, color):
        plt.figure(figsize=(14, 10))
        m = Basemap(projection='mill',llcrnrlat=-60,urcrnrlat=90,\
                llcrnrlon=-180,urcrnrlon=180,resolution='c')
        m.drawcoastlines()
        m.drawcountries()
        m.drawmapboundary(fill_color='aqua')
        m.fillcontinents(color='lightgreen',lake_color='aqua')
        m.drawparallels(np.arange(-90., 91., 30.), labels=[1, 0, 0, 0])
        m.drawmeridians(np.arange(-180., 181., 60.), labels=[0, 0, 0, 1])

# Convert longitude and latitude to map projection coordinates
        x, y = m(lon, lat)

    # Plot the coordinates on the map
        m.scatter(x, y, marker=marker_style, color=color, zorder=5)
        plt.title(title)
        plt.show()

# Read the 'sitecol' dataset from both HDF5 files
    sitecol_68 = read_hdf5_dataset('calc_68.hdf5', 'sitecol')
    sitecol_67 = read_hdf5_dataset('calc_67.hdf5', 'sitecol')

# Extract longitude and latitude from the 'sitecol' datasets
    lon_68 = sitecol_68['lon']
    lat_68 = sitecol_68['lat']
    lon_67 = sitecol_67['lon']
    lat_67 = sitecol_67['lat']

# Plot the map for calc_68.hdf5
    plot_map(lon_68, lat_68, "Geographical Distribution of Sites from calc_68", 'o', 'r')

# Plot the map for calc_67.hdf5
    plot_map(lon_67, lat_67, "Geographical Distribution of Sites from calc_67", 'x', 'b')
    def list_hdf5_contents(file_path):
        with h5py.File(file_path, 'r') as f:
            return list(f.keys())
    hdf5_file_path = 'calc_67.hdf5'
    print("Contents of HDF5 file:", list_hdf5_contents(hdf5_file_path))
    df_dic = pd.DataFrame.from_dict(list_hdf5_contents(hdf5_file_path))
    df_dic
    def list_npz_contents(file_path):
```

```
        with np.load(file_path) as f:
            return list(f.keys())
    npz_file_path = 'Asset Damage Distributions_output-131-damages-rlzs_68.npz'
    print("Contents of NPZ file:", list_npz_contents(npz_file_path))

# Function to read a dataset from an HDF5 file
    def read_hdf5_dataset(file_path, dataset_name):
        with h5py.File(file_path, 'r') as f:
            return f[dataset_name][()]

# Function to save a zoomed map to a file
    def save_zoomed_map_to_file(lon, lat, title, marker_style, color, file_path, llcrnrlat, urcrnrlat, llcrnrlon, urcrnrlon):
        plt.figure(figsize=(14, 10))
        m = Basemap(projection='mill', llcrnrlat=llcrnrlat, urcrnrlat=urcrnrlat,
                    llcrnrlon=llcrnrlon, urcrnrlon=urcrnrlon, resolution='c')
        m.drawcoastlines()
        m.drawcountries()
        m.drawmapboundary(fill_color='aqua')
        m.fillcontinents(color='lightgreen',lake_color='aqua')
        m.drawparallels(np.arange(-90., 91., 30.), labels=[1, 0, 0, 0])
        m.drawmeridians(np.arange(-180., 181., 60.), labels=[0, 0, 0, 1])

# Convert longitude and latitude to map projection coordinates
        x, y = m(lon, lat)

# Plot the coordinates on the map
        m.scatter(x, y, marker=marker_style, color=color, zorder=5)
        plt.title(title)
        plt.savefig(file_path)

# Re-read the 'sitecol' dataset from both HDF5 files
    sitecol_68 = read_hdf5_dataset('calc_68.hdf5', 'sitecol')
    sitecol_67 = read_hdf5_dataset('calc_67.hdf5', 'sitecol')

# Extract longitude and latitude from the 'sitecol' datasets
    lon_68 = sitecol_68['lon']
    lat_68 = sitecol_68['lat']
    lon_67 = sitecol_67['lon']
    lat_67 = sitecol_67['lat']

# Load the NPZ file and extract longitude and latitude
    with np.load('Asset Damage Distributions_output-131-damages-rlzs_68.npz') as data:
        sample_data = data['rlz-000']
    lon_npz = sample_data['lon']
    lat_npz = sample_data['lat']

# Define zoom boundaries for focusing on Canada
    llcrnrlat = 41  # Lower left corner latitude
    urcrnrlat = 84  # Upper right corner latitude
    llcrnrlon = -141  # Lower left corner longitude
    urcrnrlon = -52  # Upper right corner longitude

# File paths to save the zoomed maps focused on Canada
    zoomed_canada_map_file_68_path = 'zoomed_canada_map_from_calc_68.png'
```

```
    zoomed_canada_map_file_67_path = 'zoomed_canada_map_from_calc_67.png'
    zoomed_canada_map_file_npz_path = 'zoomed_canada_map_from_npz_file.png'

# Save the zoomed maps focused on Canada
    save_zoomed_map_to_file(lon_68, lat_68, "Zoomed Geographical Distribution of Sites from calc_68 Focused on
    Canada", 'o', 'r', zoomed_canada_map_file_68_path, llcrnrlat, urcrnrlat, llcrnrlon, urcrnrlon)
    save_zoomed_map_to_file(lon_67, lat_67, "Zoomed Geographical Distribution of Sites from calc_67 Focused on
    Canada", 'x', 'b', zoomed_canada_map_file_67_path, llcrnrlat, urcrnrlat, llcrnrlon, urcrnrlon)
    save_zoomed_map_to_file(lon_npz, lat_npz, "Zoomed Geographical Distribution of Sites from NPZ File Focused
    on Canada", 's', 'g', zoomed_canada_map_file_npz_path, llcrnrlat, urcrnrlat, llcrnrlon, urcrnrlon)
```

References

Abo El Ezz, Ahmad, Marie-José Nollet, and Miroslav Nastev. 2014. *Methodology for Rapid Assessment of Seismic Damage to Buildings in Canadian Settings*. https://doi.org/10.4095/293874.

Abo El Ezz, Ahmad, Alex Smirnoff, Miroslav Nastev, Marie-José Nollet, and Heather McGrath. 2019. "ER2-Earthquake: Interactive Web-Application for Urban Seismic Risk Assessment." *International Journal of Disaster Risk Reduction* 34 (March): 326–36. https://doi.org/10.1016/j.ijdrr.2018.12.022.

Adams, John, Garry Rogers, Stephen Halchuk, David McCormack, and John Cassidy. 2002. "The Case for an Advanced National Earthquake Monitoring System for Canada's Cities at Risk." In *Proceedings of the 7th US National Conference on Earthquake Engineering, Boston, United States. Paper*. Vol. 42.

Agrawal, Nirupama. 2018. *Natural Disasters and Risk Management in Canada*. Springer.

Aguilar Meléndez, Armando, Mario Gustavo Ordaz Schroeder, Josep De la Puente, Sergio Natan González Rocha, Héctor Enrique Rodriguez Lozoya, Alejandro Córdova Ceballos, Alejandro García Elías, et al. 2017. "Development and Validation of Software CRISIS to Perform Probabilistic Seismic Hazard Assessment with Emphasis on the Recent CRISIS2015." *Computación y Sistemas* 21 (1). https://doi.org/10.13053/cys-21-1-2578.

Asgharzadeh Sadegh, Parisa. 2012. "Focal Mechanisms and Variations in Tectonic Stress Fields in Eastern Canada (Western Quebec and Southern Ontario)."

"ATC-40 Seismic Evaluation and Retrofit of Concrete Buildings | PDF | Economic Sectors | Solid Mechanics." n.d. Accessed May 29, 2023. https://www.scribd.com/document/223455280/ATC-40-Seismic-Evaluation-and-Retrofit-of-Concrete-Buildings.

Atik, L. A., N. Abrahamson, J. J. Bommer, F. Scherbaum, F. Cotton, and N. Kuehn. 2010. "The Variability of Ground-Motion Prediction Models and Its Components." *Seismological Research Letters* 81 (5): 794–801. https://doi.org/10.1785/gssrl.81.5.794.

Baker, J. W. 2008. *An Introduction to Probabilistic Seismic Hazard Analysis (PSHA). Stanfordedu 1–72 (2008)*.

Bakun, W. H., M. C. Stickney, and Gary C. Rogers. 2011. "The 16 May 1909 Northern Great Plains EarthquakeShort Note." *Bulletin of the Seismological Society of America* 101 (6): 3065–71.

Bay, Francesca, Stefan Wiemer, Donat Fäh, and Domenico Giardini. 2005. "Predictive Ground Motion Scaling in Switzerland: Best Estimates and Uncertainties." *Journal of Seismology* 9 (2): 223–40.

Bent, Allison L., John Cassidy, Claude Prépetit, Maurice Lamontagne, and Sophia Ulysse. 2018. "Real-time Seismic Monitoring in Haiti and Some Applications." *Seismological Research Letters* 89 (2A): 407–15.

Bent, Allison L., Maurice Lamontagne, Veronika Peci, Stephen Halchuk, Gregory R. Brooks, Dariush Motazedian, James A. Hunter, et al. 2015. "The 17 May 2013 M 4.6 Ladysmith, Quebec, Earthquake." *Seismological Research Letters* 86 (2A): 460–76. https://doi.org/10.1785/0220140138.

Bernal, Gabriel, and Omar Cardona. 2018. *NEXT GENERATION CAPRA SOFTWARE*.

Bhattacharya, Baidurya, Roger Basu, and Kai-tung Ma. 2001. "Developing Target Reliability for Novel Structures: The Case of the Mobile Offshore Base." *Marine Structures*, Very Large Floating Structures (VLFS) Part II, 14 (1): 37–58. https://doi.org/10.1016/S0951-8339(00)00024-1.

Bommer, Julian J. 2002. "Deterministic vs. Probabilistic Seismic Hazard Assessment: An Exaggerated and Obstructive Dichotomy." *Journal of Earthquake Engineering* 06 (spec01): 43–73. https://doi.org/10.1142/S1363246902000644.

Bommer, Julian J., and Helen Crowley. 2006. "The Influence of Ground-Motion Variability in Earthquake Loss Modelling." *Bulletin of Earthquake Engineering* 4: 231–48.

Bommer, Julian J., Helen Crowley, and Rui Pinho. 2015. "A Risk-Mitigation Approach to the Management of Induced Seismicity." *Journal of Seismology* 19: 623–46.

Bommer, Julian, Robin Spence, Mustafa Erdik, Shigeko Tabuchi, Nuray Aydinoglu, Edmund Booth, Domenico del Re, and Oliver Peterken. 2002. "Development of an Earthquake Loss Model for Turkish Catastrophe Insurance." *Journal of Seismology* 6 (3): 431–46. https://doi.org/10.1023/A:1020095711419.

Boore, David M., and Gail M. Atkinson. 2008. "Ground-Motion Prediction Equations for the Average Horizontal Component of PGA, PGV, and 5%-Damped PSA at Spectral Periods between 0.01 s and 10.0 s." *Earthquake Spectra* 24 (1): 99–138. https://doi.org/10.1193/1.2830434.

Borzi, Barbara, Rui Pinho, and Helen Crowley. 2008. "Simplified Pushover-Based Vulnerability Analysis for Large-Scale Assessment of RC Buildings." *Engineering Structures* 30 (3): 804–20.

Bostrom, Ann, Luc Anselin, and Jeremy Farris. 2008. "Visualizing Seismic Risk and Uncertainty: A Review of Related Research." *Annals of the New York Academy of Sciences*, Annals of the New York Academy of Sciences, 1128 (1): 29–40. https://doi.org/10.1196/annals.1399.005.

Bostwick, Todd Kendall. 1984. "A Re-Examination of the August 22, 1949 Queen Charlotte Earthquake." University of British Columbia.

Brooks, Gregory R., and Didier Perret. 2023. "A Long-Term Context for the 1663 Charlevoix CE Earthquake Interpreted from the Postglacial Landslide Record in the Gouffre Valley, Quebec, Canada." *Quaternary Science Reviews* 309 (June): 108096. https://doi.org/10.1016/j.quascirev.2023.108096.

Bruhn, Ronald L., Jeanne Sauber, Michelle M. Cotton, Terry L. Pavlis, Evan Burgess, Natalia Ruppert, and Richard R. Forster. 2012. "Plate Margin Deformation and Active Tectonics along the Northern Edge of the Yakutat Terrane in the Saint Elias Orogen, Alaska, and Yukon, Canada." *Geosphere* 8 (6): 1384–1407.

"CAPRA-GIS | CAPRA | Probabilistic Risk Assessment Platform." n.d. Accessed May 29, 2023. https://ecapra.org/topics/capra-gis.

Cardone, Donatello, Amedeo Flora, Mauro De Luca Picione, and Adriano Martoccia. 2019. "Estimating Direct and Indirect Losses Due to Earthquake Damage in Residential RC Buildings." *Soil Dynamics and Earthquake Engineering* 126: 105801.

Cassidy, J F, G C Rogers, and S Halchuk. 2010. "Canada's Earthquakes: 'The Good, the Bad, and the Ugly.'" *GEOSCIENCE CANADA* 37 (1).

Cassidy, J. F., G. C. Rogers, M. Lamontagne, S. Halchuk, and J. Adams. 2010. "Canada's Earthquakes: 'The Good, the Bad, and the Ugly.'" *Geoscience Canada* 37 (1): 1–16.

Cassidy, John F., and Allison L. Bent. 1993. "Source Parameters of the 29 May and 5 June, 1940 Richardson Mountains, Yukon Territory, Earthquakes." *Bulletin of the Seismological Society of America* 83 (3): 636–59.

Cassidy, John F., Garry C. Rogers, and J. Ristau. 2005. "Seismicity in the Vicinity of the SNORCLE Corridors of the Northern Canadian Cordillera." *Canadian Journal of Earth Sciences* 42 (6): 1137–48.

Choi, Eunsoo, Reginald DesRoches, and Bryant Nielson. 2004. "Seismic Fragility of Typical Bridges in Moderate Seismic Zones." *Engineering Structures* 26 (2): 187–99. https://doi.org/10.1016/j.engstruct.2003.09.006.

Choy, George L., and John Boatwright. 1988. "Teleseismic and Near-Field Analysis of the Nahanni Earthquakes in the Northwest Territories, Canada." *Bulletin of the Seismological Society of America* 78 (5): 1627–52.

Coburn, Andrew, and Robin Spence. 2002. *Earthquake Protection*. John Wiley & Sons.

Cook, Frederick, Donald White, Alan Jones, David Eaton, Jeremy Hall, and Ron Clowes. 2010. "How the Crust Meets the Mantle: Lithoprobe Perspectives on the Mohorovii Discontinuity and Crust-Mantle Transition." *Canadian Journal of Earth Sciences* 47 (April): 315–51. https://doi.org/10.1139/E09-076.

Cook, Shane Edmond. 1999. "Evaluation of Non-Structural Earthquake Damage to Buildings in Southwestern B.C." University of British Columbia. https://doi.org/10.14288/1.0063786.

Coordinator, Office of the United Nations Disaster Relief. 1980. “Natural disasters and vulnerability analysis :: report of Expert Group Meeting, 9-12 July 1979.” In . UN,. https://digitallibrary.un.org/record/95986.

Crowley, Helen, and Julian J. Bommer. 2006. “Modelling Seismic Hazard in Earthquake Loss Models with Spatially Distributed Exposure.” *Bulletin of Earthquake Engineering* 4 (3): 249–73. https://doi.org/10.1007/s10518-006-9009-y.

Crowley, Helen, Rui Pinho, Barbara Polidoro, and Jan Van Elk. 2017. “Developing Fragility and Consequence Models for Buildings in the Groningen Field.” *Netherlands Journal of Geosciences* 96 (5): s247–57.

Daniell, J. E. 2011. “Open Source Procedure for Assessment of Loss Using Global Earthquake Modelling Software (OPAL).” *Natural Hazards and Earth System Sciences* 11 (7): 1885–99. https://doi.org/10.5194/nhess-11-1885-2011.

“Daniell J, Simpson A, Murnane R, Tijssen A, Nunez A, Deparday V, Gunasekera R, Baca A, Ishizawa O, Schäfer A. Review of Open Source and Open Access Software Packages Available to Quantify Risk from Natural Hazards. Washington, DC: World Bank and Global Facility for Disaster Reduction and Recovery. 2014.” n.d. Accessed May 29, 2023.

De Bono, Andrea, and Miguel G. Mora. 2014a. “A Global Exposure Model for Disaster Risk Assessment.” *International Journal of Disaster Risk Reduction* 10 (December): 442–51. https://doi.org/10.1016/j.ijdrr.2014.05.008.

———. 2014b. “A Global Exposure Model for Disaster Risk Assessment.” *International Journal of Disaster Risk Reduction*, Global probabilistic assessment of risk from natural hazards for the Global Assessment Report 2013 (GAR13), 10 (December): 442–51. https://doi.org/10.1016/j.ijdrr.2014.05.008.

Dhu, Trevor, David Robinson, Dan Clark, D Gray, and P Row. 2008. *EVENT-BASED EARTHQUAKE RISK MODELLING*.

Dineva, Savka, David Eaton, and Robert Mereu. 2004. “Seismicity of the Southern Great Lakes: Revised Earthquake Hypocenters and Possible Tectonic Controls.” *Bulletin of the Seismological Society of America* 94 (5): 1902–18. https://doi.org/10.1785/012003007.

Doser, Diane I., and Hugo Rodriguez. 2011. “A Seismotectonic Study of the Southeastern Alaska Region.” *Tectonophysics* 497 (1): 105–13. https://doi.org/10.1016/j.tecto.2010.10.019.

Dowrick, David J. 2003. *Earthquake Risk Reduction*. Chichester, West Sussex, England ; Hoboken, NJ, USA: J. Wiley.

“Earthquake Engineering Research Institute.” n.d. EERI. Accessed November 20, 2023. https://www.eeri.org/.

Elnashai, Amr S., Shawn Hampton, Himmet Karaman, Jong Sung Lee, Terrence Mclaren, James Myers, Christopher Navarro, Muhammed Şahin, Billie Spencer, and Nathan Tolbert. 2008. “Overview and Applications of Maeviz-Hazturk 2007.” *Journal of Earthquake Engineering* 12 (sup2): 100–108. https://doi.org/10.1080/13632460802013750.

“Ergo – Multi-Hazard Assessment, Response, and Planning.” n.d. Accessed May 29, 2023. https://ergo.ncsa.illinois.edu/.

Esmaeilzadeh, Amin, and Dariush Motazedian. n.d. “3D Nonlinear Ground Motion Simulation for Postglacial Sediments in Kinburn Basin.”

Esposito, Simona, Iunio Iervolino, Anna d’Onofrio, Antonio Santo, Francesco Cavalieri, and Paolo Franchin. 2015. “Simulation-Based Seismic Risk Assessment of Gas Distribution Networks.” *Computer-Aided Civil and Infrastructure Engineering* 30 (7): 508–23. https://doi.org/10.1111/mice.12105.

Estève, Clément, Jeremy Gosselin, Pascal Audet, Andrew Schaeffer, Derek Schutt, and Richard Aster. 2021. “Surface-Wave Tomography of the Northern Canadian Cordillera Using Earthquake Rayleigh Wave Group Velocities.” *Journal of Geophysical Research: Solid Earth* 126 (August). https://doi.org/10.1029/2021JB021960.

Feng, Wanpeng, Sergey Samsonov, Cunren Liang, Junhua Li, François Charbonneau, Chen Yu, and Zhenhong Li. 2019. “Source Parameters of the 2017 M w 6.2 Yukon Earthquake Doublet Inferred from Coseismic GPS and ALOS-2 Deformation Measurements.” *Geophysical Journal International* 216 (3): 1517–28.

Fereidoni, Azadeh. 2014. “Seismicity Processes in the Charlevoix Seismic Zone, Eastern Canada.” *Electronic Thesis and Dissertation Repository*, October. https://ir.lib.uwo.ca/etd/2515.

Fowler, Christine Mary Rutherford, Clarence Mary R. Fowler, and Mary Fowler. 1990. *The Solid Earth: An Introduction to Global Geophysics*. Cambridge University Press.

Franchin, P., and F. Cavalieri. 2013. “18 - Seismic Vulnerability Analysis of a Complex Interconnected Civil Infrastructure.” In *Handbook of Seismic Risk Analysis and Management of Civil Infrastructure Systems*, edited by S. Tesfamariam and K. Goda, 465–514e. Woodhead Publishing Series in Civil and Structural Engineering. Woodhead Publishing. https://doi.org/10.1533/9780857098986.4.465.

“GEMScienceTools.” n.d. GitHub. Accessed August 1, 2023. https://github.com/GEMScienceTools.

“Global Assessment Report on Disaster Risk Reduction 2015.” n.d. Accessed May 26, 2023. https://www.undrr.org/publication/global-assessment-report-disaster-risk-reduction-2015.

“Global Earthquake Maps | Global Earthquake Model Foundation | Italy.” n.d. GEM Foundation. Accessed May 29, 2023. https://www.globalquakemodel.org/gem.

“Google Earth.” n.d. Accessed November 23, 2023. https://earth.google.com/web/@48.28672267,-81.22002271,-306.19829825a,2577904.08889711d,35y,0h,0t,0r/data=OgMKATA.

Government of Canada, Natural Resources Canada. n.d. “Earthquake Map of Canada.” Accessed June 21, 2023a. https://earthquakescanada.nrcan.gc.ca/historic-historique/caneqmap-en.php.

———. n.d. “Earthquakes Canada.” Accessed November 20, 2023b. https://www.seismescanada.rncan.gc.ca/index-en.php.

Government of Canada, Statistics Canada. 2022. “Profile Table, Census Profile, 2021 Census of Population - Kazabazua, Municipalité (MÉ) [Census Subdivision], Quebec.” February 9, 2022. https://www12.statcan.gc.ca/census-recensement/2021/dp-pd/prof/index.cfm?Lang=E.

Gueguen, Philippe. 2013. *Seismic Vulnerability of Structures*. John Wiley & Sons.

Gutenberg, Beno. 2013. *Seismicity of the Earth and Associated Phenomena*. Read Books Ltd.

Hallegatte, Stéphane, and Valentin Przyluski. 2010. “The Economics of Natural Disasters: Concepts and Methods.” *World Bank Policy Research Working Paper*, no. 5507.

Hasegawa, H. S. 1991. “Four Seismogenic Environments in Eastern Canada.” *Tectonophysics*, Intraplate Deformation, Neotectonics, Seismicity, and the State of Stress In Eastern North America, 186 (1): 3–17. https://doi.org/10.1016/0040-1951(91)90382-3.

“Hazus User & Technical Manuals | FEMA.Gov.” n.d. Accessed May 28, 2023. https://www.fema.gov/flood-maps/tools-resources/flood-map-products/hazus/user-technical-manuals.

Hazus-MH, F. 2003. “HAZUS-MH Technical Manual.” *Federal Emergency Management Agency, Washington*.

He, X., S. Ni, P. Zhang, and J. Freymueller. 2018. “The 1 May 2017 British Columbia-Alaska Earthquake Doublet and Implication for Complexity Near Southern End of Denali Fault System.” *Geophysical Research Letters* 45 (12): 5937–47. https://doi.org/10.1029/2018GL078014.

Heidebrecht, A. C. 1995. “Insights and Challenges Associated with Determining Seismic Design Forces in a Loading Code.” *Bulletin of the New Zealand Society for Earthquake Engineering* 28 (3): 224–46.

Hill, M, and Tiziana Rossetto. 2023. “DO EXISTING DAMAGE SCALES MEET THE NEEDS OF SEISMIC LOSS ESTIMATION?,” November.

Hobbs, T E, J M Journeay, A S Rao, L Martins, P LeSueur, M Kolaj, M Simionato, et al. 2022. “Scientific Basis of Canada’s First Public National Seismic Risk Model.” 8918. https://doi.org/10.4095/330927.

Hobbs, T E, J M Journeay, and D Rotheram. 2021. “An Earthquake Scenario Catalogue for Canada: A Guide to Using Scenario Hazard and Risk Results.” 8806. https://doi.org/10.4095/328364.

Hobbs, Tiegan E, J Murray Journeay, Anirudh S Rao, Michal Kolaj, Luis Martins, Philip LeSueur, Michele Simionato, et al. 2023. "A National Seismic Risk Model for Canada: Methodology and Scientific Basis." *Earthquake Spectra*, May, 87552930231173446. https://doi.org/10.1177/87552930231173446.

Holzer, Thomas L., and James C. Savage. 2013. "Global Earthquake Fatalities and Population." *Earthquake Spectra* 29 (1): 155–75.

Horner, R. B., M. Lamontagne, and R. J. Wet-miller. 1987. *Rock and Roll in the NWT: The 1985 Nahanni Earthquakes: GEOS (Energy Mines and Resources Canada), v. 16, No. 2*.

Hosseinpour, Vahid, Ali Saeidi, Marie-José Nollet, and Miroslav Nastev. 2021. "Seismic Loss Estimation Software: A Comprehensive Review of Risk Assessment Steps, Software Development and Limitations." *Engineering Structures* 232 (April): 111866. https://doi.org/10.1016/j.engstruct.2021.111866.

Hosseinpour, Vahid, Ali Saeidi, Marie-Jose Nollet, and Miroslav Nastev. 2022. "A Comprehensive Review of Seismic Hazard and Loss Estimation Software."

Hough, Susan E. 2009. "Cataloging the 1811–1812 New Madrid, Central U.S., Earthquake Sequence." *Seismological Research Letters* 80 (6): 1045–53. https://doi.org/10.1785/gssrl.80.6.1045.

Hunter, J., Heather Crow, Gregory Brooks, M Pyne, Dariush Motazedian, M Lamontagne, A Pugin, et al. 2010. *Seismic Site Classification and Site Period Mapping in the Ottawa Area Using Geophysical Methods*.

Hyndman, Roy D., and Garry C. Rogers. 2010. "Great Earthquakes on Canada's West Coast: A Review." *Canadian Journal of Earth Sciences* 47 (5): 801–20.

"Inasafe.Org | 521: Web Server Is Down." n.d. Accessed May 29, 2023. https://inasafe.org/index.html@lang=fr.html.

Jaiswal, Kishor, D.J. Wald, and M. Hearne. 2010. "Estimating Casualties for Large Earthquakes Worldwide Using an Empirical Approach." In *Earthquake Research: Background and Select Reports*, 47–105.

Jena, Ratiranjan, Biswajeet Pradhan, Ghassan Beydoun, Abdullah Al-Amri, and Hizir Sofyan. 2020. "Seismic Hazard and Risk Assessment: A Review of State-of-the-Art Traditional and GIS Models." *Arabian Journal of Geosciences* 13 (2): 50. https://doi.org/10.1007/s12517-019-5012-x.

Journeay, M, P LeSueur, W Chow, and CL Wagner. 2022. "Physical Exposure to Natural Hazards in Canada." 8892. https://doi.org/10.4095/330012.

Karaca, E., and N. Luco. 2008. "Development of Hazard-Compatible Building Fragility and Vulnerability Models." In *Proceedings of the 14th World Conference on Earthquake Engineering, Beijing, China*, 12–17.

Karaman, Himmet, Muhammed Şahin, and Amr S. Elnashai. 2008. "Earthquake Loss Assessment Features of Maeviz-Istanbul (Hazturk)." *Journal of Earthquake Engineering* 12 (sup2): 175–86. https://doi.org/10.1080/13632460802014006.

Kircher, C.A., R.V. Whitman, and W.T. Holmes. 2006. "HAZUS Earthquake Loss Estimation Methods." *Natural Hazards Review* 7 (2): 45–59. https://doi.org/10.1061/(ASCE)1527-6988(2006)7:2(45).

Kolaj, M, S Halchuk, and J Adams. 2023. "Sixth-Generation Seismic Hazard Model of Canada: Grid Values of Mean Hazard to Be Used with the 2020 National Building Code of Canada." 8950. Version 1.0. https://doi.org/10.4095/331497.

Lamontagne, M., S. Halchuk, and J. Adams. n.d. "JF Cassidy Geological Survey of Canada PO Box 6000 Sidney, BC, Canada, V8L 4B2 Jcassidy@ Nrcan. Gc. ca GC Rogers Geological Survey of Canada PO Box 6000 Sidney, BC, Canada, V8L 4B2."

Lamontagne, M., S. Halchuk, J. F. Cassidy, and G. C. Rogers. 2008. "Significant Canadian Earthquakes of the Period 1600–2006." *Seismological Research Letters* 79 (2): 211–23. https://doi.org/10.1785/gssrl.79.2.211.

Lamontagne, M, S Halchuk, J F Cassidy, and G C Rogers. 2018. "Significant Canadian Earthquakes 1600-2017." 8285. https://doi.org/10.4095/311183.

Lamontagne, Maurice. 2002. "An Overview of Some Significant Eastern Canadian Earthquakes and Their Impacts on the Geological Environment, Buildings and the Public." *Natural Hazards* 26: 55–68.

Lamontagne, Maurice, Allison L. Bent, Catherine R. D. Woodgold, Shutian Ma, and Veronika Peci. 2004. "The 16 March 1999 mN 5.1 Côte-Nord Earthquake: The Largest Earthquake Ever Recorded in the Lower St. Lawrence Seismic Zone, Canada." *Seismological Research Letters* 75 (2): 299–316. https://doi.org/10.1785/gssrl.75.2.299.

Langford, Dale. 2018. "The Early Shield Archaic in Northwestern Ontario." *Ontario Archaeology* 98: 24–43.

Langhammer, Tobias, Jochen Schwarz, Panagiotis Loukopoulus, Lars Abrahamczyk, Fillitsa Karantoni, and Dominik Lang. 2006. *INTENSITY-BASED RISK ASSESSMENT FOR EUROPEAN EARTHQUAKE REGIONS – THE 1995 AIGIO EARTHQUAKE*.

Lay, Thorne, Lingling Ye, Hiroo Kanamori, Yoshiki Yamazaki, Kwok Fai Cheung, Kevin Kwong, and Keith D. Koper. 2013. "The October 28, 2012 Mw 7.8 Haida Gwaii Underthrusting Earthquake and Tsunami: Slip Partitioning along the Queen Charlotte Fault Transpressional Plate Boundary." *Earth and Planetary Science Letters* 375: 57–70.

Lizundia, B., S. Durphy, M. Griffin, W. Holmes, A. Hortacsu, B. Kehoe, K. Porter, and B. Welliver. 2015. "Update of FEMA P-154: Rapid Visual Screening for Potential Seismic Hazards." In *Improving the Seismic Performance of Existing Buildings and Other Structures 2015*, 775–86.

Lochead, Janet, Darlene Gillespie, and Claudia Hand. 2012. "Storm-Induced Anastrophic Burial of the Pacific Geoduck (Panopea Generosa) on the West Coast of Vancouver Island." *Journal of Shellfish Research* 31 (4): 959–67.

Ludwin, Ruth S., Gregory J. Smits, D. Carver, K. James, C. Jonientz-Trisler, A. D. McMillan, R. Losey, R. Dennis, J. Rasmussen, and A. De Los Angeles. 2007. "Folklore and Earthquakes: Native American Oral Traditions from Cascadia Compared with Written Traditions from Japan." *Geological Society, London, Special Publications* 273 (1): 67–94.

Ma, Shutian, and Pascal Audet. 2014. "The 5.2 Magnitude Earthquake near Ladysmith, Quebec, 17 May 2013: Implications for the Seismotectonics of the Ottawa–Bonnechere Graben." *Canadian Journal of Earth Sciences* 51 (5): 439–51.

Ma, Shutian, and Dariush Motazedian. 2012. "Studies on the June 23, 2010 North Ottawa MW 5.2 Earthquake and Vicinity Seismicity." *Journal of Seismology* 16: 513–34.

Makhoul, Nisrine, and Sotiris Argyroudis. 2018. "Loss Estimation Software: Developments, Limitations and Future Needs." In *16th European Conference on Earthquake Engineering, Thessaloniki, Greece*.

Marano, Kristin, David J. Wald, and Trevor Allen. 2010. "Global Earthquake Casualties Due to Secondary Effects: A Quantitative Analysis for Improving PAGER Losses." *Natural Hazards* 52: 319–28. https://doi.org/10.1007/s11069-009-9372-5.

McCormack, Thomas C., and Franz N. Rad. 1997. "An Earthquake Loss Estimation Methodology for Buildings Based on ATC-13 and ATC-21." *Earthquake Spectra* 13 (4): 605–21.

McGuire, Robin K. 2004. "Seismic Hazard and Risk Analysis." *(No Title)*.

Milne, W. G., and Alan Garnett Davenport. 1969. "Distribution of Earthquake Risk in Canada." *Bulletin of the Seismological Society of America* 59 (2): 729–54.

Mitchell, Denis, René Tinawi, and Tim Law. 1990. "Damage Caused by the November 25, 1988, Saguenay Earthquake." *Canadian Journal of Civil Engineering* 17 (3): 338–65. https://doi.org/10.1139/l90-041.

Molina, S. 0. "The SELENA-RISe Open Risk Package - Towards the next Generation of ELE Software." https://www.norsar.no/r-d/publications/2015/the-selena-rise-open-risk-package-towards-the-next-generation-of-ele-software.

Molina, S., D. H. Lang, and C. D. Lindholm. 2010. "SELENA – An Open-Source Tool for Seismic Risk and Loss Assessment Using a Logic Tree Computation Procedure." *Computers & Geosciences* 36 (3): 257–69. https://doi.org/10.1016/j.cageo.2009.07.006.

Molina, Sergio, Dominik Lang, Abdelghani Meslem, C.D. Lindholm, and Noelia Agea-Medina. 2017. "A Next-Generation Open-Source Tool for Earthquake Loss Estimation." *International Journal of*

Safety and Security Engineering 7 (November): 585–96. https://doi.org/10.2495/SAFE-V7-N4-585-596.

Molina, Sergio, and Conrad Lindholm. 2005. "A Logic Tree Extension of the Capacity Spectrum Method Developed to Estimate Seismic Risk in Oslo, Norway." *Journal of Earthquake Engineering* 09 (06): 877–97. https://doi.org/10.1142/S1363246905002201.

Mouroux, P., and B. Le Brun. 2006. "Risk-Ue Project: An Advanced Approach to Earthquake Risk Scenarios With Application to Different European Towns." In *Assessing and Managing Earthquake Risk: Geo-Scientific and Engineering Knowledge for Earthquake Risk Mitigation: Developments, Tools, Techniques*, edited by Carlos Sousa Oliveira, Antoni Roca, and Xavier Goula, 479–508. Geotechnical, Geological And Earthquake Engineering. Dordrecht: Springer Netherlands. https://doi.org/10.1007/978-1-4020-3608-8_23.

Nastev, Miroslav. 2014. "Adapting Hazus for Seismic Risk Assessment in Canada." *Canadian Geotechnical Journal* 51 (2): 217–22. https://doi.org/10.1139/cgj-2013-0080.

Nations, United. n.d. "Databases." United Nations. United Nations. Accessed September 3, 2023. https://www.un.org/en/library/page/databases.

Neumann, Frank. 1954. "Earthquake Intensity and Related Ground Motion." *(No Title)*.

Newman, Jeffrey Peter, Holger Robert Maier, Graeme Angus Riddell, Aaron Carlo Zecchin, James Edward Daniell, Andreas Maximilian Schaefer, Hedwig van Delden, Bijan Khazai, Michael John O'Flaherty, and Charles Peter Newland. 2017. "Review of Literature on Decision Support Systems for Natural Hazard Risk Reduction: Current Status and Future Research Directions." *Environmental Modelling & Software* 96 (October): 378–409. https://doi.org/10.1016/j.envsoft.2017.06.042.

News ·, C. B. C. 2011. "2010 Quake Led Ottawa to Change Policies | CBC News." CBC. June 23, 2011. https://www.cbc.ca/news/canada/ottawa/2010-quake-led-ottawa-to-change-policies-1.996472.

Nielson, Bryant G., and Reginald DesRoches. 2007. "Seismic Fragility Methodology for Highway Bridges Using a Component Level Approach." *Earthquake Engineering & Structural Dynamics* 36 (6): 823–39.

Nollet, Marie-José, Ahmad Abo El Ezz, Oliver Surprenant, Alex Smirnoff, and Miroslav Nastev. 2018. "Earthquake Magnitude and Shaking Intensity Dependent Fragility Functions for Rapid Risk Assessment of Buildings." *Geosciences* 8 (1): 16. https://doi.org/10.3390/geosciences8010016.

"OpenQuake Platform." n.d. Accessed August 1, 2023. https://platform.openquake.org/.

Otto, Stefan. 2010. "Applications and Challenges to Using HAZUS-MH for Building Seismic Risk Awareness." *Improving the Seismic Performance of Existing Buildings and Other Structures*, 1241–46.

Pagani, M., D. Monelli, G. Weatherill, L. Danciu, H. Crowley, V. Silva, P. Henshaw, et al. 2014. "OpenQuake Engine: An Open Hazard (and Risk) Software for the Global Earthquake Model." *Seismological Research Letters* 85 (3): 692–702. https://doi.org/10.1785/0220130087.

Pagani, M., V. Silva, A. Rao, M. Simionato, and K. Johnson. 2023. "OpenQuake Engine Manual."

Pagani, M, V Silva, A Rao, M Simionato, and K Johnson. n.d. "OpenQuake Engine Manual."

Perret, Didier, André Pugin, Rémi Mompin, and Denis Demers. 2017. "The Possible Role of Topographic and Basin-Edge Effects in Triggering the Mulgrave and Derrylandslide during the 2010 Val-Des-Bois Earthquake, Québec (Canada)." In *Proceedings of the 70th Annual Canadian Geotechnical Conference GeoOttawa, Ottawa, Canada*.

Pesaresi, Martino, M. Melchiorri, A. Siragusa, and T. Kemper. 2016. "Atlas of the Human Planet 2016." *Mapping Human Presence on Earth with the Global Human Settlement Layer*.

Pitilakis, K., H. Crowley, and A.M. Kaynia, eds. 2014. *SYNER-G: Typology Definition and Fragility Functions for Physical Elements at Seismic Risk: Buildings, Lifelines, Transportation Networks and Critical Facilities*. Vol. 27. Geotechnical, Geological and Earthquake Engineering. Dordrecht: Springer Netherlands. https://doi.org/10.1007/978-94-007-7872-6.

Porter, Keith. 2009. "Cracking an Open Safe: More HAZUS Vulnerability Functions in Terms of Structure-Independent Intensity." *Earthquake Spectra* 25 (3): 607–18. https://doi.org/10.1193/1.3153330.

———. 2015. “A Beginner’s Guide to Fragility, Vulnerability, and Risk.” *Encyclopedia of Earthquake Engineering* 2015: 235–60.
Pranantyo, Ignatius, and Mahardika Fadmastuti. 2014. *InaSAFE Applications in Disaster Preparedness*. Vol. 1658. https://doi.org/10.1063/1.4915053.
Robinson, D. J., T. Dhu, and P. Row. 2007. “EQRM: An Open-Source Event-Based Earthquake Risk Modeling Program” 2007 (December): PA33A-1027.
Robinson, David, Glenn Fulford, and Trevor Dhu. 2005. *EQRM: Geoscience Australia’s Earthquake Risk Model: Technical Manual: Version 3.0*.
Rogers, Garry C., and Henry S. Hasegawa. 1978. “A Second Look at the British Columbia Earthquake of June 23, 1946.” *Bulletin of the Seismological Society of America* 68 (3): 653–76.
Rojahn, Christopher. 1988. *Rapid Visual Screening of Buildings for Potential Seismic Hazards: A Handbook*. Vol. 21. Federal Emergency Management Agency.
Rojahn, Christopher, Roland L. Sharpe, Roger E. Scholl, Anne S. Kiremidjian, Richard V. Nutt, and R. R. Wilson. 1986. “Earthquake Damage and Loss Evaluation for California.” *Earthquake Spectra* 2 (4): 767–82.
Rossetto, Tiziana, Dina D’Ayala, Ioanna Ioannou, and Abdelghani Meslem. 2014. “Evaluation of Existing Fragility Curves.” In *SYNER-G: Typology Definition and Fragility Functions for Physical Elements at Seismic Risk: Buildings, Lifelines, Transportation Networks and Critical Facilities*, edited by K. Pitilakis, H. Crowley, and A.M. Kaynia, 47–93. Geotechnical, Geological and Earthquake Engineering. Dordrecht: Springer Netherlands. https://doi.org/10.1007/978-94-007-7872-6_3.
Sabetta, Fabio, Gabriele Fiorentino, Flavio Bocchi, Martina Sinibaldi, Gaetano Falcone, and Amerigo Mendicelli. 2023. “Influence of Local Site Effects on Seismic Risk Maps and Ranking of Italian Municipalities.” *Bulletin of Earthquake Engineering* 21 (February). https://doi.org/10.1007/s10518-023-01619-9.
Schäfer, D., and M. Pietsch & H. Wenzel. 2013. “EQvis: A Consequence Based Risk Management Software Tool.” In *Research and Applications in Structural Engineering, Mechanics and Computation*. CRC Press.
“Sendai Framework for Disaster Risk Reduction 2015 - 2030.” n.d.
Silva, Vitor, Desmond Amo-Oduro, Alejandro Calderon, Catarina Costa, Jamal Dabbeek, Venetia Despotaki, Luis Martins, et al. 2020. “Development of a Global Seismic Risk Model.” *Earthquake Spectra*, February. https://doi.org/10.1177/8755293019899953.
Silva, Vitor, Helen Crowley, Marco Pagani, Damiano Monelli, and Rui Pinho. 2014a. “Development of the OpenQuake Engine, the Global Earthquake Model’s Open-Source Software for Seismic Risk Assessment.” *Natural Hazards* 72 (July). https://doi.org/10.1007/s11069-013-0618-x.
———. 2014b. “Development of the OpenQuake Engine, the Global Earthquake Model’s Open-Source Software for Seismic Risk Assessment.” *Natural Hazards* 72 (3): 1409–27. https://doi.org/10.1007/s11069-013-0618-x.
Silva, Vitor, and Nick Horspool. 2019. “Combining USGS ShakeMaps and the OpenQuake-Engine for Damage and Loss Assessment.” *Earthquake Engineering & Structural Dynamics* 48 (6): 634–52. https://doi.org/10.1002/eqe.3154.
Statistics Canada, Statistics Canada. 2023. “Consumer Price Index, Monthly, Not Seasonally Adjusted.” 2023. https://www150.statcan.gc.ca/t1/tbl1/en/tv.action?pid=1810000401.
Stott, D. F. 1984. “Cretaceous Sequences of the Foothills of the Canadian Rocky Mountains,” 85–107.
“The Basics of Seismic Risk Analysis.” 1989. *Earthquake Spectra* 5 (4): 675–702. https://doi.org/10.1193/1.1585549.
Thibert, Katherine Marie. 2008. “A Methodology for Assessing the Seismic Risk of Buildings.” University of British Columbia. https://doi.org/10.14288/1.0063092.
TOOLKiT, RisK MODELLERs. 2015. “OPENQUAKE.”

Trifunac, M. D., and A. G. Brady. 1975. “On the Correlation of Seismic Intensity Scales with the Peaks of Recorded Strong Ground Motion.” *Bulletin of the Seismological Society of America* 65 (1): 139–62.

Tyagunov, Sergey, Lothar Stempniewski, Gottfried Grünthal, Rutger Wahlström, and Jochen Zschau. 2004. “Vulnerability and Risk Assessment for Earthquake Prone Cities.” In *13th World Conference on Earthquake Engineering (Vancouver 2004)*.

U. S. Geological Survey. 2017. “The Preliminary Determination of Epicenters (PDE) Bulletin.” U.S. Geological Survey. https://doi.org/10.5066/F74T6GJC.

“USGS Website.” n.d. Accessed September 11, 2023. https://earthquake.usgs.gov/earthquakes/map/?extent=7.10089,-155.91797&extent=60.32695,-34.01367.

Vecere, Annibale, Ricardo Monteiro, and Walter J. Ammann. 2016. “Comparative Analysis of Existing Tools for Assessment of Post-Earthquake Short-Term Lodging Needs.” *Procedia Engineering*, World Multidisciplinary Civil Engineering-Architecture-Urban Planning Symposium 2016, WMCAUS 2016, 161 (January): 2217–21. https://doi.org/10.1016/j.proeng.2016.08.818.

Ventura, Carlos E., and Norman D. Schuster. 1994. “Seismic Risk and Hazard Reduction in Vancouver, British Columbia.” In *Issues in Urban Earthquake Risk*, edited by Brian E. Tucker, Mustafa Erdik, and Christina N. Hwang, 221–36. NATO ASI Series. Dordrecht: Springer Netherlands. https://doi.org/10.1007/978-94-015-8338-1_14.

Ventura, Carlos, Tuna Onur, and Liam Finn. 2005. “Regional Seismic Risk in British Columbia - Damage and Loss Distribution in Victoria and Vancouver.” *Canadian Journal of Civil Engineering* 32 (April): 361–71. https://doi.org/10.1139/l04-098.

Wald, David J., Vincent Quitoriano, Thomas H. Heaton, Hiroo Kanamori, Craig W. Scrivner, and C. Bruce Worden. 1999. “TriNet ‘ShakeMaps’: Rapid Generation of Peak Ground Motion and Intensity Maps for Earthquakes in Southern California.” *Earthquake Spectra* 15 (3): 537–55.

Walker, Blake Byron, Nadine Schuurman, David Swanlund, and John J. Clague. 2021. “GIS-Based Multicriteria Evaluation for Earthquake Response: A Case Study of Expert Opinion in Vancouver, Canada.” *Natural Hazards* 105: 2075–91.

Wetmiller, R. J., J. Adams, F. M. Anglin, H. S. Hasegawa, and A. E. Stevens. 1984. “Aftershock Sequences of the 1982 Miramichi, New Brunswick, Earthquakes.” *Bulletin of the Seismological Society of America* 74 (2): 621–53.

Wetmiller, R. J., R. B. Horner, H. S. Hasegawa, R. G. North, M. Lamontagne, D. H. Weichert, and S. G. Evans. 1988. “An Analysis of the 1985 Nahanni Earthquakes.” *Bulletin of the Seismological Society of America* 78 (2): 590–616.

Wyss, Max, and Yuzo Toya. 2000. “Is Background Seismicity Produced at a Stationary Poissonian Rate?” *Bulletin of the Seismological Society of America* 90 (5): 1174–87.

Yeh, Chin-Hsun, Chin-Hsiung Loh, and Keh-Chyuan Tsai. 2006. “Overview of Taiwan Earthquake Loss Estimation System.” *Natural Hazards* 37 (1): 23–37. https://doi.org/10.1007/s11069-005-4654-z.

Zameeruddin, Mohd, and Keshav K. Sangle. 2016. “Review on Recent Developments in the Performance-Based Seismic Design of Reinforced Concrete Structures.” In *Structures*, 6:119–33. Elsevier.